TÜBİTAK

TÜRKİYE BİLİMSEL VE
TEKNİK ARAŞTIRMA KURUMU

THE SCIENTIFIC AND TECHNICAL
RESEARCH COUNCIL OF TURKEY



# EMİSYON KONTROLÜNDE KULLANILAN DEĞERLİ METAL KATALİZÖRLER ÜZERİNDE CO OKSİTLENMESİ REAKSİYONU YAPISAL DUYARLILIK (STRUCTURE SENSITIVITY) GÖSTERİR Mİ?'

**PROJE NO: MİSAG 188**

**Makina Kimyasal Teknolojiler, Malzeme ve İmalat Sistemleri Araştırma Grubu**

**Mechanical Engineering, Chemical Technologies,Material Sciences and Manufacturing Systems Research Grant Committee**

**TÜBİTAK**

**ARAŞTIRMA PROJESİ SONUÇ RAPORU**

2004-282

# EMİSYON KONTROLÜNDE KULLANILAN DEĞERLİ METAL KATALİZÖRLER ÜZERİNDE CO OKSİTLENMESİ REAKSİYONU YAPISAL DUYARLILIK (STRUCTURE SENSITIVITY) GÖSTERİR Mİ?'

**PROJE NO: MİSAG 188**

**Doç. Dr. Deniz Üner**

**Murat Üner**

**Bora Atalık**

**Aralık 2003**

**ANKARA**

# İÇİNDEKİLER

## ŞEKİL LİSTESİ

## TABLO LİSTESİ

# ÖNSÖZ

TÜBİTAK MİSAG 188 projesi çerçevesinde ODTÜ Kimya Mühendisliği bölümünde gerçekleşirilen 'Emisyon kontrolünde kullanılan değerli metal katalizörler üzerinde CO oksitlenmesi reaksiyonu yapısal duyarlılık (Structure sensitivity) gösterir mi?' başlıklı projede tek ve çift metalli destekli katalizörler üzerinde CO oksitlenmesi reaksiyonunun yapısal duyarlılığı incelenmiştir. Elde edilen sonuçlar hem egzoz emisyon kontrolünde kullanılan değerli metal katalizörlerin işleyişini yorumlamakta kullanılabilecek, hem de proton takaslı membran yakıt pillerinde kullanılan seçici CO oksitlenmesi katalizörlerinin de tasarımına ışık tutacak niteliktedir.

# ÖZ

Karbon monoksitin karbon dioksite oksitlenmesi tepkimesi oksijen molekülünün yüzeyde parçalanarak adsorplanması sonucunda oluşan oksijen atomu ile adsoplanmış karbon monoksit molekülünün etkileşimi ile gerçekleşir. Karbon monoksitin Pt üzerinde yol açtığı zehirleme etkisi yüzünden oksijen adsoplanması daha da önem kazanır. Bu çalışmanın amacı oksijen, hidrojen ve karbon monoksitin $Pt/\gamma\text{-}Al_2O_3$ üzerindeki adsorplanması ve yapısal duyarlılığını incelemektir. Metallerin parçacık büyüklüğü kalsinasyon sıcaklığı ve süresini yükselterek artırılmış ve bu şekilde katalizörlerin yapısı değiştirilmiştir. Bu şekilde aynı miktarda metal yüklenmiş fakat farklı parçacık büyüklüğünde dolayısı ile farklı kenar, köşe ve düzlem atom oranları içeren katalizörler hazırlanmıştır. Temiz yüzey adsorplanma ısıları ölçüldüğünde karbon monoksit ve oksijenin yapıya duyarlılık göstemedikleri, ancak hidrojenin temiz yüzey adsorplanma ısısının parçacık büyüklüğü ile ters orantılı olduğu belirlenmiştir. Bu sonuç hidrojenin CO veya $O_2$ den daha fazla yapısal duyarlılık gösterdiğinin bir işareti olarak alınmıştır. CO oksitlenmesi tepkimesinin yapısal duyarlılık gösterdiği ise reaksiyon deneyleri ile açığa çıkarılmıştır. Tepkimenin aktivasyon enerjisinin artan parçacık büyüklüğü ile sistematik olarak azaldığı ortaya çıkarılmıştır.

*Anahtar kelimeler:* Katalizör, Destekli metal katalizör, ikili metaller, karbon monoksit oksitlenmesi, seçici karbon monoksit oksitlenmesi, platin , adsorplanma ısısı, mikrokinetik analiz.

## ABSTRACT

The oxidation of CO to form $CO_2$ reaction proceeds via the combination of a chemisorbed CO molecule with a chemisorbed oxygen atom, the latter produced through the dissociative adsorption of $O_2$ on the Pt surface. Due to the poisoning effect of the CO adsorption on the Pt surface, amount of adsorbed oxygen on the surface gains more importance. The aim of the study is to investigate the adsorption characteristics and the structure sensitivity of oxygen, hydrogen and carbon monoxide adsorption on $Pt/\gamma\text{-}Al_2O_3$ catalysts. The surface structure of the catalysts was manipulated by increasing the particle size of the metals by increasing the calcination duration and temperature. As a result catalysts with the same metal loading but different surface composition in terms of edge, corner and low index plane atoms could be prepared. The zero coverage differential heat of adsorptions measured for CO and $O_2$ do not show any change with the changing particle size. On the other hand, $H_2$ shows a sharp decrease of zero coverage heat values as the average particle diameter of Pt increases. This can be concluded as $H_2$ adsorption is more structure sensitive than the CO and $O_2$ adsorptions. The structure sensitivity of the CO oxidation reaction was confirmed by reaction experiments. In addition, it was observed that the reaction apparent activation energy decreased sytematically with increasing particle size.



*Key words:* Catalysts, supported metal catalysts, bimetallics, carbon monoxide oxidation, selective cabon monoxide oxidation, platinum, heats of adsorption, microkinetic analysis.

# 1. GİRİŞ

## 1.1. Konu ve amaç

Çeşitli katalizörler üzerinde gerçekleşen karbon monoksit oksidasyonu reaksiyonu reaksiyonun basitliği nedeni ile yüzey kimyacıları tarafından yaygın olarak çalışılmış bir reaksiyondur. Egzoz emisyonlarında açığa çıkan karbon monoksit gazını karbon dioksit'e dönüştürerek zehirsiz hale getirmek için kullanılan Pt ve Pd gibi değerli metallerin yüksek fiyatları nedeni ile (yaklaşık 500 $/ons) en verimli şekilde kullanılmaları gerekmektedir. Bu nedenle bu metaller üzerinde gerçekleşen reaksiyonun gerçek mekanizmasını algılamak ve katalitik olarak metallerin en aktif oldukları yapıda katalizörleri tasarlamak ve hazırlamak gerekmektedir. Katalitik karbon monoksit oksidasyonu reaksiyonunun mekanizmasının Langmuir-Hinshelwood veya Eley-Riedal olup olmadığı konusunda yoğun çalışmalar yapılmış ve genel konsensus olarak reaksiyonun mekanizmasının Langmuir-Hinshelwood olduğu kabullenilmiştir. Bu reaksiyon sırasında Pt ve Pd gibi değerli metallerin yüzeyde yeniden yapılandıkları belirlenmiş (Ladas *et al.*, 1993;Thiel *et al.*, 1982; Eiswirth ve Ertl, 1986; Fink *et al.*,1991) bu yeniden yapılanmadan kaynaklanan reaksiyon salınımları incelenmiştir. Ayrıca, düşük sıcaklıklarda yüzeyin ağırlıkla karbon monoksit kaplanmasından kaynaklanan bir zehirlenme, yüksek sıcaklıklarda oksitlenebilir metallerde, örneğin Pd, kısmi oksit oluşturma şeklinde sıcaklığa bağlı bir reaksiyon salınımı da gerçekleşebilmektedir (Özkan *et al.*,1997).

Gurubumuzda gerçekleşen bir tez çalışmasında oksijen ve CO adsorplanması ve oksitlenme reaksiyonu, yüksek karbon monoksit kısmi basınçlarında $Pt/TiO_2$ üzerinde termal ve fotokatalitik olarak iki şekilde incelenmiştir (Ozen, 2001; Ozen ve Uner, 2001). Karbon monoksitin bu tür katalizörler üzerinde oksitlenmesi reaksiyonuna ilişkin ayrıntılı bir literatür taraması adı geçen tezde yer almaktadır. Yine gurubumuzda yapılan bir tez çalışmasında CO oksitlenmesi oksidan olarak NO'nun ortamda bulunduğu durumlarda Rh katalizörleri üzerinde mikrokinetik analiz kullanılarak çalışılmıştır(Ernur, 1998; Ernur ve Üner, 2000). 400-500 K civarındaki sıcaklıklara kadar değerli metallerin yüzeyleri %100'e varan oranlarda karbon monoksit ile kaplıdır (Ernur, 1998; Ernur ve Üner, 2000 ve içindeki referanslar). Bu sıcaklıklar karbon monoksit ve oksijenin adsorplanma ısılarının göreceli büyüklüklerinin

karbon monoksitin yüzeyde kaplanmasını ağırlıklı kılacak sıcaklıklardır. Sıcaklık yükseldikçe karbon monoksit yüzeydeki yerini oksijene terketmekte ve reaksiyonun mekanizması, mertebeleri ve aktivasyon enerjileri de buna bağlı olarak değişmektedir (Ernur, 1998; Ernur ve Üner, 2000). 400-500 K sıcaklık aralığı ise otomobil egzozunun katalitik konvertere ulaştığı sıradaki sıcaklığı olması itibarı ile önemli bir aralıktır. Bu aralıkta yukarıda da bahsedildiği gibi karbon monoksit yüzeyin %100'e yakın kısmını kaplamakta, karbon dioksit oluşumu ise katalizörün yüzeyinin açıkta kalan yaklaşık %0,1'lik kısmında gerçekleşebilmektedir.

Karbon monoksit literatürde yapısal duyarlılık gösteren bir reaksiyon olarak geçmez (Gates, 1992; Masel; 1996). Ancak oksijen adsorplanması toplam reaksiyon mekanizması içinde yapısal duyarlılık gösteren bir basamaktır (Masel, 1996). Bunlara ek olarak literatürde yer alan yoğun çalışmaların özünde, karbon monoksit oksitlenmesi reaksiyonu sırasında hız belirleyici basamağın oksijen adsorplanması, yüzey oksidasyonu reaksiyonu veya karbon dioksit desorplanması (Nijhuis *et al.*,1997) basamağı olabileceği konusunda fikir birliğine varılamamıştır. Ancak oksijen adsorplanmasının hız belirleyici basamak olması halinde tepkimenin yapısal duyarlılık göstermesi beklenmelidir.

Literatür'deki mevcut çalışmalar, ve halihazırda sürdürdüğümüz farklı oksit desteklerin CO oksitlenmesi reaksiyonu üzerindeki etkisi konusunda elde ettiğimiz bulgular, metaller üzerinde oksijen adsorplanmasının yapısal duyarlılık gösterdiği şeklindedir. Aslında bu yapısal duyarlılığın, parçalanarak adsorplanmayı gerektiren moleküller için bir yaygınlık arzettiği düşünülmektedir (Kumar *et al.*,2000; Savargaonkar *et al.*,1998; Vanderwiel *et al.*,1999). Bu çalışmada, CO oksitlenmesi reaksiyonunun yapısal duyarlılık gösterdiği konusundaki literatürdeki ipuçlarına (Zafiris ve Gorte, 1993) destek olacak veya yadsıyacak verileri toplamak ve bu verilerin yüzey reaksiyon modelleri ve mikrokinetik analiz yöntemi kullanılarak (Dumesic *et al.*,1993) global kinetik modellere dönüştürülmesi planlanmış ve bu doğrultuda veriler toplanmış ve modeller kurulmuştur.

### 1.2. İncelenen Parametreler:

Bu çalışmada, $\gamma$-$Al_2O_3$ üzerinde desteklenmiş Pt ve Pd tek metalli ve Pt-Pd ikili metal alaşım katalizörleri üzerinde karbon monoksit ve oksijen adsorplanmalarının ve karbon monoksit oksitlenmesi tepkimesinin yapısal duyarlılığı incelenmiştir. Tek metalli Pt katalizörler ıslaklık başlangıcı yöntemi ile hazırlanmış, metal parçacık büyüklüğü katalizör

kalsinasyon sıcaklığı bir parametre olarak kullanılarak değiştirilmiştir. İkili metal katalizörler ise kullanılan katalizör hammaddesine göre birlikte empregne veya sıralı empregne yöntemleri kullanılarak hazırlanmıştır. Tek metalli Pt katalizörleri üzerinde yapısal duyarlılık bu katalizörler üzerindeki CO, $H_2$ ve $O_2$ gazlarının diferansiyel ve integral adsorplanma ısıları ölçülerek incelenmiştir. Tepkenlerin diferansiyel adsorplanma ısıları laboratuvarımızda bulunan Setaram C80® model Tian-Calvet tipi bir mikrokalorimetre kullanılarak ölçülmüştür. Tepkimenin yapısal duyarlılığı ise dolgulu yatak bir diferansiyel reaktörde tepkenlerin reaksiyon mertebeleri ve tepkimenin aktivasyon enerjisi ve bunların sıcaklığa bağlı değişimleri izlenerek incelenmiştir. Ayrıca karbon monoksitin hidrojen açısından zengin ortamlarda değerli metaller üzerinde gerçekleşen seçici oksidasyon reaksiyonunun yapısal duyarlılık gösterip göstermediği sorusuna modelleme yolu ile cevap aranmıştır. Bu nedenle metal parçacık büyüklüğünün kontrol edilerek değiştirildiği katalizörler kullanılarak reaksiyon adsorplanma ve tepkime basamaklarında ayrı ayrı incelenmiş, ve metal yüzeyinde bulunan düşük koordinasyonlu metal atomlarının konsantrasyonu ile adsorplanma ve tepkime basamaklarının hızları ve enerjetik davranışları izlenmiştir.

**1.3 Projenin değerlendirilmesi:**

Başvuru sırasında bu projenin kapsamında egzoz emisyon kontrolünde yaygın olarak kullanılan iki oksidasyon katalizörü, Pt ve Pd, ve yine aynı amaçla kullanılan oksit malzemeler, $\gamma$-$Al_2O_3$, $CeO_2$ ve $ZrO_2$, yanı sıra fotokatalitik etkinliği ispatlanmış $TiO_2$ altlıkları kullanılarak metaller farklı parçacık büyüklüklerinde hazırlanması planlanmıştır. Çalışmada ise esas olarak $\gamma$-$Al_2O_3$ altlık kullanılmış, $TiO_2$ üzerinde desteklenmiş Pt katalizörlerinin oksijen adsorplanma ısıları ölçülmüş ancak bu katalizörlerde tepkime deneyleri yapılmamıştır. $TiO_2$ destekli katalizörler üzerinde yapılan adsorplanma ısısı ölçümü çalışmalarında katalizör ile desteğin kalsinasyon sırasında doğrudan elektronik etkileşime geçtiğine yönelik bulgular bu destek malzemesi üzerindeki çalışmaların daha ileri fazda yapılmasının yanıltıcı olabileceği gerekçesi ile durdurulmuştur. Destek olarak $CeO_2$ kullanılan çalışmada ise bu malzemenin hammadesinin içerdiği klordan kaynaklanan etkileşim incelenmiş, daha temiz bir hammmade olan ceryum asetat kullanılarak hazırlanan $CeO_2$ üzerinde desteklenen Pt katalizörleri üzerinde CO oksitlenmesi reaksiyonunun mertebeleri ve aktivasyon enerjileri ölçülebilmiştir. Bu katalizör üzerinde oksijen sıcaklık programlı desorplanma çalışmaları ise halen devam etmektedir. Hedeflenen altlıklar arasında sadece $ZrO_2$ çalışılamamıştır. Laboratuvarımızda bulunan $ZrO_2$ yeterince yüksek yüzey

alanına sahip olmadığından, önmaddesi (precursor) de proje bütçesinde öngörülmediğinden bu altlık çalışılmamıştır.

Parçacık büyüklüğünü ayarlayabilmek için metal yükleme ortamının pH'sı, başlangıç maddeleri (precursor) ve metalleştirme yöntemleri (kalsinasyon ve indirgeme basamakları) değiştirilerek aynı yükleme oranında, yani aynı metal/oksit altlık stokiyometrisinde katalizörler hazırlanması planlanmıştır. Ancak, kalsinasyon sıcaklığını değiştirerek gerekli kontrolün sağlanabildiği gözlemlendiğinden hazırlama koşullarının kimyası incelenmemiştir. Bu katalizörlerin metal parçacık büyülüklerinin hidrojen adsorplanması ve katı hal NMR spektroskopisi yöntemi ile ölçülmesi planlanmıştır. Hidrojen adsorplanması yöntemi kullanılabilmiştir. Ancak ODTÜ Kimya bölümünde bulunan NMR spekrometresinin katı hal izleyicisi (probe) ve düzeneği ile ilgili sorunlar yaşandığı ve bu ölçümün yapılamayacağı öğrenilmiştir. ODTÜ Merkezi Laboratuvarlarına cihaz alımlarının yaklaşık üç yıl gecikmesinden kaynaklanan sorundan ötürü burada bulunması planlanan NMR spektrometresi de kullanılamadığından NMR ölçümleri yapılamamıştır. Bu katalizörlerin hidrojen, oksijen ve karbon monoksit adsorplanma kapasiteleri hacimsel yöntemlerle ölçülmüş, paralelinde gerçekleşen mikrokalorimetre ölçümleri ile de statik ortamda diferansiyel adsorplanma ısı eğrileri elde edilebilmiştir. Karbon monoksit oksidasyonu reaksiyonu light-off eğrileri de tek ve çift metalli katalizörlerde elde edilebilmiştir. Elde edilen bilgilerin mikrokinetik analiz yöntemi ile modellenmesi hedeflenmiştir(Dumesic *et al.*, 1993), ancak gerekli bilgisayar programlarının yetersizliği nedeni ile (FEMLAB ve CHEMKİN) çalışma global kinetik modelleme ile sınırlı kalmıştır.

Proje çerçevesinde öngörülen ancak desteklenemeyen kütle akım kontrolorü cihazlarının olmayışı nedeni ile dinamik adsorplanma yöntemi ile yapılacak kalorimetre ölçümleri yerine statik ölçümler benimsenmiştir. Statik ortamda yapılan ölçümlerle yüzey kaplanma oranına karşı gelen diferansiyel adsorplanma ısısı grafiği çizilerek yapısal duyarlılık incelenmiştir.

# 2. GELİŞME

## 2.1 Teorik Esaslar

### 2.1.1 Yapısal duyarlılık:

Yapısal duyarlılık, destekli metal katalizörlerin işlevsel mekanizmalarından yalnızca birisidir. Herhangi bir reaksiyonun yapısal duyarlılık gösterip göstermediğini anlamak için, toz örneklerde katalitik reaksiyonun hızının kütle aktarımı ile sınırlanmadığı bölgede gerçekleşirken, kinetiğin metal parçacık büyüklüğüne bağlılığı incelenmelidir. Metal parçacık büyüklüğü, reaksiyonun hızını farklı şekillerde etkileyebilmektedir. Birincil olarak yapısal duyarlılık nedeni ile düşük çaplı paraçacıklarda bulunan yüksek miktardaki düşük koordinasyonlu atomların etkinlikleri reaksiyon hızını etkileyebilmektedir. İkincisi, ensemble etkisi olarak adlandırılır ve bazı reakiyonların gerçekleşebilmesi için belli miktarda aynı özelliği taşıyan atomların belli bir geometride yüzeyde varolmasını gerektirir. Üçüncüsü ise metal/destek arayüzünün büyüklüğünün metal parçacık büyüklüğü ile etkilenmesi sonucunda ve taşma olayları veya arayüz reaksiyonlarının hızları etkilenmektedir. Eğer ince filmlerde bu çalışmanın yapılması söz konusu ise yapısal duyarlılık, metallerin farklı kristal düzlemleri üzerinde reaksiyonun farklı hızlarda gerçekleşip gerçekleşmediği incelenerek anlaşılabilir. Bu projede hedeflenen konu, farklı oksit malzemeler üzerinde hazırlanacak olan değerli metal katalizörlerin aktifliğinin metal parçacık büyüklüğü ile olan ilişkisini dolayısı ile karbon monoksit oksitlenmesi tepkimesinin yapısal duyarlılık gösterip göstermediği sorusunun cevabını aramaktır.

### 2.1.2. CO adsorplanması:

Karbon monoksit, değerli metaller üzerinde karbon ucu metale bağlı olmak üzere lineer, di-karbonil ($M\text{-}(CO)_2$) multikarbonil ($M\text{-}(CO)_n$) ya da köprü bağlı ($M_2CO$) olarak adsorplanabilir. Bu bağlanma şekilleri yüzeye, yüzey kaplanma oranına ve adsorplandığı metala göre değişiklik gösterir (Uner, 1994). Karbon monoksit, hem oksitlenme, hem hidrojenleme tepkimelerinde kullanıldığı için adsorplanması yaygın olarak çalışılmış bir moleküldür. Buna ek olarak yüzey karakterizasyonu amacı ile karbon monoksit izleyici molekül olarak kullanılabilmektedir. Pt üzerine yapılmış CO adsorplanması çalışmalarını burada özetlemek yerine, çalışmada kıyaslamak amacı ile Pt yüzeyleri üzerinde yapılan karbon monoksit adsorplanması ısısı ölçümü değerlerinin kısa bir derlemesi Tablo 1'de verilmektedir.

Tablo 1. Destekli Pt üzerinde karbon monoksit adsorplanma ısıları ile ilgili literatür verileri

| Yüzey | % Pt | Sıfır kaplama oranı adsorplanma ısısı (kJ/mol) | İntegral adsorplanma ısısı (kJ/mol) | Doygunluk yüzey kaplanma oranı (μmol/g kat) | Disperslenme (mol H ads/mol Pt) oranı | Kaynak |
|---|---|---|---|---|---|---|
| $Pt/SiO_2$ | 1.2 | 144 | 104 | 48.7 | 1.18 | Cortright ve Dumesic, 1995 |
| $Pt-K/SiO_2$ | 1.2 | 140 | 101 | 26.7 | 1.31 | Cortright ve Dumesic, 1995 |
| $Pt-Sn/SiO_2$ | 0.93 | 135 | 83 | 19.6 | 0.51 | Cortright ve Dumesic, 1995 |
| $Pt-Sn-K//SiO_2$ | 0.93 | 138 | 91 | 10.4 | 0.89 | Cortright ve Dumesic, 1995 |
| $Pt/SiO_2$ | 4.0 | 140 | 105.1 | 130 | 0.51 | Sharma *et al.*, 1994 |
| $Pt/SiO_2$ | 7.0 | 140 | 113.8 | 162 | 0.63 | Sharma *et al.*, 1994 |

### 2.1.3. Oksijen adsorplanması:

Metaller üzerinde oksijen adsoplanması oksijenin polar bir molekül olmasının yarattığı sorunlardan ötürü karbon monoksit veya hidrojen kadar yagın çalışılmamış olmakla beraber, literatürde konu ile ilgili yapılmış yayınlardan derlenen bilgiler Tablo 2'de verilmiştir. Bu yayınlar incelendiğinde oksijenin metaller üzerinde adsorplanmasının ağırlıkla düşük Miller endeksli düzlemler üzerinde gerçekleştiği görülmektedir. Oksijenin adsorplanırken parçalanması veya moleküler olarak adsorplanması için belirleyici faktör adsorplanacağı yüzey ile olan etkileşimi adsorplanacağı yüzeyin yapısı olmaktadır.

Oksijen adsorplanmasının mekanizmaları, katalitik toplam oksidasyon ya da kısmi oksidasyon tepkimelerinde kısıtlayıcı ve/veya seçiciliği belirleyici basamak olabilir. Oksitleyici molekül olarak NO kullanıldığı zaman, tepkimenin yapısal duyarlılığının, NO molekülünün metal yüzeyleri ile olan özel etkileşiminden kaynaklandığı bilinmektedir. Suyun ya da karbon monoksitin oksitlenmesi sırasında oksijen yerine NO kullanıldığında farklı metal yüzeylari arasında tepkimenin hız oranları 21 mertebe değişebilmektedir. Ancak oksijen kullanıldığında bu farklılık ancak 6 mertebe düzeyindedir (Masel, 1996).

Oksijenin adsorplanması kinetiğindeki yapısal duyarlılık, molekülün izotop değiş-tokuş dinamiğinde belirgin bir biçimde gözlemlenmekle birlikte (Descorme ve Duprez, 2001) adsorplanma ısısı verilerinin destekli metal katalizörler üzerinde yaygın olarak çalışılmamış olması bu konudaki kesin yargıyı ertelemektedir.

Tablo 2. Oksijenin yüzeyde adsoplanma şekilleri, adsorplanma ısıları ve desorplanma aktivasyon enerjileri (Uner *et al.*, 2003)

| **Yüzey** | **Oksijen adsorplanma biçimi** | **Doygunluk üzey kaplanma oranı (ML)** | **Yapışma katsayısı, $S_0$** | **$E_{a,\ des}$ (kJ/mol)** | **$\Delta H_{ads}$ (kJ/mol)** | **Kaynak** |
|---|---|---|---|---|---|---|
| Pt(111) | atomsal | | 0.064 | | 339±32 | Yeo *et al.*, 1997 |
| Pt(110) | atomsal | 0.35 | 0.34 | | 332±10 | Wartnaby *et al.*, 1996 |
| Pt(111) | | 0.25 | 0.06 | 213.4 -175.7 | | Campbell *et al.*,, 1981 |
| Pt(S)-[9(111)x(111)] | | 0.5 | 0.06 | 205-171.5 | | Schwaha ve Bechtold, 1977 |
| Pt(111) | Moleküler | 0.6 | | | 37±2 | Gland *et al.*, 1980 |
| Pt(111) | atomsal | 0.4 | | | 470±10 | Gland *et al.*, 1980 |
| Pt(111) | | 0.25 | 0.048±0.006 | | | Monroe ve Merill, 1980 |
| Pt(111) | | 0.25 | | | | Puglia *et al.*,, 1995 |
| Pt(111) | Moleküler, peroxo | | | | 40.5 | Nolan *et al.*, 1999 |
| Polycristalline Pt | | 0.75 | | | | Tong ve van der Klink , 1995 |
| Pt(111) | Moleküler | | 0.12 | | | Cudok *et al.*, 1994 |
| $TiO_2$(110) | Moleküler | | $8\times10^{-5}$ | 94 | | Gopel *et al.*, 1983 |
| $TiO_2$(110) | Moleküler | | 0.5-0.6 | 108 | | Henderson *et al.*, 1996 |

### 2.1.4. Hidrojen adsorplanması:

Hidrojen adsorplanması literatürde hem destekli metaller üzerinde hem de tek kristalli metaller üzerinde yaygın olarak çalışılmıştır. Bunun gerekçesi hem hidrojenin yaygın bir endüstriyel hammadde olması hem de adsorplanmış hidrojenin metal karakterizasyonunda yaygın olarak kullanılmaşıdır. Pt üzerinde hidrojen adsorplanmasının mikrokalorimetrik ölçümleri sonucunda elde edilen başlangıç adsorplanma ısıları ve integral adsorplanma ısıları Tablo 3'de, değişik metaller üzerinde hidrojen adsorplanması yapışma katsayıları da Tablo 4'te derlenmiştir. Hidrojen adsorplanmasının yapısal duyarlılığı, yakın zamanda NMR spektroskopisi kullanılarak incelenmiştir (Savargaonkar *et al.*, 1998, Savargaonkar *et al.*, 2002). Tek ve çift metalli katalizörler üzerinde yapılan ölçümlerde Ru üzerinde hidrojen adsorplanmasının başlangıç ısılarının değişmediği ancak orta ve düşük ısılı adsorplanma merkezlerinin azaldığı belirlenmiştir (Savargaonkar *et al.*, 1998; Narayan ve King, 1998). NMR spektroskopisi ile ölçülen gaz fazı-yüzey arasındaki hidrojen değiş tokuş parametresi kullanılarak hesaplanan adsorplanma ve desorplanma hız sabitleri kullanılarak metal üzerinde hidrojenin görünür yapışma katsayıları yüzey kaplanma oranlarının bir fonksiyonu olarak belirlenebilmiştir. Bu sonuçların gösterdiği en belirgin özellik tek metalli Ru parçacıkları üzerinde hidrojenin 'prekursor' adsoplanması gerçekleştirdiği zaman göstereceği yapışma katsayısının kaplanma oranı ile değişmediği durumdur. Buradan yola çıkılarak oluşturulan bir modelde metal parçacıkları üzerinde adsorplanma portal'larının olduğu, bu portalların elektron fakiri kenar ve köşe atomlarından oluştuğu, adorplanmanın ağırlıkla bu portallara aracılığı ile gerçekleşirken desorplanmanın yüzey üzerinde hareket halinde olan moleküllerin herhangi bir noktada karşılaşmaları sonucunda gerçekleşeceği varsayımı denenmiş ve NMR sonuçları ile uyumu gösterilmiştir (Kumar et al., 2000).

Bu çalışmaların ışığında, hidrojen adsorplanması dinamiğinin yapısal duyarlılığı varsayımının geçerliliği dikkate alınarak bu çalışmada katalizörlerin yapısal karakterisazyonu hidrojen adsorplanması ve hidrojenin adsorplanma ısılarının yapısal farklılıkları belirlenmesi amacı ile kullanılması kararlaştırılmıştır.

Tablo 3. Pt Üzerinde hidrojen adsorplanma ısıları ile ilgili literatür verileri

| Yüzey | % Pt | Sıfır kaplama oranı adsorplanma ısısı (kJ/mol) | İntegral adsorplanma ısısı (kJ/mol) | Doygunluk yüzey kaplanma oranı (μmol/g kat) | Disperslenme (mol H ads/mol Pt) oranı | Kaynak |
|---|---|---|---|---|---|---|
| $Pt/SiO_2$ | 1.2 | 93 | 66 | 38.6 | 1.18 | Cortright ve Dumesic, 1995 |
| Pt-$K/SiO_2$ | 1.2 | 95 | 67 | 46.0 | 1.31 | Cortright ve Dumesic, 1995 |
| Pt-$Sn/SiO_2$ | 0.93 | 92 | 59 | 16.1 | 0.51 | Cortright ve Dumesic, 1995 |
| Pt-Sn-$K//SiO_2$ | 0.93 | 97 | 52 | 26.0 | 0.89 | Cortright ve Dumesic, 1995 |
| $Pt/SiO_2$ | 4.0 | 91 | 67 | 69 | 0.51 | Sharma *et al.*, 1994 |
| $Pt/SiO_2$ | 7.0 | 92 | 68 | 94 | 0.63 | Sharma *et al.*, 1994 |

Tablo 4. Çeşitli tek kristal metal yüzeylerinde hidrojen yapışma katsayıları (Savargaonkar *et al.*, 1998)

| Yüzey | Sıcaklık (K) | Hidrojen kaplanma oranı | Yapışma katsayısı | Kaynak |
|---|---|---|---|---|
| Pt (111) | 150 | 0.0 | 0.06 | Seebauer *et al.*, 1988 |
| | | 0.4 | 0.00 | |
| | – | 0.0 | 0.016 | Lu ve Rye, 1974 |
| Pt (100) | – | 0.0 | 0.07 | Lu ve Rye, 1974 |
| Pt (211) | – | 0.0 | 0.14 | Lu ve Rye, 1974 |
| Pt (110) | – | 0.0 | 0.33 | Lu ve Rye, 1974 |
| Pt Filament | 189 | 0.0 | 0.13 | Norton ve Richards, 1974 |
| | | 0.4 | 0.017 | Norton ve Richards, 1974 |
| | 350 | 0.0 | 0.06 | Norton ve Richards, 1974 |
| | 273 | 0.4 | 0.4 | Lisowski, 1988 |
| | 298 | 0.4 | 0.0 | Lisowski, 1988 |
| | – | 0.0 | 0.0045 | Procop ve Volter, 1972 |
| | – | 0.0 | 0.1-0.16 | Lisowski, 1988 |

### 2.1.5. Seçici CO oksitlenmesi tepkimesi:

Seçici karbon monoksit oksidasyonu reaksiyonu, yakıt pilleri teknolojisi açısından çok önemli bir reaksiyondur. Hidrojen, polimer elektrolit membran yakıt pillerinde (PEMFC) yakıt olarak kullanılmaktadır. Hidrojen yaygın olarak hidrokarbonların kısmi oksidasyon veya oto-termal riformlama yöntemleri ile elde edilmektedir. Riformlama sonucunda açığa çıkan gazda önemli ölçüde karbon monoksit(CO) bulunmaktadır. CO molekülleri yakıt pilleri anotlarındaki Pt katalizörlerle çok güçlü etkileşime girdiklerinden bir süre sonra elektrot

katalizörlerinin yüzeyleri ağırlıkla CO kaplanmakta ve bu da elektrotların zehirlenmesi olarak adlandırılmaktadır. Karbon monoksit'in yakıt piline beslenecek gazdaki konsantrasyonunu düşürebilmek için su gaz kaydırma (water gas shift) reaksiyonu kullanılmaktadır. Bu sayede çıkan gaz hidrojen açısından daha da zenginleşirken, karbon monoksitin konsantrasyonu ise toplam gazın hacminin 1%'ine kadar düşmektedir. Ancak, PEMFC yakıt pillerinin anotlarında platin metalinin kaldırabileceği karbon monoksit derişiminin 10 ppm olması nedeni ile hazırlanan gazların ek bir reaktörde tercihan CO'yu oksitleyen bir katalizör üzerinden geçirilmesi gerekmektedir. Bu gereksinimden ötürü, hidrojen gazı varlığında seçici karbon monoksit oksidasyonu reaksiyonuna en uygun katalizörün araştırılması güncel bir problem olarak yaygın bir şekilde incelenmektedir. Bu konuda başarılı bir katalizör üretebilmek için katalizörün sağlaması gereken koşullar: (i) karbon monoksit oksidasyonu reaksiyonu açısından aktif olması; (ii) istenmeyen hidrojen oksidasyonu reaksiyonuna karşı olarak fazlasıyla seçici olması(ideal olarak hidrojen oksidasyonuna aktif olmaması) şeklinde sıralanabilir.

## 2. 2 Yöntem:

Bu proje kapsamında hem projenin başında hedeflenen değerli metaller üzerinde karbon monoksit oksidasyonu reaksiyonunun yapısal duyarlılık gösterip göstermediği doğrultusundaki çalışma hipotezi hem de seçici karbon monoksit oksidasyonu reaksiyonu perspektifleri sınanmıştır. Projenin daha önce öngörülmeyen ikinci kısmının gündeme alınması öncelikle değerli metaller üzerindeki adsorplanma hızlarının yapısal duyarlılığı ispatlanmış olan (Savargaonkar *et al.*1998; Kumar *et al.*, 2000) hidrojen adsorplanmasının katalizörlerin yapısal değişikliğinin bir ölçeği olarak kullanılması kararı ile başlamıştır. Daha sonra hidrojen ve karbon monoksitin bir arada bulunduğu ve seçici oksitlenme reaksiyonunun güncel bir problem olması nedeni ile elde edilen sonuçların her iki amaca yönelik kullanılabilmesi için çalışma metodolojisi kısmen proje başvurusunda öngörülen metodolojiden daha farklı bir seyir alacak şekilde değiştirilmiştir.

### 2.2.1 Deney düzenekleri:

#### 2.2.1.1 Kimyasal tepkime ölçüm düzeneği:

Orta Doğu Teknik Üniversitesi araştırma ve eğitim fonlarından sağlanan kaynaklarla kurulmuş olan bu düzenekte en fazla 200 ml/dak debi ile 100 ila 1000 mg katalizörün

sınanabildiği, 1200 °C sıcaklığa kadar çıkabilen sıcaklık programlı bir fırın ve tepkime gazlarının doğrudan örneklenerek gaz analizine gönderilebildiği bir gaz kromatografi ve örnekleme sisteminden oluşmaktadır. Bu sistemle ilgili ayrıntılar, gurubumuzda gerçekleştirilmiş Yüksek Lisans Tezleri (Dernaika, 2001; Kaya, 2002; Demirkol,2002; Özen, 2001; Oran, 2001) ve yayınlarda (Özen and Uner, 2001, Dernaika and Uner, 2003, Mbaraka and Uner, 2003) bulunabilir.

### 2.2.1.2. Kimyasal adsorplanma ölçüm düzeneği:

Bu düzenek MİSAG 96 kodlu TÜBİTAK projesinin sağladığı kaynaklarla kurulmuş, ve gurubumuzda yapılan çalışmalarda ana katalizör karakterizasyonu cihazı olarak kullanılagelmektedir. Bu cihazla ilgili detaylar MİSAG 96 kodlu proje raporunda ve ilgili yüksek lisans tezlerinde bulunmaktadır (Tapan, 1999; Ozen, 2001).

### 2.2.1.3 Adsorplama ısısı ölçüm düzeneği:

Bu deney düzeneği kısmen Devlet Planlama Teşkilatı ileri araştırma projeleri desteği kullanılarak kısmen de MİSAG 188 aracılığı ile sağlanan kaynaklardan alınmıştır. Cihazın ana bileşeni SETARAM C-80 Tian-Calvet Mikrokalorimetre DPT desteği ile alınmış, cihazın vakumlu ortamlarda çalışabilmesini sağlamak üzere ilgili basınç ölçer ve vakum pompaları MİSAG 188 kaynakları kullanılarak tedarik edilmiştir. Bu amaçla alınan soğuk katot tipi basınç ölçerin tasarımı gereği gaz değişikliğinde kalibrasyona gereksinim duyması nedeni ile MİSAG 96 ödeneği ile alınan basınç ölçerlerden 10 mm Hg sınırındaki basınç ölçer kimyasal adsorplanma düzeneğinden bu düzeneğe aktarılmıştır. Kimyasal adsorplanma düzeneğinde ise sadece 1000 mm Hg duyarlılığındaki basınç ölçerle kullanılmaya devam edilmiştir. 2003 yılında Orta Doğu Teknik Üniversitesi tarafından sağlanan kaynaklarla bu düzeneğe de Baratron tipi basınçölçerler alınarak cihazlar arası basınçölçer paylaşımı ortadan kaldırılmıştır. Şekil 1'de bu düzeneğin şematik bir çizimi verilmektedir.

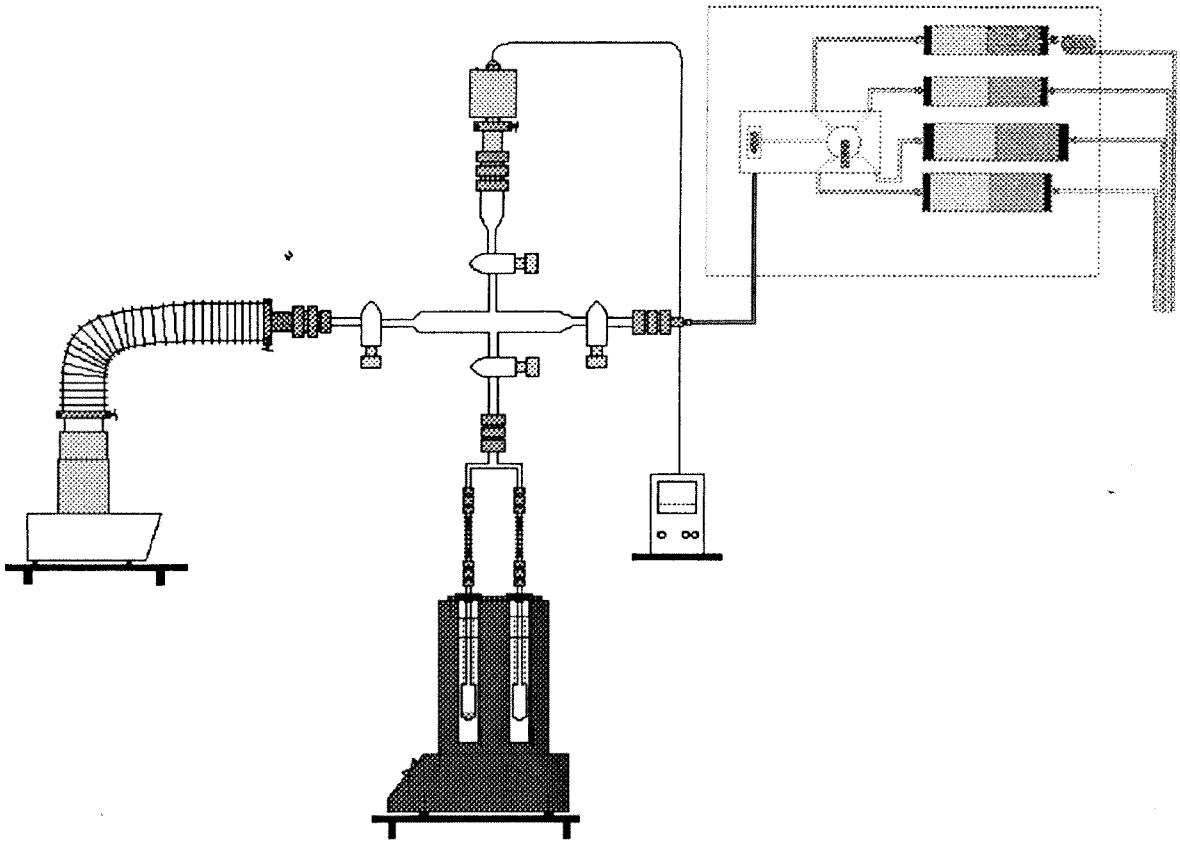

Şekil 1. Adsorplanma kalorimetresi düzeneği

**2.2.1.4 Sıcaklık programlı desorplanma düzeneği:**

Bu ünite devreye en geç alınabilen ünite olmuştur. Yaşanılan sorunlar kaynak yetersizliği ile tedarik edilemeyen bilgisayar ve kütle akım kontrol cihazlarından kaynaklanmıştır. Veri akışını sağlamak üzere kullanılan bilgisayar 2003 yılında Orta Doğu Teknik Üniversitesi kaynakları kullanılarak tedarik edilmiş, ancak kütle akım kontrolü cihazlarının tedariki mümkün olamamıştır. Bu nedenle, ölçümlerde gerekli hassasiyeti sağlamak ancak tepkime düzeneğindeki kütle akım kontrol cihazlarının dönüşümlü olarak kullanılması ile gerçekleşmiştir. Bu sistemde kullanılan sıcaklık programlı fırın MİSAG 96 kaynakları kullanılarak tedarik edilmiş olan fırındır. Sistemin ilk devreye alınmasından sonra yüksek basınçlı tepkime gazlarının RGA vakum sistemine verilmesi için kullanılan adaptörün tasarımının birkaç defa değiştirilmesi gerekmiştir. Orjinal bağlantı parçası esas alınarak yapılan tasarımda adaptör iç hacminin çok yüksek olması örneklemede ciddi ölü zamanlar yaratmıştır (Şekil 2.a). 20 dakikaya varan bu ölü zamanların giderilmesi için parçanın hacmi küçültülmüş (Şekil 2.b) ancak sorun yine de giderilememiştir. Bu nedenle örneğin giriş ve

çıkış yönlerinin değiştirilmesi kararlaştırılmış ve bakır ve pirinç parçalardan Şekil 3'de gösterilen parça imal edilmiştir. Bu şekilde cihazın örnekleme tepki süresi 30 saniye mertebelerine indirilebilmiştir.

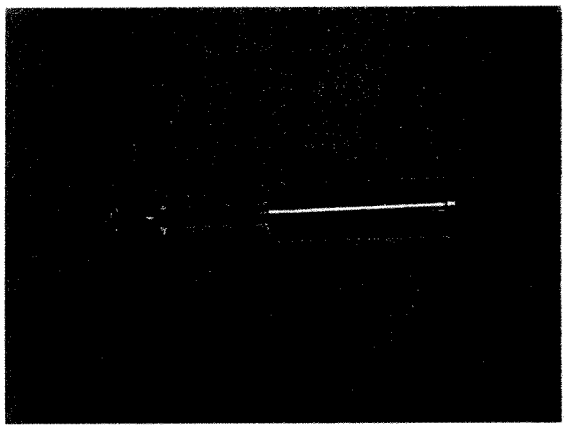

Şekil 2 a Örnekleme adaptörü: ilk tasarım

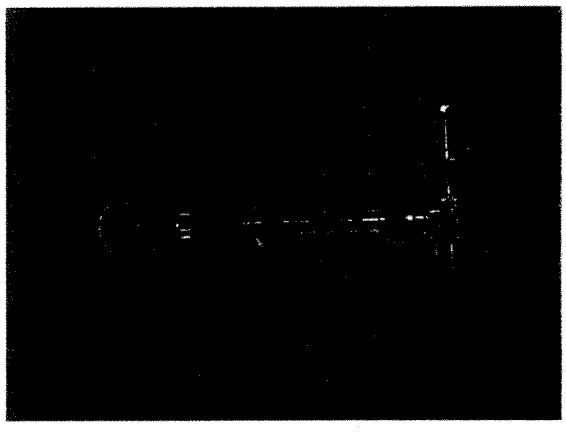

Şekil2.b Örnekleme adaptörü: ikinci tasarım

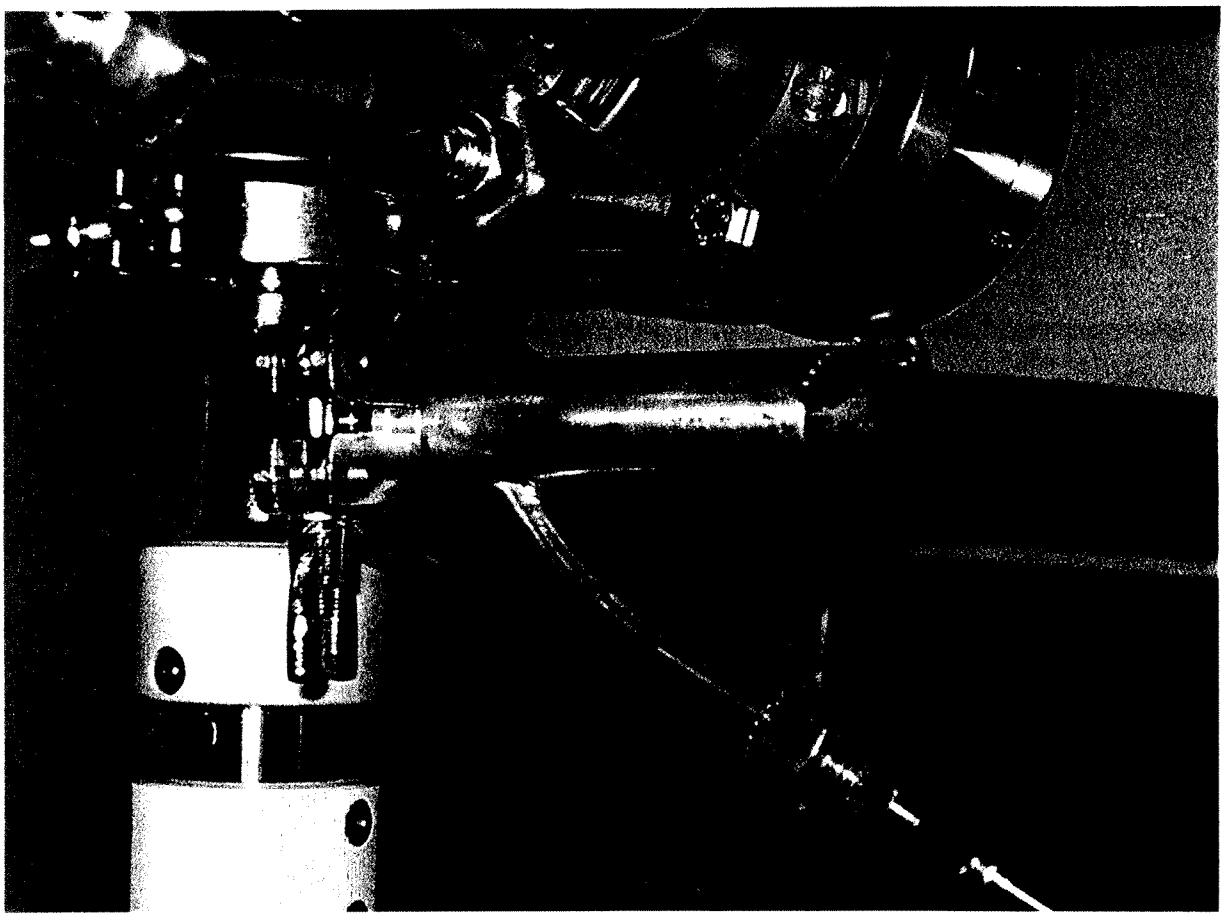

Şekil 3. Örnekleme adaptörü: halen kullanılan tasarım

### 2.2.2. Katalizörler ve hazırlama yöntemleri:

Bu proje kapsamındaki deneysel çalışmada 2%Pt/γ-$Al_2O_3$ katalizörü ıslaklık başlangıcı metoduyla tetraammine platinum (II) klorit $Pt(NH_3)_4Cl_2.H_2O$ (Johnson Matthey) tuzunun gerekli miktarını saf suda çözerek elde edilen çözeltinin γ-$Al_2O_3$ (Johnson Matthey) ile karıştırılmasıyla hazırlanmıştır. Bu karışım Pt metalinin γ-$Al_2O_3$ gözeneklerine difüzyonu için oda sıcaklığında bir gece bekletilmiştir ve ardından 400 K de iki saat bekletilerek kalan suyunda uçması sağlanmıştır. Hazırlanan katalizör dörde ayrılmış ve her örnek farklı sıcaklıkta kalsine edilmiştir. Kalsinasyon sıcaklıkları 683K, 723K, 773K ve 873K dir. Elde edilen katalizörler farklı sıcaklıklarda kalsine edilerek metal parçacık büyüklüğü değiştirilmiştir. Bu yapıdaki katalizörün ortalama metal dağılım oranı hacimsel hidrojen adsorplama yöntemi kullanılarak belirlenmiştir.

İkili metal katalizörler $Pt(NH_3)_4Cl_2.H_2O$ (Johnson Matthey), $PdCl_2$ (Johnson Matthey) ve $Pd(NO_3)_2$ (Johnson Matthey) tuzları kullanılarak hazırlanmıştır. $PdCl_2$ (Johnson Matthey)

tuzu kullanıldığında ikili metal katalizörler birlikte empregnasyon yöntemi ile $Pd(NO_3)_2$ (Johnson Matthey) tuzu kullanılıdığında ise sıralı empregnasyon yöntemi ile hazırlanabilmiştir. İkinci durumda Pt ve Pd tuzları empregransyon öncesi çökeldiklerinden sıralı empregnasyon yöntemi tercih edilmiştir. Bu katalizörler de 723 K'de dört saat kalsine edildikten sonra kullanım öncesi hidrojen ortamında indirgenmişlerdir.

$CeO_2$ destekli katalizörleri hazırlamak için $CeCl_3.XH_2O$ (Johnson Matthey) ve $Ce(C_2H_3O_2)_3.1.5H_2O$ (Johnson Matthey) tuzları kullanılmıştır. Bu tuzların 873 K sıcaklıkta dört saat kalsinasyonu sonucunda $CeO_2$ oluşumu sağlanmış ve XRD ile de teyit edilmiştir.

### 2.2.3. Deneysel yöntemler:

#### 2.2.3.1. Tepkime deneyleri:

Tepkime deneyleri, fakir, zengin ve stokiyometrik CO ve $O_2$ karışımları azot, kuru hava ve karbon monoksit'in kütle akım kontrol cihazlarından geçirilerek karıştırılmasından sonra elde edilen gaz karışımları kullanılarak kütle ve ısı aktarımı kısıtlamalarının olmadığı test edilmiş koşullarda yapılmıştır. Öncelikle hazırlanan katalizörler 100 mg katalizör 900 mg $Al_2O_3$ ile karıştırılarak quartz cam tüpler içinde sıcaklık kontrollü tüp fırının içine yerleştirilmiştir. Gaz karışımındaki oksijen CO oranı stokiyometrik ayarlandığında 5% CO ve 2.5% oksijen mevcuttur. Gazın akış hızı 200 ml/dak olarak sabit tutulmuştur. Karbon monoksit, kuru hava ve azottan oluşan gaz karışımı tepken olarak kullanılmış ve CO oksidasyon reaksiyonu sonucu çıkan ürünler gaz kromotografı yardımı ile ölçülmüştür. RGA ünitesinin devreye alınmasından sonra bu deneylerin bir kısmı yatışkın hal ortamında RGA kullanılarak gerçekleştirilmiştir. Gaz kromatografının hidrojen duyarlılığının yetersiz olması nedeniyle seçici hidrojen oksitlenmesi deneyleri tamamen RGA sistemi kullanılarak çalışılmaktadır.

#### 2.2.3.2 Adsorplanma ısısı ölçüm deneyleri:

Adsorplanma ısısı ölçüm deneyleri Şekil 1'de gösterilen düzenekte yapılmıştır. Bu düzenekte erişilebilecek en yüksek sıcaklığın 573 K olması nedeni ile önceden indirgenmiş 500 mg ila 1 g arasında tartılmış katalizörler örnek hücresine yerleştirilmekte, referans hücresi boş olarak deney düzeneğine monte edilmektedir. Bu düzenekte 573K sıcaklıkta hidrojen ortamında katalizörler yaklaşık iki saat indirgendikten sonra basınç $10^{-5}$ Torr'a ininceye kadar vakum uygulanmaktadır. Yüzeyde adsorplanmış maddelerin tamamen desorplandığı varsayılan bu basınç düzeyinde sistem 303 K sıcaklığa çekilerek adsorplanma ısıları ve miktarları

ölçülmektedir. Kalorimetre cihazı ile adsorplanma ısıları ölçülürken volümetrik olarak adsorplanmış gaz miktarları belirlenmekte ve her bir ölçümde bu iki değerin oranı diferansiyel adsorplanma ısılarını vermektedir.

Adsorplanma ısısı ölçümü için kullanılan düzenekte ilk olarak Full Range Cold Cathode Gauge basınç ölçer kullanılarak deneyler yapılmış fakat bu deneylerin bir çoğunda adsorplanan gazın miktarında tutarsızlık ve gazın türüne bağımlı ölçüm yapmasından dolayı hatalar oluşmuştur. Bu sorunlardan kurtulmak için kullanılmakta olan basınç ölçer (Cold Cathode Gauge), gazın türüne bağımlı ölçüm yapmayan ve kalibrasyonsuz kullanılabilen Baratron Gauge ile değiştirilmiştir. Böylelikle gaz basınç ölçümleri hatalardan arındırılmıştır. Sistemde kullanılan bağlantı noktalarındaki sızdırmazlık parçalarının da (O-ring) yenilenmesiyle sağlıklı ölçüm alınmaya başlanmıştır.

## 2.3. Bulgular ve Tartışma

### 2.3.1. Yapısal duyarlılık çalışmaları:

#### 2.3.1.1 Tepkime deneyleri:

Öncelikle karbon monoksit oksidasyonu reaksiyonun yapısal duyarlılığı incelenmiştir. Bu nedenle öncelikle dört değişik katalizör hazırlanmıştır. 2% platinyum katalizörü hazırlandıktan sonra 410, 450, 500 ve 600$^0$C derecelerde dört saat boyunca kalsine edilmiş dört katalizör elde edilmiştir. Bu katalizörlerin metal dağılım oranları hacimsel hidrojen adsorplama yöntemi kullanılarak belirlenmiştir. 450 $^o$C sıcaklıkta kalsine olmuş katalizörün hacimsel adsoprlanma sonuçları Şekil 4'te tüm katalizörlerin toplam, zayıf ve güçlü hidrojen adsorplanma oranları ise Tablo 5'te verilmektedir.

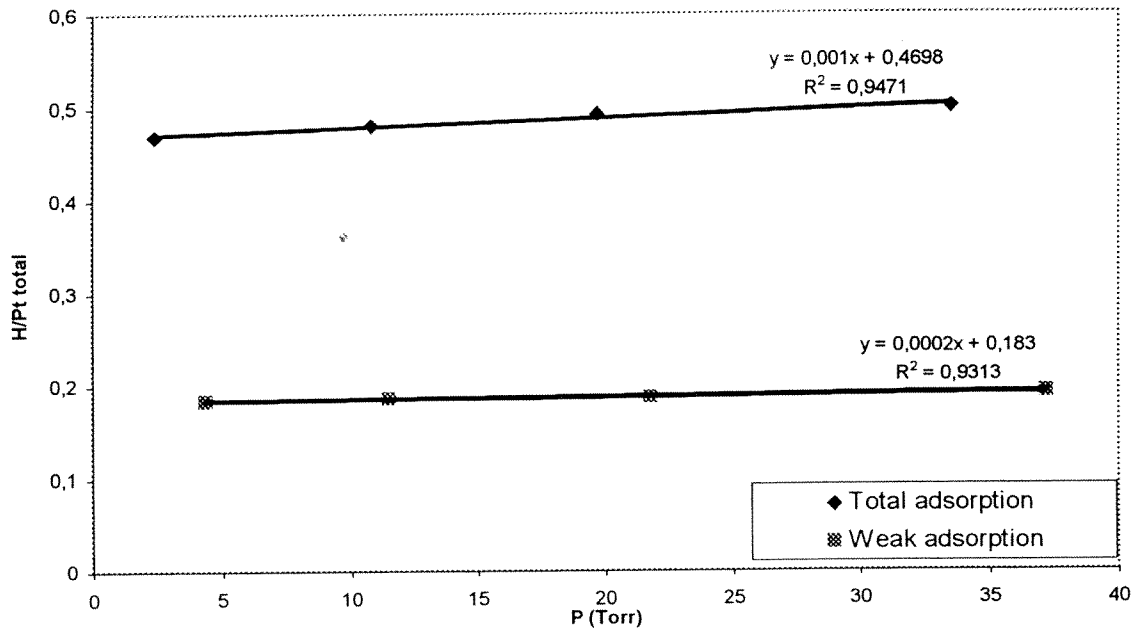


Şekil 4. 450°C de kalsine olmuş 2%Pt/γ-$Al_2O_3$ katalizörü için hidrojen adsorplanma isotermi

Tablo 5. Farklı sıcaklıklarda hazırlanmış 2%Pt/γ-$Al_2O_3$ katalzörlerinin toplam, zayıf ve güçlü adsorplanma değerleri

| Kalsinasyon sıcaklığı (°C) | Toplam Adsorplanma ($H/Pt_{toplam}$) | Zayıf Adsorplanma ($H/Pt_{toplam}$) | Güçlü Adsorplanma ($H/Pt_{toplam}$) |
|---|---|---|---|
| 410 | 0,83 | 0,20 | 0,63 |
| 450 | 0,47 | 0,18 | 0,29 |
| 500 | 0,26 | 0.06 | 0,20 |
| 600 | 0,09 | 0,05 | 0,04 |

Dört değişik sıcaklıkta kalsine edilmiş (410, 450, 500, 600$^0$C) 2% Pt/γ-$Al_2O_3$ katalizörleri katalitik performans testine tabi tutulmuştur. Sıcaklık sabit aralıklarla arttırılarak, sıcaklığa bağlı olarak karbon monoksitin yüzde dönüşümü elde edilmiştir (Şekil 5). Yüzde dönüşümün 10%'a kadar olan kısmı göz önüne alınarak da reaksiyonun hız değerleri elde edilebilmiştir. Reaktör aslında bir dolgulu yatak reaktörü olmasına rağmen 0-10% yüzde dönüşüm bölümü dikkate alınarak bu reaktörün diferansiyel reaktör gibi davrandığı varsayımıyla reaksiyon

hızları kolayca hesaplanabilmiştir. Böylece her yüzde dünüşüm değerine göre reaksiyon hızı hesaplanmıştır.

Aktivasyon enerjisi değerleri, reaksiyon hızının üstel bir fonksiyon ve hız sabitinin Arrhenius denklemine uygun olduğu varsayımına göre hesaplanmıştır. Denklemin iki tarafının doğal logaritmaları alınarak, reaksiyon hızının doğal logaritmasının sıcaklığa ters orantılı olduğu bir denklem elde edilmiştir. Böylece ln(hız)'a karşılık olarak 1/T grafiğini çizerek (Şekil 6), bu grafiğin eğiminden aktivasyon enerjisi heasaplanmaktadır. Dört farklı katalizör için elde edilen aktivasyon enerji değeri Tablo 6'te gösterilmiştir.

Katalizörlerin devri-daim sıklıkları ise reaksiyon hızları ve metal parçacığının yüzey dağılım oranı kullanılarak hesaplanmıştır. Öncelikle bir gram katalizördeki metal ağırlık oranı, platinyumun moleküler ağırlığı ve yüzey dağılım oranı kullanılarak bir gram metaldeki aktif sitelerin sayısı hesaplanmıştır. Daha sonra reaksiyon hızının aktif site yoğunluğuna oranı alınarak katalizörlerin devri-daim sıklıkları elde edilmiştir (Şekil 7).

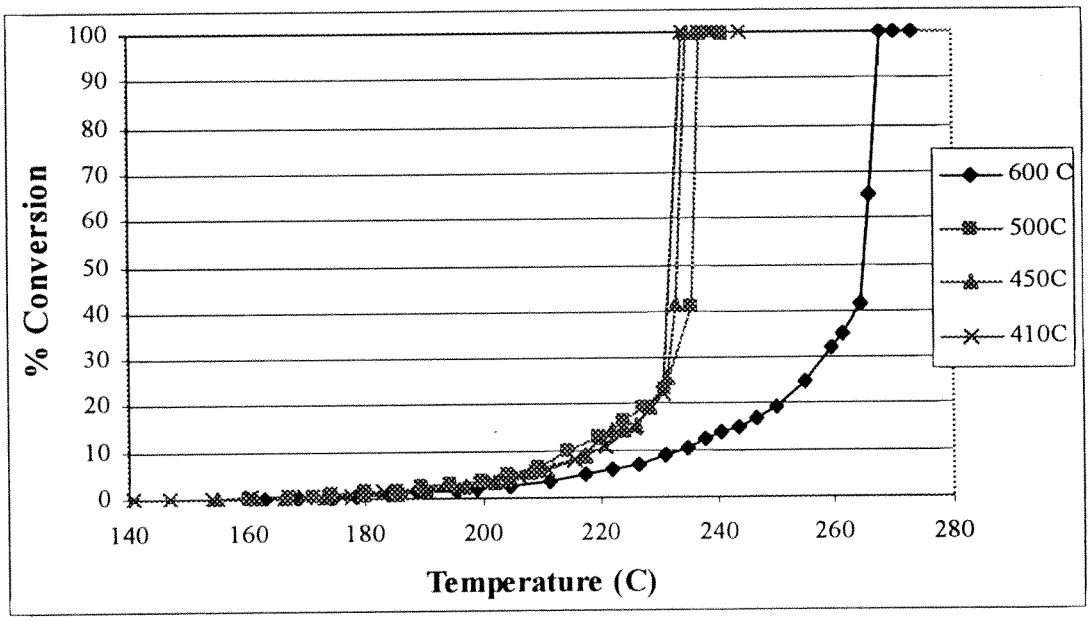


Şekil 5. 410°C, 450°C, 500°C ve 600°C de kalsine edilmiş 2%Pt/$\gamma$-$Al_2O_3$ üzerine CO oksitlenmesi tepkimesinin sıcaklıkla gerçekleşme oranını değişimi.

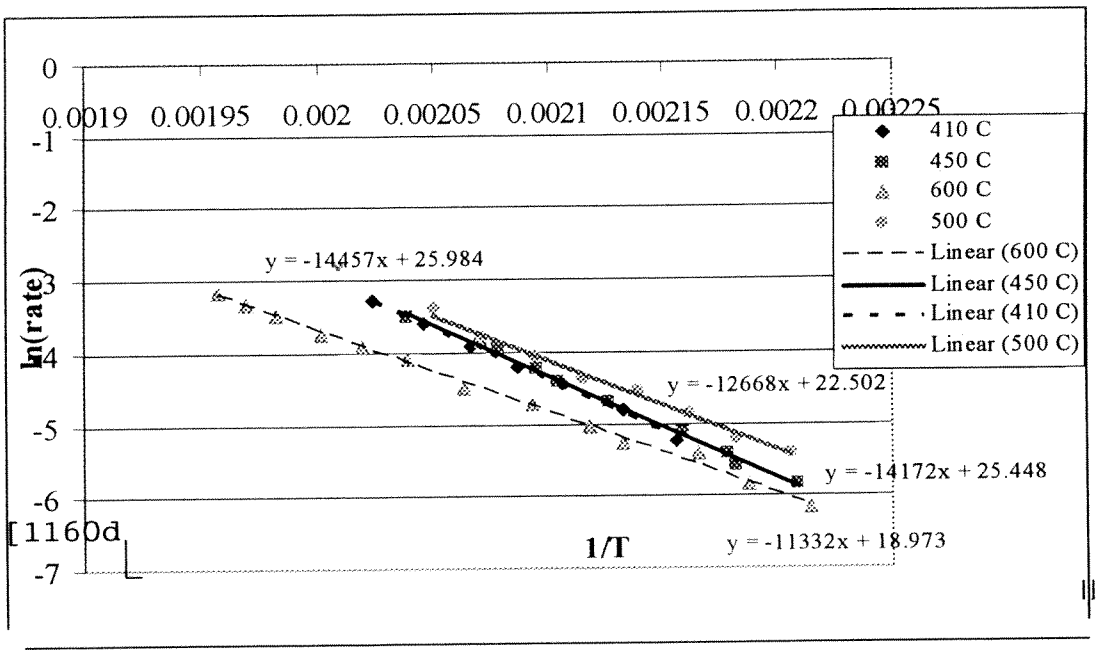


Şekil 6. 410°C, 450°C, 500°C ve 600°C de kalsine edilmiş 2%Pt/γ-$Al_2O_3$ üzerinde CO oksidasyon tepkime hızının 1/T ye göre değişimi.

Tablo 6. Farklı sıcaklıklarda kalsine edilmiş 2%Pt/γ-$Al_2O_3$ katalizörlerinin üzerinde gerçekleşen CO oksidasyonu tepkimesinin aktivasyon enerjileri.

| **Sıcaklık (°C)** | **Ea (kJ/mol.K)** |
|---|---|
| 410 | 120,2 |
| 450 | 117,8 |
| 500 | 105,3 |
| 600 | 94,2 |

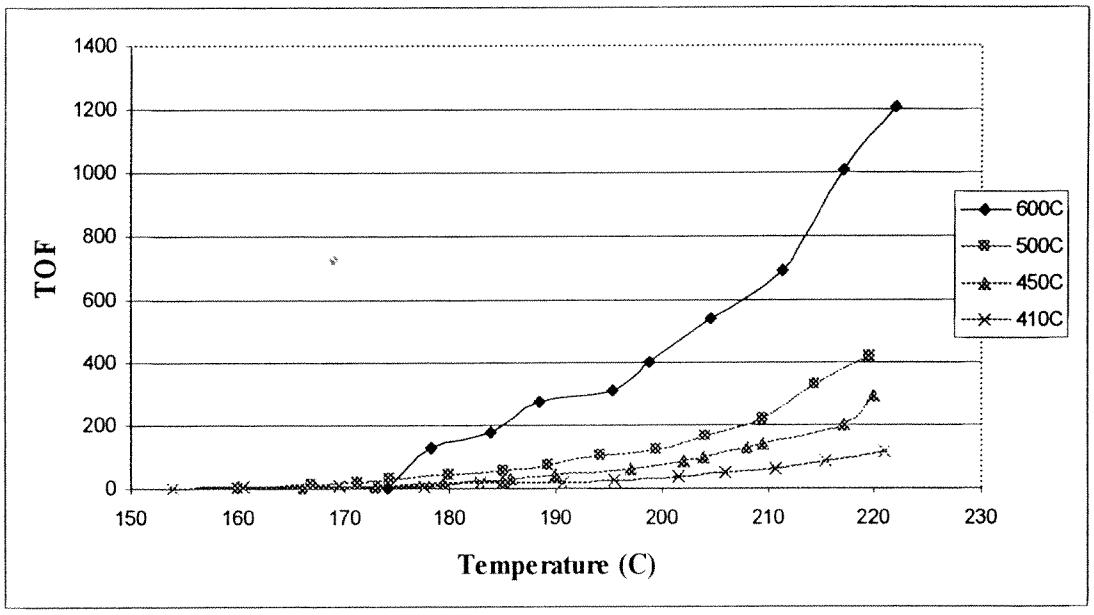


Şekil 7. 410°C,450°C, 500°C ve 600°C' de kalsine edilmiş 2%Pt/γ-$Al_2O_3$ üzerinde CO oksidasyon tepkimesinin devir-daim sıklığının sıcaklığa göre değişimi.

Elde edilen tepkime deneyleri sonucunda karbon monoksit oksitlenmesi tepkimesinin yüzeyin yapısına bağımlı olarak değişim kaydettiği kesin olarak görülmüştür. Daha önce de belirtildiği gibi aktif metal parçacık büyüklüğü kalsinasyon sıcaklığının arttırılmasıyla değiştirilmiş ve yüzey metal dağılımıyla belirlenmiştir. Metal parçacık büyüklüğündeki değişim ise gazla etkileşimde olan yüzeylerinin oranının değişmesine neden olmaktadır. Daha büyük parçacıklarda düzlem yüzeylerinde olan atomların, kenar ve köşe atomlarına göre oranı artmaktadır. Toplam katalizör yüzeyine bakıldığında ise metal parçacıklarının büyümesi sonucunda gaz ile temas etmeyen ve parçacık yapısının içinde kalan metal miktarı artarak yüzeydeki toplam aktif merkez sayısı azalmaktadır. Bu tespitler ışığında elde edilen deneysel sonuçlar irdelenmeye çalışılacaktır.

**a.** Farklı sıcaklıklarda hazırlanmış Pt/γ-$Al_2O_3$ katalizörleri üzerinde gerçekleşen karbon monoksit oksitlenmesi tepkimesinin sıcaklık ile değişimi Şekil 5'te verilmiştir. Bu grafikte görüldüğü üzere karbon monoksit oksitlenmesi tepkimesi farklı katalizörlerde farklı alevlenme (light-off) ve tamamlanma sıcaklıkları göstermektedir.

**b.** Bu tepkime testleri deneysel çalışma bölümünde belirtildiği gibi mikro reaktör analiziyle incelenmiş ve bunun sonucunda aktivasyon enerjileri Tablo 6'te verilmiştir. Tabloda görüldüğü gibi kalsinasyon sıcaklığı arttıkça aktivasyon enerjisi düşmektedir.

**c.** Tepkime testlerinin devir-daim sıklığı incelemesi (Şekil 7) sonucunda görülmüştür ki aktif metal parçacık büyüklüğünün artmasıyla devir-daim sıklığı artmıştır.

Yukarıdaki üç sonuç bir biriyle ilintili olarak açıklanabilir. Metal parçacık büyüklüğü arttıkça devir-daim sıklığının artması, aktifleşme enerjisindeki azalma ile açıklanabilir. Bunun sonucu olarak mevcut olan sitelerin aktifliğinin artması gözlemlenmiştir. Aynı zamanda büyük metal parçacıklarının daha yüksek sıcaklıklarda alevlenme göstermesi ise toplam site sayısındaki azalmadan dolayıdır.

### 2.3.1.2. Adsorplanma ısısı ölçümleri:

Yüzeyde adsorplanan CO'nun adsorplanma ısısı ve bu ısının yüzeyin kaplanma oranıyla değişimi CO/metal sitemi hakkında temel bilgiler verir. Adsorplanma ısısı yüzeyde dengedeki absorplanma noktalarının kaplanma oranlarının niteliğini belirler. Ama bu konu destekli katalizörlerde deneysel zorluklardan ötürü çok nadir olarak çalışılmıştır. Bu konuyu inceleyebilecek metotlardan sıcaklık-programlı desorplanma (TPD) difüzyon ve yüzeyde tekrar adsorplanma gibi problemlerden dolayı kullanım bulamamıştır. Adsorption mikrokalorimetresi, alternatif bir yöntem olarak gazdaki kirliliklerden (safsızlık) yada yüzeyde kalmış olabilecek diğer maddelerle reaksiyonlardan etkilenebilir (Bianchi *et al.*, 2001). Adsorplanma ısısının elde edilebildiği metotlar içinde sadece kalorimetre her hangi bir varsayıma dayanmadan doğrudan ölçüm yapmaktadır.

Literatürde bulunan adsorplanma ısısı verilerinin hemen hemen hepsi ya saf metallerde yada metal kristal yüzeylerinde ölçülmüştür. Bununla birlikte destekli katalizörlerde genellikle metal parçalarının büyüklüğü 10 nm ile 1 nm arasında değişmektedir. Katalizördeki metallerin yüzey/yığın oranı metal parçacık büyüklüğü azaldıkça artar ve böylelikle yüzeydeki metallerin yığındakilerden farklı elektronik özelliklere sahip olması beklenir. Daha da önemlisi, metallerin özellikleri destek tarafından etkilenmektedir (Vannice ve Chu, 1987). Metal kristal yüzlerinde ölçülmüş adsorplanma ısıları çok yüksek vakum ve düşük sıcaklıklarda TPD metoduyla elde edilmiştir. Bu deney koşulları gerçek hayat katalitik operasyon koşullarından çok farklıdır (Bianchi, ve Dulaurent, 2000). Literatürde yer alan sınırlı sayıdaki destekli metal katalizörler üzerindeki adsorplanma ısısı verileri (örneğin Narayan ve King, 1998; Spiewak ve Dumesic,1996) katalizörlerin atom ölçeğinde yapıları hakkında yoğun bilgiler verebilmektedir.

Bu çalışmada yapılan ilk ölçümler $TiO_2$ üzerinde desteklenmiş Pt katalizörleri üzerinde oksijen adsorplanması ısıları üzerine idi. TÜBİTAK tarafından desteklenen MİSAG 96 kodlu

projede başlanmış çalışmaların devamı niteliğinde yapılan bu ölçümlerde temiz yüzey diferansiyel adsorplanma ısıları ve doygunluk yüzey kaplanma oranları incelendiğinde metal parçacık büyüklüğü ile diferansiyel adsorplanma ısılarının ters orantılı olduğu görülmektedir (Tablo 7). Bu sonuçlar ve detaylı tartışması Uner *et al.*(2003)'de ayrıntısı ile bulunabilir. Şekil 8'den de görüleceği gibi diferansiyel oksijen adsorplanması ısıları yüzey kaplanma oranı ile düşmektedir. Ayrıca metal parçacık büyüklüğü düştükçe diferansiyel adsoplanma ısıları da yükselmektedir. Metal paçacık büyüklükleri azaldıkça düşük koordinasyon sayılı kenar ve köşe atomlarının oranının arttığı bilindiğinden, gözlemlenen bu değişiklik oksijen adsorplanmasının yapısal duyarlılığı olarak yorumlanabilir. Ancak $TiO_2$'nin katalizör hazırlama süreci sırasında kısmen indirgenebildiği ve oluşan $TiO_x$ yarı indirgenmiş moitelerinin yüksek hareketliliğe sahip olmaları nedeni ile metal parçacıklarını üzerini kapladıkları ve metallerle elektron alışverişinde bulundukları bilinmektedir. Dolayısı ile Şekil 8 ve Tablo 7'da ayrıntısı ile gösterilen verilerden bir yargıya varmadan önce göreceli olarak inert bir altlık malzeme ile bu deneyleri tekrarlamak gerekmiştir.

Tablo 7. $TiO_2$ destekli Pt katalizörleri üzerinde diferansiyel adsorplanma ısıları ve bunun metal parçacık büyüklüğü ile ilişkisi

| Pt % | BET Yüzey alanı ($m^2$/g katalizör) | Pt yüklemesi (μmol Pt/g katalizör) | Güçlü H (μmol H/g katalizör) | Güçlü H/Pt | $O_2$ doygunluk kaplanma oranı Pt (μmol/g katalizör) | Temiz yüzey diferansiyel adsoplanma ısısı (kJ/mol) |
|---|---|---|---|---|---|---|
| 0.5 | 44.5 | 51.30 | 0.86 | 0.03 | 1.5 | 320 |
| 1.0 | 44.5 | 51.30 | 6.36 | 0.12 | 3.0 | 380 |

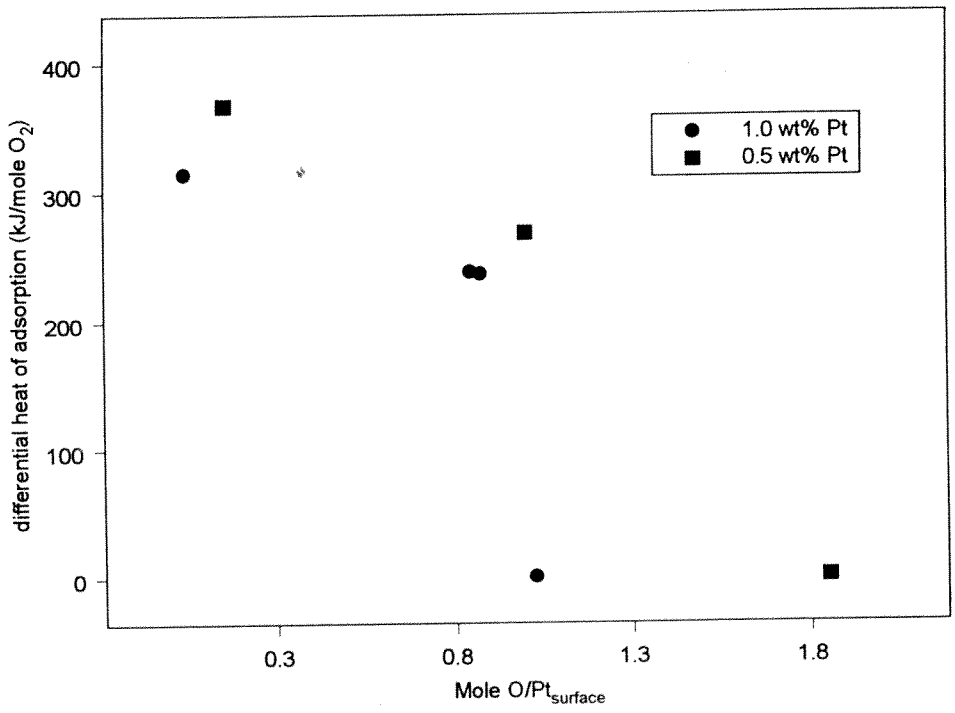


Şekil 8. $Pt/TiO_2$ üzerinde oksijen adsorplanma ısısı ölçümleri

Farklı ısıl işlemlerle hazırlanmış katalizörlerin yüzeyinde $H_2$, CO ve $O_2$ gazları ayrı ayrı adsorplanmış ve yüzey kaplanma oranının değişimine göre adsorplanma ısılarındaki değişimler Şekil 9'da gösterilmektedir. Şekil 9'daki verilerden kolayca anlaşılacağı gibi düşük parçacık boyutlarında katalizör üzerinde yoğun miktarda gerçekleşen hidrojen adsorplanması metal paçacık büyüklüğü arttıkça düşmektedir. Ayrıca hidrojen adsorplanması enerjisi dağılımı da daha dar bir aralığa çekilmektedir. Aynı şekilde yapılan karbon monoksit ve oksijen adsorplanma ısıları ölçümleri de sırasıyla Şekil 10 ve 11'de verilmektedir. Şekil 12'de temiz yüzey adsorplanma ısıları gösterilmektedir. Temiz yüzey adsoplanma ısıları adsorban katalizör arasındaki ilk etkileşimin işareti olduğundan, yapıdaki elektronik değişimlerin de bir göstergesi olarak kullanılabilir. Bu veriler incelendiğinde hidrojen'in temiz yüzey diferansiyel adsoplanma ısısında artan kalsinasyon sıcaklığı, yani artan parçacık büyüklüğü ile bir düşme olduğu, yine Şekil 9'dan da görülebileceği gibi doygunluk kaplanma oranları da kalsinasyon sıcaklığı ile belirgin bir şekilde düşmektedir.

Hidrojen gazının adsorplanmasının yapısal duyarlılığı konusu literatürde kabul gören bir gerçektir (van Der Viel *et al.* ,1999; Kumar *et al.* ,2000; Savargaonkar *et al.* ,1998). Bu çalışmanın sonuçları da bu bulguları hem teyid etmiş, hem de katalizördeki yapısal değişiklikleri dolaylı olarak ölçme imkanı olmuştur.

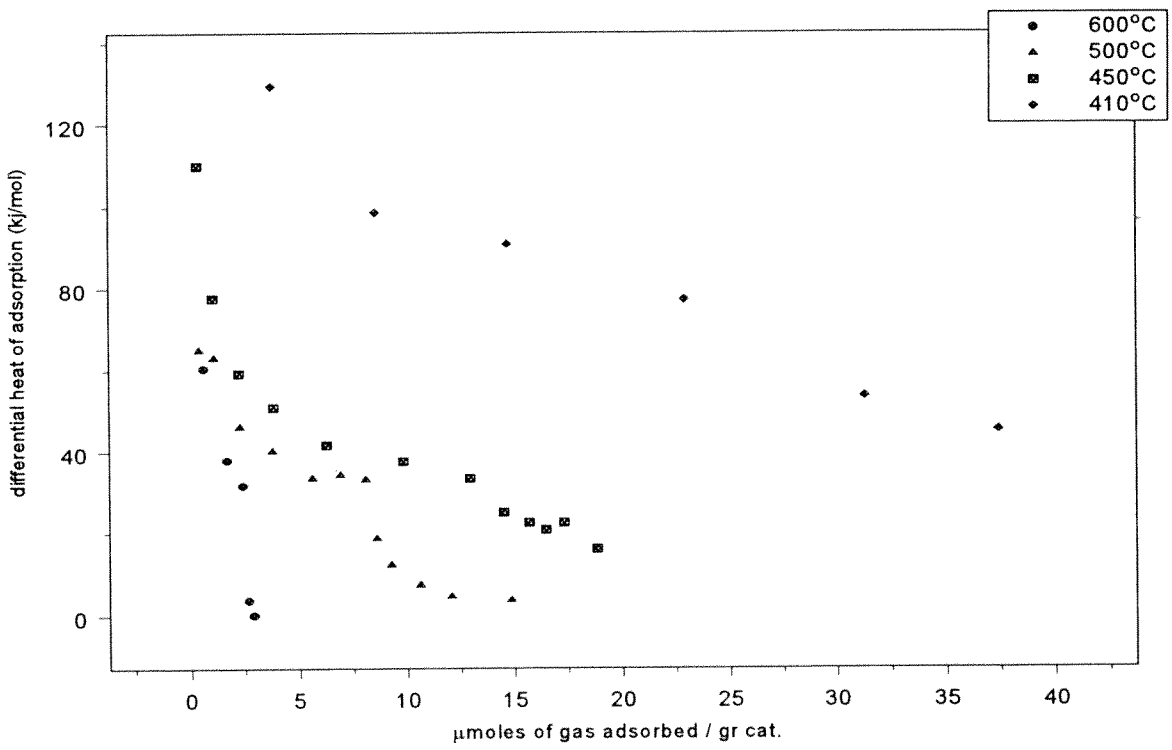


Şekil 9. 410, 450, 500 ve 600°C'de kalsine olmuş 2%Pt/γ-$Al_2O_3$ katalizörü yüzeyinde hidrojen gazı adsorplanma ısıları.

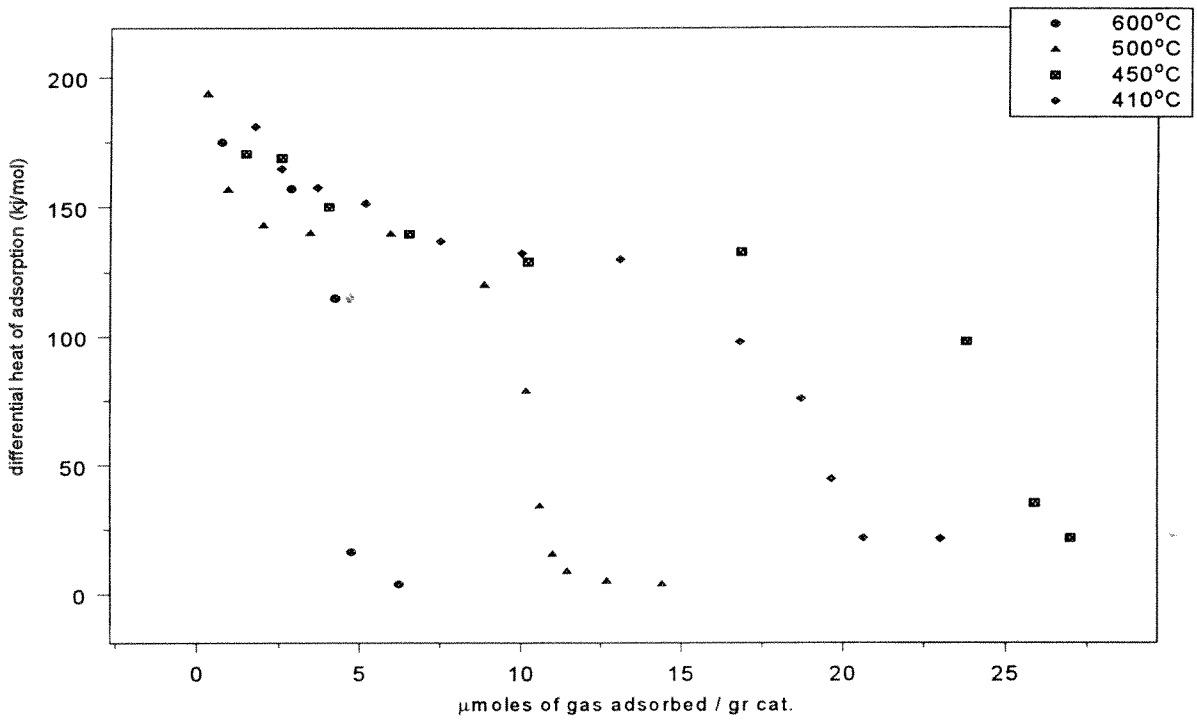


Şekil 10. 410, 450, 500 ve 600°C'de kalsine olmuş 2%Pt/γ-$Al_2O_3$ katalizörü yüzeyinde karbon monoksit gazı adsorplanma ısıları.

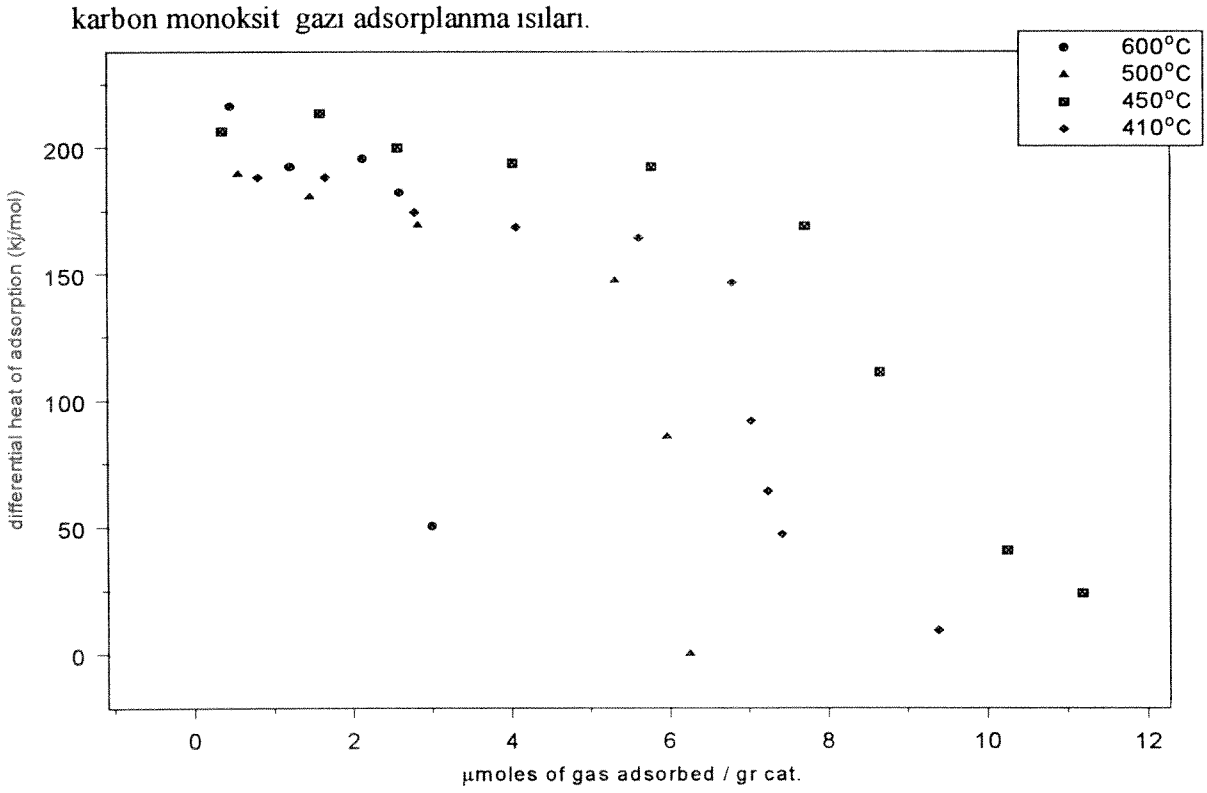


Şekil 11. 410, 450, 500 ve 600°C'de kalsine olmuş 2%Pt/γ-$Al_2O_3$ katalizörü yüzeyinde oksijen gazı adsorplanma ısıları.

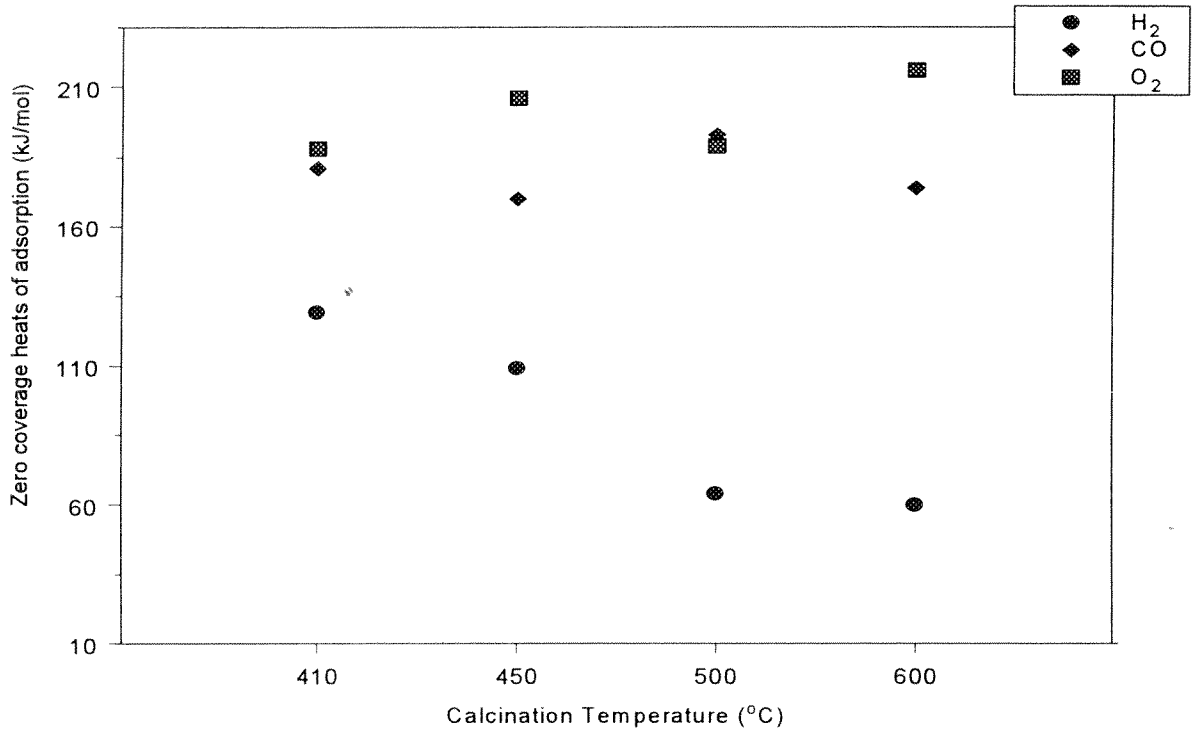


Şekil 12. Temiz yüzey adsorplanma ısılarının kalsinasyon sıcaklığı ile değişimi

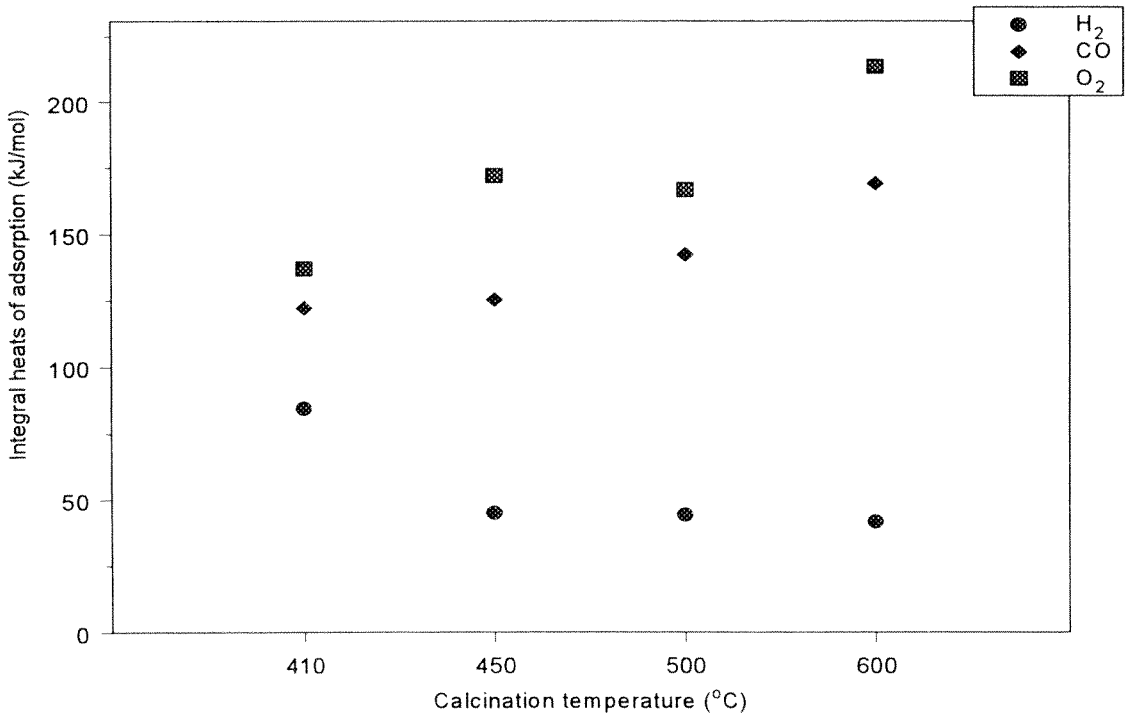


Şekil 13. İntegral adsorplanma ısılarının kalsinasyon sıcaklığı ile değişimi

Hidrojen adsorplanma ısıları ile karbon monoksit ve oksijen adsorplanma ısıları grafiklerinde 410 °C sıcaklıkta kalsine edilmiş katalizörün davranışında bir değişiklik olduğu ve doygunluk kaplanma oranlarının 450 °C sıcaklıkta kalsine edilmiş katalizörün doygunluk kaplanma oranlarının altına düştüğü Şekil 11 ve 12'den de görülebilir. Bu katalizör üzerinde hidrojen adsorplanmasından sonra gerçekleşen bir bozunmadan olduğu düşünülmekte, ancak yeterli miktarda taze katalizör bulunmadığından bu deneyler tekrarlanamamıştır. Bu günlerde yeni katalizör hazırlayarak bu ölçümlerin tekrarlanması planlanmaktadır.

İntegral adsorplanma ısıları diferansiyel adsorplanma ısısı eğrilerinin boyutsuz yüzey kaplanma oranına karşı çizildiği grafiklerin altındaki alanlar hesaplanarak bulunur. İntegral adsorplanma ısılarının parçacık büyüklüğüne göre değişimi ilginç bir sonuç göstermektedir (Şekil 13). Hidrojen gazının integral adsorplanma ısısı parçacık büyüklüğü arttıkça düşmesi hidrojen adsorplanmasının yapısal duyarlılığını göstermektedir (Savargaonkar *et al.*, 1998). Buna karşılık oksijen ve karbon monoksit'in integral adsorplanma ısıları, parçacık boyutu arttıkça yükselmektedir. Bu ters yöndeki değişim karbon monoksit seçici oksitlenmesi tepkimesinde hidrojen ve karbon monoksitin parçacık büyüklüğü arttıkça tersine bir seyir izleyeceğinin kesin bir kanıtı olmamakla beraber bir indikatörüdür. Buna ek olarak, ölçülen adsorplanma ısıları benzer katalizörler üzerinde yapılan adsorplanma ısıları ölçümleri ile benzerlik göstermesi yaptığımız ölçümlerin tekrarlanabilirliğinin bir göstergesidir (Tablo 1, 2, ve 3).

### 2.3.2. İkili metal katalizörlerde CO oksitlenmesi:

Bu çalışma kapsamında Pt-Pd ikili metal katalizörler incelenmiştir. Bu metaller egzoz emisyon kontrolünde yaygın olarak kullanılırlar. Ayrıca ikili metal ortamlarında bu katalizörlerin kükürte karşı dirençlerinin de arttığı bilinmektedir. Dolayısı ile petrol rafinerilerinde hidrojenleme ve izomerleme tepkimelerinde kullanılmak üzere bu türden ikili metal aday katalizörler geliştirilmektedir.

Bu çalışmada incelenen birlikte emdirilmiş toplam metal yükleme oranı ağırlıkça %1 olan Pt-Pd ikili metal katalizörleri, bu katalizörlerin sıcak su ile klor giderilmeden önce (yıkanmamış) ve sonra (yıkanmış) hidrojen adsorplanması yöntemi ile ölçülmüş yüzey/yığın metal atom oranları ve her bir gram katalizörde bulunan yüzey metal atom miktarları Tablo 8'de gösterilmektedir.

Tablo 8. Pt-Pd ikili metal katalizörleri ve yıkanmadan önce ve sonra hidrojen adsorplanması yöntemi ile ölçülen yüzey/yığın atom oranları

| | | Yüzeydeki atom miktarı, % | | μmol yüzey atomu/g katalizör |
|---|---|---|---|---|
| Katalizör | Pd:Pt | (yıkanmamış) | (yıkanmış) | (yıkanmış) |
| 1 % $Pt/\gamma\text{-}Al_2O_3$ | 0:1 | 70.4 | 60.8 | 31.2 |
| 1 % $Pd\text{-}Pt/\gamma\text{-}Al_2O_3$ | 1:3 | 57.8 | 39.6 | 18.3 |
| 1 % $Pd\text{-}Pt/\gamma\text{-}Al_2O_3$ | 1:1 | 52.3 | 38.3 | 27.8 |
| 1 % $Pd\text{-}Pt/\gamma\text{-}Al_2O_3$ | 3:1 | 49.1 | 23.5 | 19.6 |
| 1 % $Pd/\gamma\text{-}Al_2O_3$ | 1:0 | 47.9 | 27.9 | 26.2 |

Bu katalizörler üzerinde yapılan karbon monoksit oksitlenmesi deneylerinde elde edilen sonuçların bir kısmı Şekil 14'te gösterilmektedir.

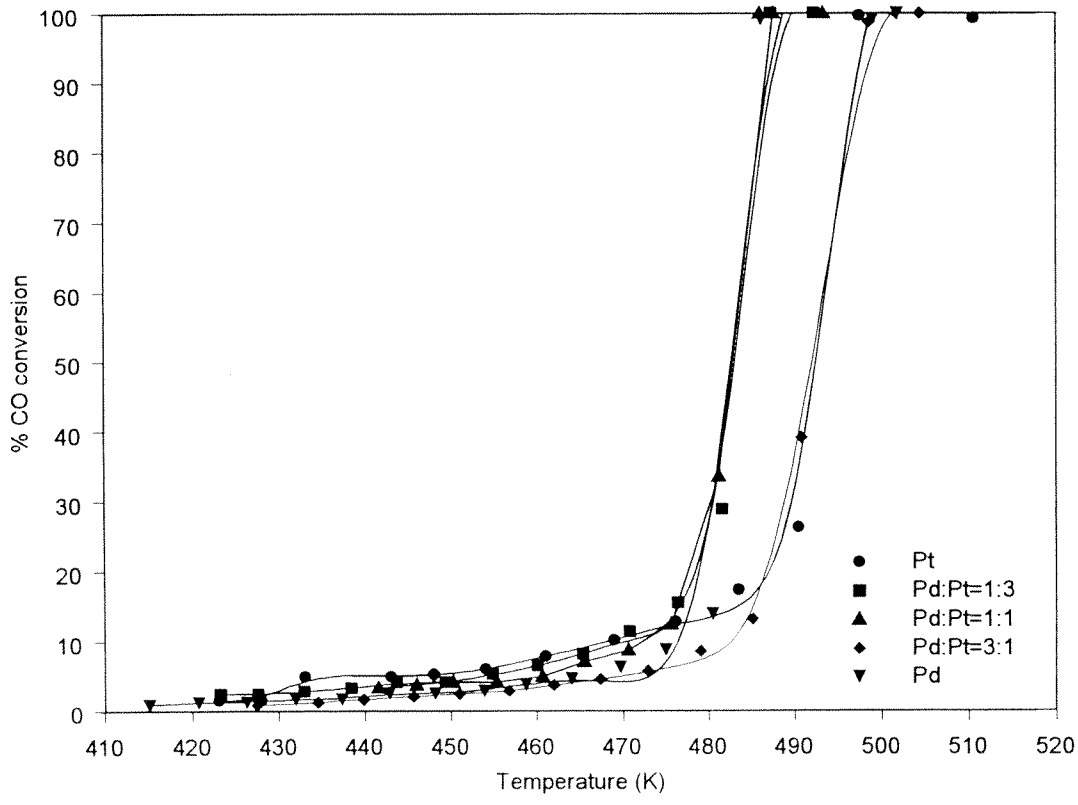

Şekil 14. Yıkanmış Pt-Pd ikili metal katalizörlerinde karbon monoksit yanma (light-off) eğrileri.

Şekil 14'ten de görüleceği gibi katalizörlerin kimyasal davranışı ağırlıkla Pd katalizörüne yakındır. Bunun temel nedeni Pt ve Pd metallerinin karışma ısılarının egzotermik olması nedeni ile bu metallerin birbirleri ile alaşım oluşturmalarıdır. Dolayısı ile her bir kataliör parçacığı Pt ve Pd içermektedir. Buna ek olarak Pd metalinin ergime noktası ve süblimleşme ısısı Pt metalinden daha düşük olduğundan, daha düşük serbest yüzey enerjisine sahiptir ve termodinamik olarak bu metal yüzeyde daha fazla bulunmayı tercih etmektedir. Bu bilgilerin doğrudan teyidi karbon monoksit oksitlenmesi tepkimesi sonucunda ortaya çıkmıştır. Bu katalizörler üzerinde yapılan ısıtma ve soğutma deneylerinde ise histeresis davranışı gözlemlenmiştir. Tüm katalizörlerde gözelmlenen bu histeresis davranışının örnek grafiği Şekil 15'te %1 $Pd/\gamma\text{-}Al_2O_3$ için verilmektedir.

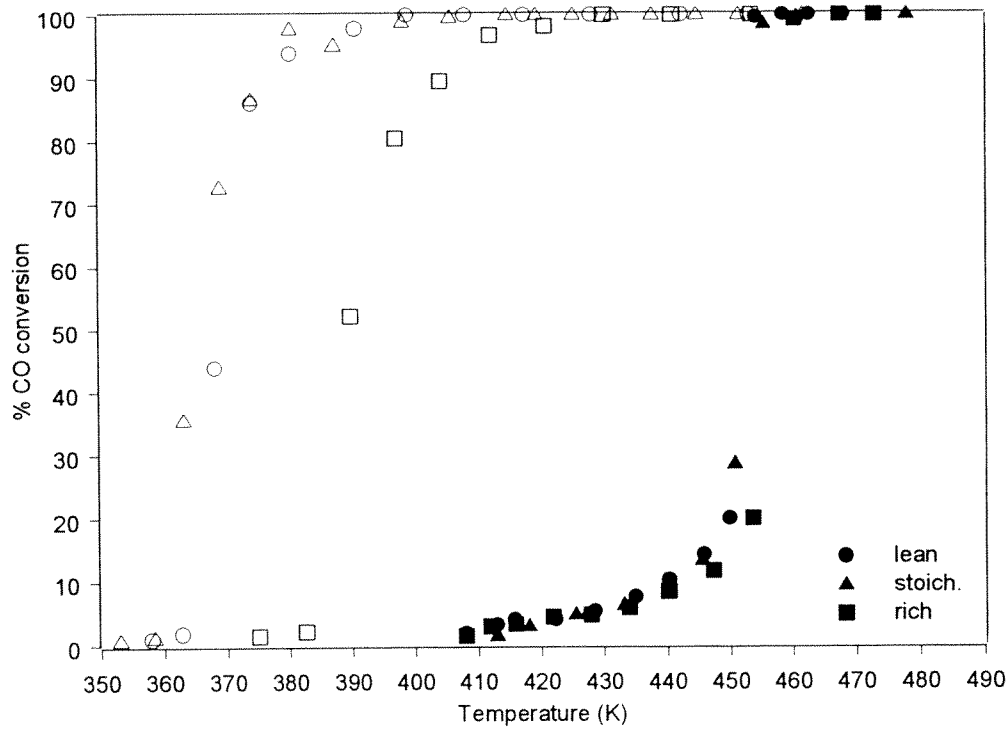


Şekil 15. %1 $Pd/\gamma\text{-}Al_2O_3$ katalizörlerinin CO oksitlenmesi sırasında ısıtma ve soğutma süreçlerindeki davranışları. Tepkime zenkin, stokiyometrik ve fakir karışımlar için ayrı ayrı incelenmiştir.

Histeresis davranışının temel gerekçesi katalizör yüzeyinin düşük sıcaklıklarda CO tarafından tamamen bloke edilerek oksijen adsorplanmasına yer bırakmayışındandır. Adsorplanma ısılarının ölçümleri sonucunda (Şekil 13) ortaya çıkan bulgu oksijenin daha yüksek adsorplanma ısıları verdiği dolayısı ile rekabet ortamında yüzeyi karbon monoksite bırakmayı tercih ettiğidir. Ancak sıcaklıklar yükseldikçe karbon monoksit desorplanma eğilimine girer ve bu da oksijenin yüzeyde daha fazla adsorplanmasına yol açar. Dolayısı ile yüzeyde tepkimeye girebilecek atomsal oksijen oranı arttıkça dönüşüm kolaylaşır ve daha düşük sıcaklıklarda gerçekleşebilir. Soğuma sırasında eğrinin daha düşük sıcaklıklarda daha yüksek dönüşüm vermesinin nedeni yüzeydeki karbon monoksit zehirlenmesinin henüz oluşmaya başlamamasındandır. Şekil 15 dikkatle incelendiğinde dönüşümün ısıtma sırasında hızla %100'e fırladığı ve soğutma sırasında da birden bire sıfıra düştüğü görülür. Bu olayların gerçekleştiği sıcaklıklar yüzeyde kinetik faz dönüşümü oluşan sıcaklıklardır.

Pd katalizörünün oksitlenmeye eğiliminin Pt'den daha fazla olduğu bilindiğinden, her iki katalizörde gerçekleşen tepkime hızları karbon monoksit kısmi basıncı değiştirilerek incelenmiştir. Şekil 16'da saf Pt ve Şekil 17'de ise saf Pd katalizörünün davranışları gösterilmektedir. Saf Pt katalizörü üzerinde CO oksitlenmesi hızları artan CO miktarı ile düzenli bir şekilde artmakta, $CO/O_2$ oranı reaksiyon stokiyometrisine eriştikten sonra da düzenli bir şekilde azalmaktadır. Bu deneyler yüzeyin karbon monoksit ile zehirlenmediği sıcaklıklarda bu eğilimi gösterirken, karbon monoksitin yüzeyi zehirlediği durumlarda hiç bir değişim olmadığı da Şekil 16'da gözlemlenmektedir.

Benzer deneyler Pd içeren katalizörler üzerinde tekrarlandığında ise tepkimede CO kısmi basıncı stokiyometrik oranın üstüne çıktığında bile hızın düşmediği gözlemlenmiştir (Şekil 17). Bunun nedeni CO oksitlenmesinin Pd-O merkezleri aracılığı ile gerçekleşmesinden ötürüdür. Gaz fazından oksijen alışverişi Pd katalizörlerinde dolaylı olarak gerçekleşmekte, ve katalizörün yığın içinde depoladığı oksijen tepkime sırasında kullanılabilmektedir.

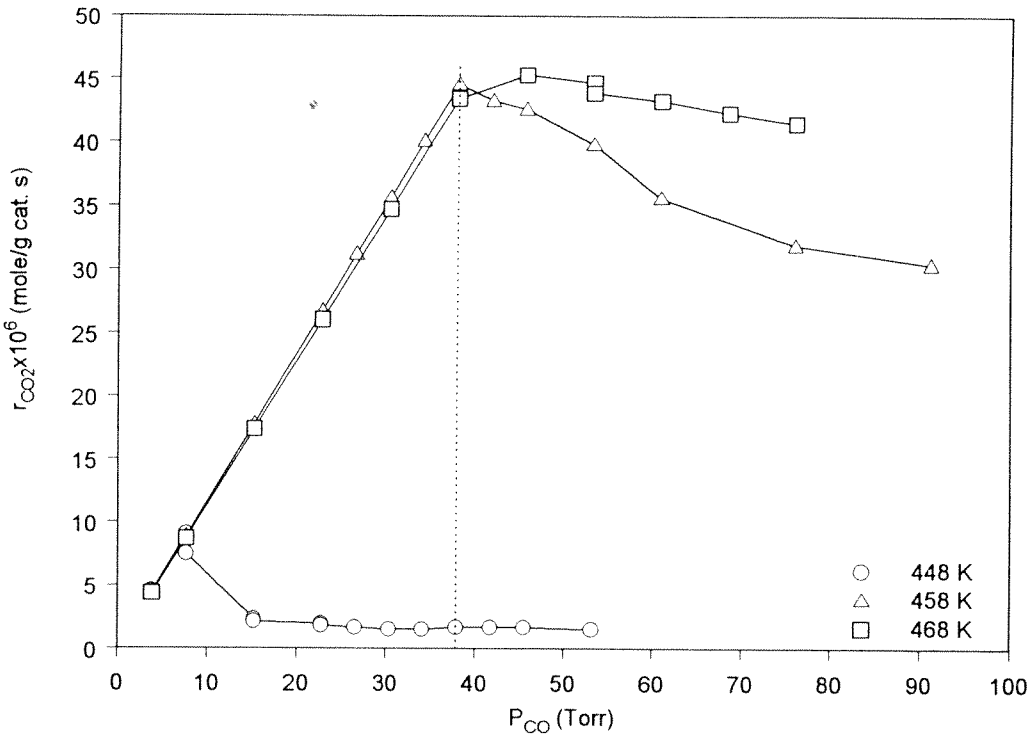


Şekil 16. Pt üzerinde CO oksitlenme hızının CO kısmi basıncı ile değişimi.

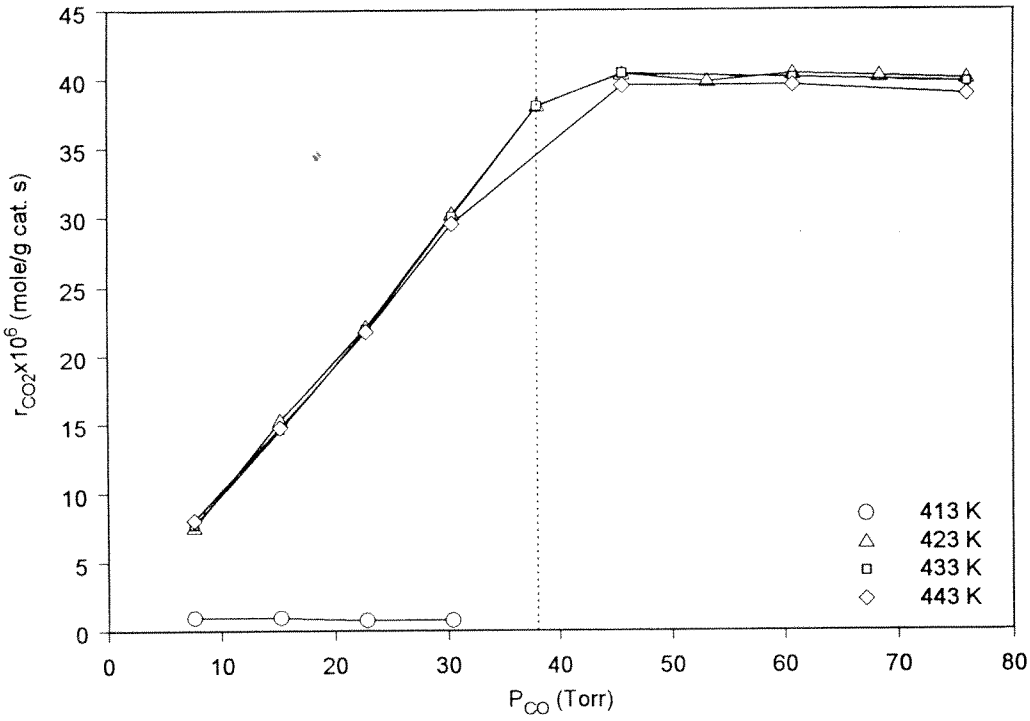


Şekil 17. Pd üzerinde CO oksitlenme hızının CO kısmi basıncı ile değişimi.

### 2.3.3. $CeO_2$ destekli Pt üzerinde CO Oksitlenmesi:

$CeO_2$ destekli Pt üzeindeki CO oksitlenmesi çalışmalarındaki bulgular yukarıda bahsi geçen konuların genel bir tekrarı olacağından burada yer alması tercih edilmemiştir. Ancak, bu çalışma sonucunda hazırlanan ve Applied Catalysis B: Environmental dergisine yayınlanmak üzere sunulacak olan elyazması ekte verilmektedir. Çalışmanın bu kısmında katalizör ön maddesinden kaynaklanan klorun katalizör üzerindeki etkisinin CO oksitlenmesi tepkimesinin yapısal duyarlılığını gösterir bulgular elde edilmiştir. Ancak kesin kanıtlar daha sistemetik bir çalışma ile ortaya konulabileceğinden detayı ile vurgulanmaktan bu aşamada uzak durulmaktadır.

### 2.3.4. Seçici CO oksitlenmesi reaksiyon modeli:

RGA ünitesi devreye alındıktan sonra kısa bir sure çalışılabilen seçici CO oksitlenmesi tepkimesinin 410 °C sıcaklıkta kalsine edilmiş katalizör üzerinde yapılan ön deney sonuçları Şekil 18'de gösterilmektedir. Bu ilk deneylerde % 2 CO % 4 $O_2$, % 10 $H_2$ ve %84 He

karışımı kullanılımıştır. Şekil 18'den de görüleceği gibi oksijen dönüşümleri hızla %100'e varmakta ve katalizör üzerinde karbon monoksit dönüşümü hidrojen dönüşümünden yüksek çıkmaktadır. Bu seçiçiliğin kalsinasyon sıcaklığı arttıkça artması beklenmektedir. Bu çalışma halen devam etmektedir, ve yapısal duyarlılık boyutu tek ve çift metalli katalizörler incelenerek sürdürülmektedir.

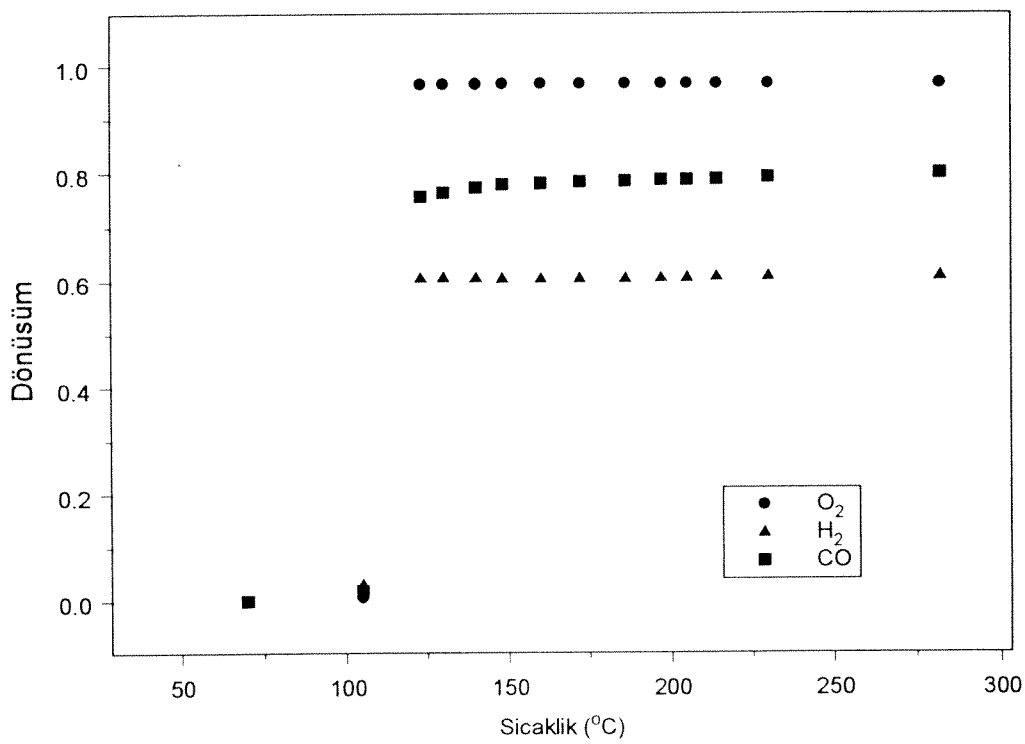


Şekil 18. RGA ünitesi kullanılarak elde edilen seçici CO oksitlenmesi tepkimesi sonuçları

Hidrojen bulunan ortamlarda karbon monoksit'in seçici oksitlenmesi tepkimesi global kinetik modelleme yöntemi ile çalışılmıştır. Modelde kullanılan tepkime silsilesi aşağıda verilmektedir.

$O_2 + * \rightarrow O_2*$ [1]

$O_2* + * \rightarrow 2O*$ [2]

$CO + * \leftrightarrow CO*$ [3]

$H_2 + 2^* \rightarrow H_2^*$ [4]

$O^* + H^* \leftrightarrow OH^*$ [5]

$OH^* + H^* \rightarrow H_2O + 2^*$ [6] (hız belirleyici adım)

$CO^* + O^* \rightarrow CO_2 + 2^*$ [7] (hız belirleyici adım)

Yüzeydeki aktif merkez dengesi aşağıdaki gibidir:

$\Theta_v + \Theta_{O2} + \Theta_O + \Theta_{CO} + \Theta_H + \Theta_{OH} = 1$

Denklemdeki $\Theta_i$, i maddesinin yüzey kaplanma oranını ve $\Theta_v$ boş sitelerin yüzey kaplanma oranını belirtmektedir. Hesaplamalar sırasında, yüzeyin genel olarak CO tarafından kaplandığı varsayılmıştır.

Bu nedenle aktif merkez dengesinin yeni hali:

$$\Theta_{CO} + \Theta_v = 1$$

$$\Theta_v = 1 - \Theta_{CO}$$

Eğer reaksiyon [3]'ü hatırlarsak;

$$CO + * \leftrightarrow CO^*$$

Bu reaksiyon için hız kanunu elde ederken reaksiyonun birincil mertebeden olduğu varsayılmıştır. Karbon monoksitin adsorblanma hızı, moleküllerin yüzeye çarpma sayılarıyla doğru orantılıdır. Bir başka deyişle, moleküllerin belli bir oranı adsorblanabilir. Bu nedenle, çarpışma hızı karbon momksitin kısmi basıncı ile doğru orantılıdır. Ayrıca, karbon monoksit molekülleri sadece boş sitelere adsorblanabileceği için moleküllerin yüzeye yapışma hızı boş sitelerin molar konsantrasyonlarıyla doğru orantılıdır. Bunları göz önünde bulundurarak karbon monoksitin yapışma hızı şu şekilde yazılabilir:

$$\text{yapışma hızı} = k_3 P_{CO} \Theta_v$$

CO moleküllerinin yüzeyden desorplanma hızları ise $\Theta_{CO}$ miktarı ile doğru orantılıdır. Bu nedenle;

$$\text{Desorplanma hızı} = k_{-3} \Theta_{CO}$$

Net adsorplanma hızı, yapışan CO moleküllerinin sayısından yüzeyden kurtulan moleküllerin sayısı çıkartılarak elde edilebilir.

$$\text{adsorplanma hızı} = k_3 P_{CO} \Theta_v - k_{-3} \Theta_{CO}$$

Denge durumunda adsorplanma hızı sıfıra eşittir.

Denklem [3]'den $\Theta_{CO} = K_3 P_{CO} \Theta_v$

$1 - \Theta_v = K_3 P_{CO} \Theta_v$ ve $K_i = \frac{k_i}{k_{-1}}$

Eğer yeni site denge denklemini ve [3]'den gelen denklemleri birleştirirsek;

$$\Theta_v = \frac{1}{1 + K_3 P_{CO}} \qquad [3a]$$

$$\Theta_{CO} = \frac{K_3 P_{CO}}{1 + K_3 P_{CO}} \qquad [3b]$$

Aynı şekilde aşağıdaki denklemler elde edilmiştir:

Denklem [1]'den $\Theta_{O2} = K_1 \times P_{O2} \times \Theta_v$

$$\Theta_{O2} = \frac{K_1 \times P_{O2}}{1 + K_3 P_{CO}} \qquad [1a]$$

Denklem [4]'den $\Theta_H = \sqrt{K_4 \times P_{H2}} \times \Theta_v$

$$\Theta_H^2 = \frac{\sqrt{K_4 \times P_{H2}}}{1 + K_3 P_{CO}} \qquad [4a]$$

Eğer oksijen atomlarının sabit olarak üretildiği ve tüketildiği varsayılırsa;

$$\frac{d\Theta_O}{dt} = 0 = k_2 \Theta_{O2} \Theta_v - k_5 \Theta_O \Theta_H - k_{-5} \Theta_{OH} - k_7 \Theta_{CO} \Theta_O$$

$$\Theta_O = \frac{k_2 \Theta_{O2} \Theta_v}{k_5 \Theta_H - \frac{k_5 k_{-5} \Theta_H}{k_{-5} + k_6 \Theta_H} - k_7 \Theta_v} \qquad [8]$$

[3a] ve [4a]'i [8]'in içinde yerine koyarsak;

$$\Theta_O = \frac{\frac{k_2 \Theta_{O2}}{1 + K_3 P_{CO}}}{k_5 \frac{\sqrt{K_4 P_{H2}}}{1 + K_3 P_{CO}} - \frac{k_5 k_{-5} \frac{\sqrt{K_4 P_{H2}}}{1 + K_3 P_{CO}}}{k_{-5} + k_6 \frac{\sqrt{K_4 P_{H2}}}{1 + K_3 P_{CO}}} + k_7 \frac{K_3 P_{CO}}{1 + K_3 P_{CO}}} \qquad [9]$$

$k_{-5} >> k_6 \frac{\sqrt{K_4 P_{H2}}}{1 + K_3 P_{CO}}$ diye varsayılırsa;

Yeni denklem;

$$\Rightarrow \Theta_O \approx \frac{k_2 \Theta_{O2}}{k_7 K_3 P_{CO}} \qquad [10]$$

ve [1a]'yı [10]'un içinde yerine koyarsak;

$$\Rightarrow \Theta_O \cong \frac{k_2}{k_7 K_3 P_{CO}} * \frac{K_1 P_{O2}}{1 + K_3 P_{CO}} \qquad [10a]$$

Eğer OH moleküllerinin sabit olarak üretildiği ve tüketildiği varsayılırsa;

$$\frac{d\Theta_{OH}}{dt} = 0 = k_5 \Theta_O \Theta_H - k_{-5} \Theta_{OH} - k_6 \Theta_{OH} \Theta_H$$

$$\Rightarrow \Theta_{OH} = \frac{k_5 \Theta_O \Theta_H}{k_{-5} + k_6 \Theta_H} \qquad [11]$$

[10a] ve [4a]'yı [11]'in içinde yerine koyarsak;

$$\Rightarrow \Theta_{OH} = \frac{k_5 \frac{k_2}{k_7 K_3 P_{CO}} * \frac{K_1 P_{O2}}{1 + K_3 P_{CO}} * \frac{\sqrt{K_4 P_{H2}}}{1 + K_3 P_{CO}}}{k_{-5} + k_6 \frac{\sqrt{K_4 P_{H2}}}{1 + K_3 P_{CO}}} \qquad [11a]$$

$k_{-5} \rangle\rangle k_6 \frac{\sqrt{K_4 P_{H2}}}{1 + K_3 P_{CO}}$ diye varsayılırsa;

Yeni denklem;

$$\Rightarrow \Theta_{OH} \cong \frac{k_2 K_5}{k_7 K_3 P_{CO}} * \frac{K_1 P_{O2}}{1 + K_3 P_{CO}} * \frac{\sqrt{K_4 P_{H2}}}{1 + K_3 P_{CO}} \qquad [12]$$

$H_2O$'nun hızı [6]'ya göre şu şekilde yazılabilir;

$$hız_{H2O} = k_6 \Theta_{OH} \Theta_H \qquad [6a]$$

[4a] ve [12]'yi [6a]'nın içinde yerine koyarsak;

$$hız_{H2O} = k_6 \frac{k_2 K_5}{k_7 K_3 P_{CO}} \cdot \frac{K_1 P_{O2}}{1 + K_3 P_{CO}} \cdot \frac{\sqrt{K_4 P_{H2}}}{1 + K_3 P_{CO}} \cdot \frac{\sqrt{K_4 P_{H2}}}{1 + K_3 P_{CO}}$$

$$= \frac{k_2 k_6 K_1 K_4 K_5}{k_7 K_3} \cdot \frac{P_{O2}}{P_{CO}} \cdot \frac{P_{H2}}{(1 + K_3 P_{CO})^3} \qquad [6b]$$

$K_3P_{CO}>>1$ diye varsıyılırsa, denklem [6b]'nin yeni hali;

$$hız_{H2O} = k_{eff}^{I} \cdot \frac{P_{O2} P_{H2}}{(P_{CO})^4} \qquad k_{eff}^{I} = \frac{k_2 k_6 K_1 K_4 K_5}{k_7 (K_3)^4} \qquad [13]$$

$$Ea_{eff}^{I} = Ea_2 + Ea_6 + \Delta H_1 + \Delta H_4 + \Delta H_5 - Ea_7 - 4\Delta H_3$$

$CO_2$'nun hızı [7]'ya göre şu şekilde yazılabilir;

$$hız_{CO} = k_7 \Theta_{CO} \Theta_O \qquad [7a]$$

[3b] ve [10a]'yi [7a]'nın içinde yerine koyarsak;

$$hız_{CO} = k_7 \frac{K_3 P_{CO}}{1 + K_3 P_{CO}} \cdot \frac{k_2}{k_7 K_3 P_{CO}} \cdot \frac{K_1 P_{O2}}{1 + K_3 P_{CO}} \qquad [7b]$$

$K_3P_{CO}>>1$ diye varsıyılırsa, denklem [7b]'nin yeni hali;

$$hız_{CO} = k_{eff}^{II} \cdot \frac{P_{O2}}{(P_{CO})^2} \qquad k_{eff}^{II} = \frac{k_2 K_1}{(K_3)^2} \qquad [14]$$

$$Ea_{eff}^{II} = Ea_2 + \Delta H_1 - 2\Delta H_3$$

Seçicilik, CO'yu $CO_2$'ye çevirmek için kullanılan oksijen miktarının toplam oksijen miktarına oranı olarak tanımlanabilir. CO'yu okside etmek için kullanılmayan oksijenin tamamının hidrojeni okside etmek için kullanıldığı varsayılabilir. Sonuç olarak seçicilik şu şekilde yazılabilir;

$$seçicilik = \frac{hız_{CO}}{hız_{CO} + hız_{H2O}} \qquad [15]$$

$$seçicilik = \frac{\frac{k_2 K_1}{(K_3)^3} \cdot \frac{P_{O2}}{(P_{CO})^2}}{\frac{k_2 K_1}{(K_3)^3} \cdot \frac{P_{O2}}{(P_{CO})^2} + \frac{k_2 k_6 K_1 K_4 K_5}{k_7 (K_3)^4} \cdot \frac{P_{O2} \cdot P_{H2}}{(P_{CO})^4}}$$

$$seçicilik = \frac{1}{1 + \frac{k_6 K_4 K_5}{k_7 (K_3)^2} \cdot \frac{P_{H2}}{(P_{CO})^2}}$$

$\frac{k_6 K_4 K_5}{k_7 (K_3)^2} \cdot \frac{P_{H2}}{(P_{CO})^2} >> 1$ diye varsıyılırsa, seçicilik denklemi;

$$seçicilik = \frac{k_7 (K_3)^2}{k_6 K_4 K_5} \cdot \frac{(P_{CO})^2}{P_{H2}} \qquad [16]$$

$k_{eff}^{III} = \frac{k_7 (K_3)^2}{k_6 K_4 K_5}$ ve $Ea_{eff}^{III} = Ea_7 + 2\Delta H_3 - Ea_5 - Ea_6 - \Delta H_4$

Son denklemdeki efektif aktivasyon enerjisinin artan CO adsorplanma ısıları ile artığı, ancak artan hidrojen adsorplanma ısıları ile azaldığı görülmektedir. Adsorplanma ısıları ölçümlerinde artan parçacık büyüklüğü ile CO'nun integral adsorplanma ısılarının arttığı, hidrojenin integral adsorplanma ısılarının ise azaldığı görülmüştür. Bu sonuçları dikkate alarak model sonuçları yorumlandığında ise artan parçacık büyüklüklerinde efektif aktivasyon enerjisinin artacağı, ve tepkimenin CO'ya yönelik seçiciliğinin yüksek sıcaklıklarda daha fazla olacağı ortaya çıkmaktadır.

## SONUÇLAR VE ÖNERİLER

Yapılan deneyler sonucunda karbon monoksit oksitlenmesi tepkimesinin yüzeyin yapısına bağımlı olarak değişim kaydettiği kesin olarak görülmüştür. Deneyler sonrasında karbon monoksit oksidasyonu reaksiyonunun düzlemsel bölgelerde köşe ve kenar bölgelerine nazaran daha hızlı bir reaksiyon olduğu görülmüştür. Bu aşamadan itibaren hidrojeni de işin içine katarak seçici karbon monoksit oksidasyonu reaksiyonunun yapısal duyarlılığıyla ilgili bulgulara ulaşmamız gerekmektedir. Bunu gözlemleyebilmek için iki yöntem takip edilecektir. Birincisi, bu çalışmada kullanılan yöntemle katalizör hazırlanırken kalsinasyon sıcaklığını ve süresini değiştirerek parçacık büyüklüğünü değiştirmektir. İkinci yöntem ise çift metalli katalizörler kullanılmasıdır. Altın, bakır veya gümüş $Pt/\gamma\text{-}Al_2O_3$ üzerine yüklenecektir. Bu tür metallerin hidrojen oksitlenmesi reaksiyonuna yetersiz olduğu bilinmektedir. Literatüre göre hidrojen oksitlenmesi reaksiyonu köşe ve kenar bölgelerde daha hızlı gerçekleşir ve altın,bakır ve gümüş türü metaller platinyum katalizörlerin köşe ve kenar bölgelerini tıkadıkları bilinmektedir. Bu sayede hidrojen oksitlenmesi reaksiyonunun önemli ölçüde ortadan kaldırılması ve yüksek CO oksitlenmesi seçicilik değerlerinin elde edilmesi amaçlanmaktadır. Sonuç olarak parçacık büyüklüğü değiştirilerek ve çift metalli katalizörler kullanılarak maksimum seçicilik değeri elde edilebilinecektir.

## PROJEDEN ÇIKAN YAYINLAR


1. D. Uner, N. A. Tapan , I. Ozen, and M. Uner, Oxygen adsorption and spillover over $Pt/TiO_2$ catalysts. *Applied Catalysis A: General*, **251** (2), 225-234 (2003).
2. D. Uner, I. Ozen and M. Uner 'Elucidating the Mechanism of $Pt/TiO_2$ Interactions in the Gas Phase Photo-catalytic Oxidation of Organic Materials', 18th NAM Catalysis Society Conference, June 1-June 6, 2003, Cancun, Mexico.
3. M. Uner and D. Uner, N.A. Tapan, "Is oxygen adsorption on supported Pt catalysts structure sensitive?", Presented at AIChE Annual Meeting, 3-8 November 2002, Indianapolis, IN.
4. D. Uner, B. Atalık, and M. Uner, Rational Design of Selective CO oxidation Catalysts, Submitted for presentation in 13th International Congress of Catalysis, to be held in July 2004, Paris France.

5. D. Uner and M. Uner, Adsorption Calorimetry In Supported Catalyst Characterization: Adsorption Structure Sensitivity On $Pt/\gamma\text{-}Al_2O_3$, Submitted for presentation in Calorimetry and Thermal Effects in Catalysis conference to be held in July 2004, Lyon, France.

## YAYINA HAZIRLANAN ELYAZMALARI

1. U. Oran and D. Uner "Mechanisms of CO Oxidation Reaction and Effect of Chlorine ions on the CO Oxidation Reaction over $Pt/CeO_2$ and $Pt/CeO_2/\gamma\text{-}Al_2O_3$ Catalysts" Prepared for publication in Applied Catalysis B: Environmental.
2. S. Kaya and D. Uner "CO Oxidation on Alumina Supported Pd-Pt mono- and bi-metallic Catalysts: Temperature Hysteresis" Prepared for publication in Journal of Catalysis.
3. D. Uner, B. Atalik and M.Uner "Structure sensitivity of CO oxidation over Pt catalysts" Prepared for publication in Journal of Catalysis.

## TEŞEKKÜR

Bu çalışmada katkıları tartışılmaz olan araştırma gurubumuzun tüm üyelerine ama özellikle, Pt-Pd ikili metal katalizör çalışmalarını yapan Sarp Kaya'ya, $CeO_2$ üzerinde çalışmaları gerçekleştiren Umut Oran'a, seçici CO oksitlemesi konusundaki modelleme çalışmasını üstlenen Berna Gençtan'a, RGA ünitesinin kurulması ve veri toplama sürecinin standartlaştırılması çalışmalarındaki katkıları nedeni ile Çağrı Savaşan'a ve RGA örnekleme ünitesinin tasarımındaki değerli katkıları nedeni ile Can Sandıkçıoğlu'na teşekkür ederiz.

## Kaynaklar


Bianchi, D., Bourane, A., Dulaurent, O., "Heats of adsorption of the linear CO species adsorbed on a $Pt/Al_2O_3$ catalyst in the presence of coadsorbed species using FTIR spectroscopy", *Langmuir* 17,5496-5502 (2001).

Bianchi, D., Dulaurent, O., "Adsorption isobars for CO on a $Pt/Al_2O_3$ catalyst at high temperatures using FTIR spectroscopy: isosteric heat of adsorption ans adsorption model.", *App.Cat.A* 196, 271-280 (2000).

Campbell, C.T. Ertl, G., Kuipers, H., Segner, J. 'A molecular-beam study of the adsorption and desorption of oxygen from a Pt(111)surface', *Surf. Sci.*, **107**, 220-236 (1981).

Cortright, R.D. and Dumesic, J.A., 'Effects of potassium on silica supported Pt and Pt/Sn catalysts for isobutane dehydrogenation' *J. Catal.*, **157**, 576-583 (1995).

Cudok, A., Froitzheim, and H. Hess, G., 'Kinetics of the dissociative adsorption of $O_2$ on Pt(111) - a TREELS study', *Surf. Sci.* **307-309**, 761-767 (1994).

Demirkol, M. K. Soot oxidation catalysis, MS Thesis ODTÜ Ankara 2002.

Dernaika, B. Catalytic combustion of diesel soot. MS Thesis ODTÜ. Ankara 2001.

Dernaika B. and Uner, D. "A simplified approach to determine the activation energies of uncatalyzed and catalyzed combustion of soot" *Applied Catalysis B: Environmental,* **40**(3) 219 – 229 (2003).

Descorme, C., Duprez, D.," Oxygen surface mobility and isotopic exchange on oxides: role of the nature and the structure of metal particles", *Applied Catalysis A-General* 202,231-241 (2001)

Dumesic, J.A., Rudd, D.F, Aparicio, L.M., Rekoske, J.E., Trevino, A.A., The Microkinetics of Heterogeeneous Catalysis, American Chemical Society, Washington, DC, 1993.

Eiswirth, M., and Ertl, G., 'Kinetic oscillations in the catalytic CO oxidation on a Pt(110) surface' *Surf. Sci.*, **177**, 90-100 (1986).

Ernur, D. De-$NO_x$ catalysis via bimetallics, MS Thesis, ODTÜ Ankara 1998.

Ernur, D. ve Üner, D. Ö., "Destekli Rh Katalizörleri ile $NO_x$ emisyonlarının İndirgenmesi Reaksiyonunda Oluşan Yüzey Ara Ürünlerinin Kaplanma Oranlarının Bulunması", *Turk. J. Engin. Environ. Sci.* **24**, 277-285 (2000).

Fink, Th., Dath, J-P., Imbihl, R., and Ertl, G., 'The mechanism of kinetic oscillations in the NO + CO reaction on Pt(100)' *Surf. Sci.*, **251/252**, 985-989 (1991).

Gates, B.C. Catalytic Chemistry, Wiley, NY, 1992.

Gland, J.L., Sexton, B.A. and Fisher, G.B. 'Oxygen interactions with the Pt(111) surface', *Surf. Sci.*, **95**, 587-602 (1980).

Gopel, W. Rocker, G. and Feierabend, R. 'Intrinsic defects of $TiO_2$(110) - interaction with chemisorbed $O_2$, $H_2$, CO, and $CO_2$', *Phys. Rev. B.*, **28**, 3427-3438 (1983).

Henderson, M.A. Epling, W.S., Perkins, C.L., Peden, C.H.F. and Diebold, U. 'Interaction of molecular oxygen with the vacuum-annealed TiO2(110) surface: Molecular and dissociative channels', *J. Phys. Chem.*, **103**, 5328-5337 (1999).

Kaya, S. CO oxidation on alumina supported Pt-Pd mono and bi-metallic catalysts: temperature hysteresis. MS Thesis ODTÜ Ankara 2002.

Kumar, N., King, T.S., and Vigil, R.D. 'A portal model for structure sensitive hydrogen adsorption on Ru-Ag/SiO2 catalysts' *Chem. Eng. Sci.*, **55**, 4973-4979 (2000).

Ladas, S, R. Imbihl and G. Ertl, 'The reactivity of high oxygen coverages on Pd(110) in catalytic CO oxidation' *Surf. Sci.*, **280**, 14-22 (1993).

Lisowski, W.," Kinetics of hydrogen adsorption and desorption on thin platinum films", Applied Surface Science 31, 451-459 (1988)

Lu, K.E., Rye, R.R., "Flash desorption and eqilibration of H2 and D2 on single-crystal surfaces of platinum", Surface Science 45, 677-695 (1974)

Masel, Principles of Adsorption and Reaction on Solid Surfaces, Wiley, NY, 1996.
Nijhuis, T.A., Makkee, M., van Lagenveld, A.D., and Mouilijn, J., 'The desorption of CO2 from the surface as a kinetically relevant step in the CO oxidation reaction over platinum' *Stud. Surf. Sci. Catal.*, **109,** 361-369 (1997).

Mbaraka I. and Uner, D. "Use of Seydisehir Alumina as a Support for CO Oxidation Catalysts", *Chemical Engineering Communications*, **190** (5-8), 1073-1084 (2003).

Monroe, D.R. and Merrill, R.P. 'Adsorption of oxygen on Pt(111) and its reactivity to hydrogen', *J. Catal.*, **65**, 461-469 (1980).

Narayan, R.L., and King, T.S., Hydrogen adsorption states on silica-supported Ru-Ag and Ru-Cu bimetallic catalysts investigated via microcalorimetry *Thermochimica Acta*, **312**, 105-114 (1998).

Nolan, P.D., Lutz, B.R.,Tanaka, P.L., Davis, J.E., Mullins, C.B. 'Molecularly chemisorbed intermediates to oxygen adsorption on Pt(111): A molecular beam and electron energy-loss spectroscopy study', *J.Chem. Phys.*, **111**, 3696-3704 (1999).

Norton, P.R., Richards, P.J., "Hydrogen isotope chemisorption and equilibration on platinum", Surface Science 41, 293-311 (1974)

Ozkan,U.S., Kumthekar, M.W. Karakas, G., 'Self-sustained oscillatory behavior of NO+CH4+O-2 reaction over titania-supported Pd catalysts' *J.Catal.*, **171**, 67-76 (1997).

Oran, U., Effect of cerium dioxide on carbon monoxide oxidation reaction mechanism over $Pt/\gamma\text{-}Al_2O_3$ catalysts. MS Thesis ODTÜ Ankara 2001.

Özen, İ, Thermal and photo-catalytic oxidation of carbon monoxide over titanium dioxide-effects of platinum deposition. MS Thesis ODTÜ Ankara 2001.

Ozen, I., and Uner, D., "Heterogeneous photo and thermal catalytic oxidation of CO: effects of metal deposition", *Studies in Surface Science and Catalysis* (Reaction Kinetics and the development and operation of catalytic processes) **133**, Netherlands , 445-452 (2001).

Procop, M., Volter, J., "Adsorption of hydrogen on platinum .1. adsorbed amounts, kinetics of adsorption and desorption", Surface Science 33, 69-81 (1972)

Puglia, C., Nilsson, A., Hernnas, B., Karis, O., Bennich, P., Martensson, N., 'Physisorbed, chemisorbed and dissociated $O_2$ on Pt(111) studied by different core-level spectroscopy methods', *Surf. Sci.* **342**, 119-133 (1995).

Savargaonkar, N., Narayan, R.L., Pruski, M., Uner, D. O., and King, T.S., 'Structure sensitive hydrogen adsorption: Effect of Ag on Ru/SiO2 catalysts' *J. Catal.* **178**, 26-33 (1998).

Savargaonkar, N., Uner, D., Pruski, M. and King, T. S. 'Kinetics of hydrogen adsorption and desorption on silica supported Pt, Rh and Ru catalysts studied by solid state $^1H$ NMR' *Langmuir*, **18**, 4005-4009 (2002).

Schwaha, K. and Bechtold, E., 'Adsorption of oxygen on stepped Pt(S)-[9(111)x(111)] face' *Surf. Sci.*, **65**, 277-286 (1977).

Seebauer, E.G., Kong, A.C.F., Schmidt, L.D.," Adsorption and desorption of CO AND H-2 on Rh(111) - laser-induced desorption", *Applied Surface Science* **31**, 163-172 (1988)

Sharma, S.B., Miller, J.T., and Dumesic, J.A., 'Microkalorimetric study of silica and zeolite supported platinum catalysts', *J. Catal.*, **148**, 198-204 (1994).

Spiewak, B.E., and Dumesic, J.A., 'Microcalorimetric measurements of differential heats of adsorption on reactive catalyst surfaces', *Thermochimica Acta*, **290**, 43-53 (1996).

Tapan, A., Adsorption dynamics and reaction kinetics at gas-solid interfaces: applications in catalysis and gas sensors. MS Thesis ODTÜ Ankara 1999.

Thiel, P.A., Behm, R.J., Norton, P.R., and Ertl, G. 'Mechanism of an adsorbate-induced surface phase-transformation - CO on Pt(100)' *Surf. Sci.*, **121**, L553-L560 (1982).

Tong, Y.Y., Van der Klink, J.J. 'Local metal to nonmetal transition on oxygen-covered platinum particles from Pt-195 nuclear-magnetic-resonance', *J. Phys.-Condens. Mat.*, 7, 2447-2459 (1995).

Uner, D.O. 'Interactions of Hydrogen with Alkali Promoted $Ru/SiO_2$ Catalysts: A Proton NMR Study', PhD Disertation Iowa State University, Ames, IA USA, 1994.

Uner, D., Tapan , N. A., Ozen, I. and Uner, M. Oxygen adsorption and spillover over $Pt/TiO_2$ catalysts. *Applied Catalysis A: General*, **251** (2), 225-234 (2003).

VanderWiel, D.P. , Pruski, M, King, TS 'A kinetic study on the adsorption and reaction of hydrogen over silica-supported ruthenium and silver-ruthenium catalysts during the hydrogenation of carbon monoxide' *J. Catal.* 188, 186-202 (1999).

Vannice, A., Chou, P., "Calorimetric Heat of adsorption measurements on palladium: Influence of crystallite size and support on $O_2$ adsorption.", *J. Catal.* 105,342-351 (1987).

Wartnaby, C.E., Stuck, A. Yeo, Y.Y. and King, D.A., 'Microcalorimetric heats of adsorption for CO, NO, and oxygen on Pt{110}', *J. Phys. Chem.* **100,** 12483-12488 (1996).

Yeo, Y.Y. Vattunoe, L., and King, D.A., 'Calorimetric heats for CO and oxygen adsorption and for the catalytic CO oxidation reaction on Pt{111}', *J. Chem. Phys.*, **106**, 392-401 (1997).

Zafiris, G.S., anf Gorte, R.J., 'CO oxidation on Pt $\alpha$-$Al_2O_3$ (0001) - evidence for structure sensitivity', *J. Catal.* **140**, 418-423 (1993).

## EKLER

### 1. Konferans sunum özetleri:

1. M. Uner and D. Uner, N.A. Tapan, "Is oxygen adsorption on supported Pt catalysts structure sensitive?", Presented at AIChE Annual Meeting, 3-8 November 2002, Indianapolis, IN.
2. D. Uner, I. Ozen and M. Uner 'Elucidating the Mechanism of $Pt/TiO_2$ Interactions in the Gas Phase Photo-catalytic Oxidation of Organic Materials', 18th NAM Catalysis Society Conference, June 1-June 6, 2003, Cancun, Mexico.
3. D. Uner, B. Atalık, and M. Uner, 'Rational Design of Selective CO oxidation Catalysts', Submitted for presentation in 13th International Congress of Catalysis, to be held in July 2004, Paris France.
4. D. Uner and M. Uner, 'Adsorption Calorimetry In Supported Catalyst Characterization: Adsorption Structure Sensitivity On $Pt/\gamma\text{-}Al_2O_3$', Submitted for presentation in Calorimetry and Thermal Effects in Catalysis conference to be held in July 2004, Lyon, France.

### 2. Proje sonucunda hazırlanan ve/veya yayınlanan makaleler:

1. U. Oran and D. Uner "Mechanisms of CO Oxidation Reaction and Effect of Chlorine ions on the CO Oxidation Reaction over $Pt/CeO_2$ and $Pt/CeO_2/\gamma\text{-}Al_2O_3$ Catalysts" Applied Catalysis B: Environmental dergisinde yayınlanmak üzere kabul edildi.
2. S. Kaya and D. Uner "CO Oxidation on Alumina Supported Pd-Pt mono- and bi-metallic Catalysts: Temperature Hysteresis" Journal of Catalysis dergisine gönderilmek üzere hazırlanıyor.
3. D. Uner, N. A. Tapan , I. Ozen, and M. Uner, Oxygen adsorption and spillover over $Pt/TiO_2$ catalysts. *Applied Catalysis A: General*, **251** (2), 225-234 (2003).
4. M. Uner and D. Uner 'Adsorption Calorimetry In Supported Catalyst Characterization: Adsorption Structure Sensitivity On $Pt/\gamma\text{-}Al_2O_3$', Thermochimica Acta dergisine yayınlanmak üzere gönderildi.

## 391e] - Is Oxygen Adsorption on Supported Pt Catalysts Structure Sensitive?

**Presented at:** [391] - Fundamentals of Supported Catalysis II

**For schedule information click here**


**Author Information:**

**Murat Uner**
Middle East Technical University
Inonu Bulvari
Ankara, 06531
Turkey
Phone: 90-312-210-4361
Fax: 90-312-210-1264
Email: muner@metu.edu.tr

**Deniz Uner** *(speaker)*
Middle East Technical University
Chemical Engineering
Ankara, 06531
Turkey
Phone: +90-312-210-4383
Fax: +90-312-210-1264
Email: uner@metu.edu.tr



**Abstract:**

The first step of a catalytic reaction on the surface of a solid catalyst is the adsorption of one or all of the reactants. The oxidation of CO to form $CO_2$ reaction proceeds via the combination of a chemisorbed CO molecule with a chemisorbed oxygen atom, the latter produced through the dissociative adsorption of $O_2$ on the Pt surface. Due to the poisoning effect of the CO adsorption on the Pt surface, amount of adsorbed oxygen on the surface gains more importance. The aim of the study is to investigate the adsorption characteristics and the structure sensitivity of oxygen adsorption on supported platinum catalysts.

The catalysts used in this study were prepared by incipient wetness impregnation of $TiO_2$ (Degussa P-25) or gamma-$Al_2O_3$ (Johnson Matthey) with a solution of tetra ammine platinum (II) chloride(Johnson Matthey). The resultant slurry was dried, calcined and reduced in hydrogen prior to the calorimetric measurements. Both of the catalysts had a final metal loading of 1 wt% Pt. The dispersion of Pt/$TiO_2$ catalyst was measured as 14% and that of Pt/gamma-$Al_2O_3$ catalyst was found to be 55% by volumetric hydrogen chemisorption. The catalysts were reduced in static hydrogen in-situ, prior to calorimety measurements.

The differential heat of adsorption measurements were conducted on a homemade constant volume Pyrex manifold coupled with Setaram C80 Tian-Calvet Calorimeter. Oxygen adsorption heats over Pt/gamma-$Al_2O_3$ was measured to be ~250 kJ/mol independent of coverage. Oxygen adsorption heats over Pt/$TiO_2$ were also independent of coverage and ~ 300 kJ/mol. Both of these surfaces were saturated at ~0.7 monolayers. Experiments for monometallic Pt and Pt-Cu bimetallic particles supported on alumina are in progress to distinguish whether the difference in the measured adsorption heats are due to the particle size effects as reflected from the dispersion data or due to an electronic or geometric effect induced by the $TiO_2$ fragments migrated on the metal particles.

## Elucidating the Mechanism of $Pt/TiO_2$ Interactions in the Gas Phase Photo-catalytic Oxidation of Organic Materials

**D. Uner[1], I. Ozen[2] and M. Uner[1]**

[1]Chemical Engineering, Middle East Technical University,Ankara 06531, TURKEY

[2]Present address: Sabancı University, Faculty of Engineering and Natural Sciences (FENS), Materials Science and Engineering Program, Orhanlı, Tuzla, 81474 İstanbul, Turkey

The rate enhancement and improved resistance to poisoning due to the presence of Pt in the $TiO_2$ assisted photo oxidation of organic materials has been very well established. However, the mechanism of the Pt-$TiO_2$ interaction is still an open debate. In this study, the kinetic effects of the presence of Pt were investigated.

A preliminary study on benzene photo-oxidation and subsequent modeling of the kinetics revealed that benzene photooxidation over pure $TiO_2$ takes place via two major reaction steps, and the final -most probably the rate limiting- oxidation step requires a single carbon containing surface intermediate (1). A detailed study was then conducted for CO oxidation reaction presuming that the single carbon containing intermediate was adsorbed CO. It was oberved that the photooxidation rate of CO over $TiO_2$ (Degussa P25) increased in the presence of 0.5, and 1 wt % Pt under both dark and illuminated conditions. Experimental details and catalyst preparation methods and tratment procedures were described elsewhere (2). The metal dispersion of 1 wt % catalyst was 3.5% while 0.5 wt% $Pt/TiO_2$ catalyst had 14% dispersion as measured by strong hydrogen chemisorption. There was a severe temperature hysteresis effect during the thermal oxidation reaction experiments. This hysteresis effect was interpreted to be due to the CO poisoning of Pt surface which implied that the catalysis was taking place over Pt surface. However, the same hysteresis effect was not observed during the illuminated experiments over the same catalysts indicating unique contribution of Pt-$TiO_2$ interaction to the overall catalysis. The light-off behavior of 1 wt% Pt containing catalyst was better than 0.5 wt% Pt containing catalyst in both thermal and photo-oxidation experiments.

Gas phase oxygen adsorption experiments over these catalysts revealed oxygen spillover from the metal to the support, which was more pronounced over 0.5 wt % Pt containing catalyst. Differential heats of adsorption measured over these catalysts indicated that oxygen adsorption heats over 0.5 wt% $Pt/TiO_2$ are systematically higher than that measured over 1.0 wt% $Pt/TiO_2$(3).

The results of the catalyst performance tests and gas adsorption studies indicate that oxygen spillover effect is not dominant during neither thermal nor photocatalytic oxidation of carbon monoxide, however, the intrinsic catalytic activity of Pt towards the reaction increases the reaction rate under both dark and illuminated conditions. Under UV illumination, oxidation takes place over both oxide and metal surface. However, under dark conditions oxidation predominantly takes place over the metal surface.

**References**


1. Ozbek, S., and Uner, D.O. "The deactivation behaviour of the $TiO_2$ used as photocatalyst for bezene oxidation", *Studies in Surface Science and Catalysis* (Catalyst deactivation) **126**, Netherlands , 411-414 (1999).
2. Ozen, I., and Uner, D., "Heterogeneous photo and thermal catalytic oxidation of CO: effects of metal deposition", *Studies in Surface Science and Catalysis* (Reaction Kinetics and the development and operation of catalytic processes) **133**, Netherlands , 445-452 (2001).
3. Uner, D., Tapan, N.A., Ozen, I. And Uner, M. "Oxygen adsorption and spillover on $Pt/TiO_2$ catalysts" Applied Catalysis A: General, Submitted for publication.

# Rational design of selective CO oxidation catalysts

**D. Uner[1], B. Atalik and M. Uner**

**Chemical Engineering**

**Middle East Technical University**

**Ankara 06531 TURKEY**

[1]uner@metu.edu.tr

Selective oxidation of CO in hydrogen-rich mixtures is an important reaction in the fuel cell technology. The hydrogen used as the feed in polymer electrolyte membrane fuel cell (PEMFC) should be significantly free of CO to avoid poisoning of the Pt anode catalyst. The aim of this study is to obtain the experimental data towards understanding the structure sensitivity of the selective CO oxidation reaction in hydrogen rich atmospheres.

The surface structure of the catalysts was manipulated by increasing the particle size of the metals by increasing the calcination duration and temperature. As a result catalysts with the same metal loading but different surface composition in terms of edge, corner and low index plane atoms could be prepared. The catalysts of 2% w/w of Pt on $\gamma$-$Al_2O_3$ were prepared by using the incipient wetness method. Four different catalysts were obtained by calcining each segment of the batch at 410, 450, 500 and 600$^0$C for four hours in air. The catalyst dispersions were measured by a modified hydrogen chemisorption technique (1). The measured dispersion values were found to be decreasing with the increasing calcination temperature as shown in Table 1. According to the carbon monoxide conversion versus reactor temperature plots, it was found that the light-off temperatures (defined here as the temperature at 50% conversion) were similar for catalysts which have dispersions of 62.5, 29.2 and 20.0% and lower than that of the catalyst with 3.7% dispersion. However, if the turnover frequencies (the ratio of the reaction rate to active site density) of these catalysts were considered, it was seen that the catalyst which has a dispersion value of 3.2% was the best catalyst for the reaction. TOF values of catalyst calcined at 600$^0$C were greater towards the four catalysts. It was also found that the activation energy of the reaction performed on catalyst calcined at 600$^0$C was less than the other catalysts.

| Calcination temperature(°C) | Dispersion (%) | Ea (kJ/mol-K) |
|---|---|---|
| 410 | 62.5 | 120.20 |
| 450 | 29.2 | 117.83 |
| 500 | 20.0 | 105.32 |
| 600 | 3.7 | 94.21 |

As the crystallite size increases, the fraction of Pt atoms at low coordination sites (corner and edge sites) decrease while the fraction of atoms on flat plates increases significantly. According to these results, it was concluded that flat surfaces have a significantly higher CO oxidation activity compared to low coordination edge and corner atoms, in accordance with the studies reported in the literature. The measured change in reaction activation energies and reaction orders with respect to catalyst dispersion indicate that the CO oxidation reaction proceeds with different mechanisms on different facets.

The structure sensitivity of hydrogen adsorption is established based on differential heat of adsorption data collected on a SETARAM C-80 Tian Calvet microcalorimeter. The results obtained are in good agreement with the previous studies(2,3) indicating that in the absence of sufficient number of edge and corner atoms the rate of adsorption of hydrogen over precious metal surfaces is severely retarded. The CO adsorption heats measured on the same catalysts exhibit a similar trend however, the saturation coverage of hydrogen as measured via microcalorimetry is lower than that of CO on low dispersion catalysts. This result can be extended to state that the selectivity of CO oxidation reaction in hydrogen containing atmospheres can be improved by using catalysts with fewer edge and corner atoms. However, when precious metals are used, the metal economy can be an important factor. In the ongoing part of this study, the ratio of planar surface metals to edge and corner atoms is manipulated by doping the catalyst with an inert metal that is capable of populating the edge and corner sites therefore production of high dispersion catalysts with a higher ratio of low index plane atoms are possible.

**References:**


1. D.O. Uner, M. Pruski, and T.S. King, " Optimization of volumetric hydrogen chemisorption as a characterization technique for $Ru/SiO_2$ catalysts" *J. Catal.*, **156**, 60-64 (1995).
2. N. Savargaonkar, D. Uner, M. Pruski and T. S. King, "Kinetics of hydrogen adsorption and desorption on silica supported Pt, Rh and Ru catalysts studied by solid state $^1H$ NMR" *Langmuir*,**18**, 4005-4009, (2002).
3. N Savargoankar, R.L. Narayan, M. Pruski, D. O. Uner and T.S. King, " Structure Sensitive Hydrogen Adsorption: effect of Ag on $Ru/SiO_2$ catalysts", *J. Catal.*, **178**, 26-33 (1998).


**Acknowledgements:**


The authors gratefully acknowledge the financial support provided by Turkish Scientific and Technical Research Council under contract no MISAG 188.

# Adsorption Calorimetry In Supported Catalyst Characterization: Adsorption Structure Sensitivity On $Pt/\gamma\text{-}Al_2O_3$

M. Uner and D. Uner[1]

Chemical Engineering, Middle East Technical University

Ankara 06531

Turkey

[1]uner@metu.edu.tr

Many catalytic reactions are structure sensitive, the rate depends on the detailed geometrical structure of the surface atoms of the catalyst. Structure sensitivity usually manifests itself as a dependence of the rate per surface atom on the average size of the catalyst particles. The understanding is that the relative number of corner and edge sites increases dramatically with decreasing particle diameter, and these very low-coordinated surface atoms could have a substantially different ability to interact with the gas phase molecules. The amount of heat evolved during the adsorption process, called the heat of adsorption, is closely related to the adsorbate-substrate bond strength. Furthermore, the differential heat of adsorption can be dependent on the surface coverage of the adsorbate due to the lateral adsorbate-adsorbate interactions or due to the surface heterogeneity.

The oxidation of CO to form $CO_2$ reaction proceeds via the combination of a chemisorbed CO molecule with a chemisorbed oxygen atom, the latter produced through the dissociative adsorption of $O_2$ on the Pt surface. Due to the poisoning effect of the CO adsorption on the Pt surface, amount of adsorbed oxygen on the surface gains more importance. The aim of the study is to investigate the adsorption characteristics and the structure sensitivity of oxygen adsorption on $Pt/\gamma\text{-}Al_2O_3$ catalysts. And also the selective CO oxidation is an important issue in the $H_2$ production for the fuel cells. Thus the first step, of a catalytic reaction on the surface of a solid catalyst, adsorption of the reactants was under the investigation.

In the study, the structure sensitivity of adsorption was studied by changing the metal particle size. All catalyst samples were prepared by incipient wetness method and calcined in air at different temperatures as: 683K, 723K, 773K and 823K in order to change the average metal particle size. The dispersion values for the catalysts were measured as 0.62, 0.28, 0.20 and 0.03 respectively.

Heat of adsorption measurements were conducted on Setaram C-80 Tian-Calvet Calorimeter coupled to a home built multi-port high-vacuum Pyrex glass manifold. The samples were reduced under atmospheric hydrogen and the differential heats of adsorption were measured by introducing small increments of the gas.

For all gases the amount of the gas adsorbed up to saturation decreases as the particle size increase. It is the case that is expected due to the number of the Pt atoms in the surface decreases as the particle size increases. The zero coverage differential heat of adsorptions for CO and $O_2$ does not show any change with the changing particle diameter. On the other hand $H_2$ shows a sharp decrease of zero coverage heat values as the average particle diameter of Pt increases. This can be concluded, as $H_2$ adsorption is more structure sensitive then the CO and $O_2$ adsorptions. The integral heat of adsorption values generally shows a decreasing trend with the increasing particle size.

The effect of the particle size on the site-energy distribution of CO, $O_2$ and $H_2$ and the resultant effect on the selective CO oxidation reaction will be discussed.

**Acknowledgement**

The financial support for this project is provided by TUBITAK under research contract no MISAG 188.

# Mechanisms of CO Oxidation Reaction and Effect of Chlorine ions on the CO Oxidation Reaction over $Pt/CeO_2$ and $Pt/CeO_2/\gamma$-$Al_2O_3$ Catalysts

U. Oran and D. Uner*

Chemical Engineering
Middle East Technical Unviersity
Ankara, 06531Turkey

## Abstract

The reaction orders and activation energies of CO oxidation reaction over $Pt/\gamma$-$Al_2O_3$, $Pt/CeO_2$ and $Pt/CeO_2/\gamma$-$Al_2O_3$ were investigated under stoichiometric gas mixtures. The effect of residual chlorine originating from catalyst precursors on the CO oxidation activity of $Pt/\gamma$-$Al_2O_3$, $Pt/CeO_2$ and $Pt/CeO_2/\gamma$-$Al_2O_3$ was also studied. Indirect evidence was collected indicating that platinum was selectively deposited on alumina surface when $Pt/CeO_2/\gamma$-$Al_2O_3$ catalyst was prepared from the physical mixture of pure oxides. The reaction orders of CO and $O_2$ was found approximately as −2.0 and +1.0 respectively over the $Pt/\gamma$-$Al_2O_3$ catalyst but as −1.0 and 0.0 over the $Pt/CeO_2$ and $Pt/CeO_2/\gamma$-$Al_2O_3$ catalysts. The activation energy of CO oxidation reaction over $Pt/\gamma$-$Al_2O_3$ catalyst under stoichiometric conditions was around 110.0 kJ/mol. On the other hand over $Pt/CeO_2$ catalysts activation energies were measured to be around 60 kJ/mol. Surface reaction mechanisms were postulated to explain the differences in the reaction orders and activation energies.

Key Words: CO oxidation, Platinum, Ceria, Alumina, Reaction mechanism, Chlorine poisoning.

* Corresponding author. Tel: +90 312 210 4383, Fax: +90 312 210 1264, e-mail adress: uner@metu.edu.tr

## 1. Introduction

$Pt/\gamma\text{-}Al_2O_3$, $Pt/CeO_2$ and $Pt/CeO_2/\gamma\text{-}Al_2O_3$ are very well known oxidation catalysts, especially used in automotive catalytic converter systems to eliminate the unburned hydrocarbons and CO. Ceria is used in catalytic converters since 1980's and it is an indispensable part of current catalytic converter technology. The reasons for so much attention being paid to cerium oxides are multiple: First, ceria stabilizes the metal dispersion, thus favoring the amount of active surface per weight of the catalyst and alumina support [1,2]. Second, it promotes the water-gas shift and hydrocarbon reforming reactions that play a fundamental role in the elimination of CO and hydrocarbons under reducing conditions as well as CO oxidation under oxidizing conditions [3-5]. Third and the most important one is the oxygen storage and releasing capacity of $CeO_2$ [6-10]. Part of the current literature on the effect of $CeO_2$ on CO oxidation reaction over $Pt/Al_2O_3$ catalysts were compiled in Table 1. The catalyst activation procedures were also listed in the same table. The information presented on this table indicates that in the presence of $CeO_2$ the light-off and 50% conversion temperatures are lower than that of $Al_2O_3$ supported catalysts, with a few exceptions.

The change in the activity of the catalyst towards CO oxidation reaction in the presence of $CeO_2$ is attributed to the change in the reaction mechanism as mentioned above. Each of the mechanistic steps, adsorption and desorption of the reactants, surface reaction, and desorption of products of CO oxidation reaction has been probed extensively with surface science techniques, as has the interaction between adsorbed O atoms and CO molecules over supported platinum, rhodium and palladium catalysts. Although the oxidation of CO over supported platinum, rhodium and palladium

catalysts has been the subject of numerous studies, there is little agreement on reaction orders in literature. The information on the reaction orders reported in the literature was compiled in Table 2 for further reference.

The catalysts in the three way catalytic converters (TWC) may be used either as pellets or as in the form of monoliths, but the preparation methods of the active materials do not differ too much. Wet impregnation is the most widely used catalyst preparation technique, which involves the impregnation of the support with a solution of the noble metal precursor with subsequent calcination and/or reduction steps [11]. Most of the noble metal precursors used in wet impregnation contains high levels of chlorine. Many studies have reported that the residual chlorine coming from the precursor chloride salts can affect the physical and chemical properties of the catalysts. For instance chlorine can improve the dispersion of supported metals and alter the activity and selectivity. Moreover, chlorine can significantly reduce both the adsorption rate and capacity of a metal surface and it can lead to a serious poisoning effect because of its stronger electronegativity [12]. In this study, the CO oxidation reaction kinetics of the $Pt/\gamma\text{-}Al_2O_3$ and $Pt/CeO_2$ powder catalysts and the effect of residual chlorine on the performance of the catalysts were comparatively investigated.

## 2. Experimental

### 2.1. Catalyst Preparation

In this study pure and mixed oxides of $CeO_2$ and $\gamma$-$Al_2O_3$ were used as catalyst supports. Powders of $\gamma$-$Al_2O_3$ and $CeO_2$ obtained from Johnson Matthey were used as received. Two other pure $CeO_2$ supports were prepared by calcination of $CeCl_3.XH_2O$ (Johnson Matthey) and $Ce(C_2H_3O_2)_3.1.5H_2O$ (Johnson Matthey) at 600 °C for 4 hours. $CeO_2$ powder obtained from Johnson Matthey will be referred to as $CeO_2$(A) and $CeO_2$ powders prepared from $CeCl_3.XH_2O$ and $Ce(C_2H_3O_2)_3.1.5H_2O$ will be referred to as $CeO_2$(B) and $CeO_2$(C) respectively. The mixed oxides were either obtained as mechanical mixtures of these pure powders, or prepared via incipient wetness impregnation of $\gamma$-$Al_2O_3$ with an aqueous solution of ceria precursors mentioned above. The mechanical mixture of oxides was obtained by wet mixing pure oxides with subsequent drying and calcination at 600 C for 4 hours. The physical characterization of this support, $CeO_2$(A)/$\gamma$-$Al_2O_3$, by X-ray Diffraction (XRD) analysis revealed little difference from the original oxides. In order to prepare the mixed oxide from $CeCl_3.XH_2O$ or $Ce(C_2H_3O_2)_3.1.5H_2O$, an appropriate amount of precursor was dissolved in 1-2 ml water/g $\gamma$-$Al_2O_3$ and this solution was impregnated on $\gamma$-$Al_2O_3$. The final slurry was dried in air at 120 °C and calcined at 600 °C for four hours. In order to increase the solubility $CeCl_3.XH_2O$ the precursor was dissolved in water in an ultrasonic bath for 30 min before impregnating over $\gamma$-$Al_2O_3$. The water stoichiometry of $CeCl_3.XH_2O$ was determined via Thermo Gravimetric Analysis (TGA). For $CeCl_3.XH_2O$, the weight loss at ~100 °C indicated that the original sample water

stoichiometry was X = 0.72. Furthermore, it was observed that a significant amount of precursor was evaporated and lost during the oxidative treatment before full calcination. The calcination started at 275 °C and was completed at 442 °C. Thus the calcination temperature to obtain pure and $\gamma$-$Al_2O_3$ supported $CeO_2$(B) was selected as 600 °C. Furthermore, the original precursor amounts for $\gamma$-$Al_2O_3$ supported $CeO_2$ was adjusted to account for the evaporative material loss to adjust the final $CeO_2/\gamma$-$Al_2O_3$ stoichiometry. No such weight loss was observed for $Ce(C_2H_3O_2)_3.1.5H_2O$. The final structure of the oxide monitored by X-Ray Diffraction analysis revealed that the $CeO_2$(B) prepared from $CeCl_3.XH_2O$ had the pure $CeO_2$ crystal structure.

Platinum was incorporated to pure or mixed oxide supports by incipient wetness technique. For this, an appropriate amount of the metal salt $Pt(NH_3)_4Cl_2.H_2O$ (tetraamine platinum-II-chloride, Johnson Mattey) was dissolved in 1-2 ml water/g support to bring the samples to incipient wetness. The solution was impregnated onto the support and the final mixture was dried overnight at room temperature and for 4 hours at 120 °C. Then the samples were ground and calcined at 450 °C for 4 hours. After calcination, half of the prepared catalysts were washed with hot water to eliminate chlorine contamination. Washing was continued until the filtered solution did not contain any $Cl^-$ ions, which was tested by $AgNO_3$ solution. The other half was used without further treatment to elucidate the effect of residual chlorine on the catalyst activity.

The resulting powders were reduced in $H_2$ under static conditions. The reduction was done in a home built Pyrex manifold of 160 ml volume, coupled with Baratron gauges (Varian) and a Turbo-molecular pump backed up by a mechanical pump (Varian Turbo V). The details of the manifold and the experimental procedure can be found

elsewhere [26]. Prior to static reduction, the samples were dehydrated under 100 Torr He at 150 °C for 15 min followed by evacuation. Subsequently, the sample was heated up to 350 °C under vacuum and dehydrated under 100 Torr He for another 15 min, again followed by evacuation. During $H_2$ reduction at 350 °C, 750 Torr of $H_2$ was dosed for 30 min intervals each followed by evacuation, for a total duration of 2 hours. The catalysts and their descriptions are given in Table 3. Pt loading in all of the catalysts were maintained at 1 wt % level, and $CeO_2$ level was adjusted to be 10 % of the total oxide weight in $Pt/CeO_2/\gamma\text{-}Al_2O_3$ catalysts.

### 2.2. Characterization of supports and catalysts

The oxidation behaviors and water contents of $CeCl_3.XH_2O$ and $Ce(C_2H_3O_2)_3.1.5H_2O$ precursors were determined by Du Pont 951 Thermo Gravimetric Analyzer (TGA). $CeO_2$(B) obtained from $CeCl_3.XH_2O$ and $CeO_2$(C) obtained from $Ce(C_2H_3O_2)_3.1.5H_2O$ were analyzed by Philips PW 1840 X-Ray Diffractometer to elucidate the final structure of the oxide. All of the supports were characterized by measuring their surface area with $N_2$ adsorption in Micromeritics ASAP 2000 BET equipment.

The metal dispersions of the finished catalysts were measured by a modified $H_2$ chemisorption experiment [17]. After reduction at 350 °C in $H_2$ under static conditions, the catalysts were cooled to room temperature under vacuum. The total and weak hydrogen adsorption isotherms were measured in the pressure range of 1 – 20 Torr at room temperature. The difference between total and weak adsorption isotherms

extrapolated to zero pressure was taken as strongly adsorbed $H_2$ and the dispersion of the Pt was calculated by assuming a 1:1 stoichiometry of H:Pt.

### 2.3 Reactivity Toward CO + $O_2$, Light-Off Tests

The CO oxidation performances of the catalysts were tested in a home built reactor system described in detail elsewhere [19]. For this purpose 0.1 g catalyst (diluted with 0.9 g $\gamma$-$Al_2O_3$) was placed in a quartz reactor inside of a temperature controlled (UDC 2300 Universal Digital Controller) tubular furnace (Protherm PTF 12/70/450). The bed temperature was increased from 300 K at 1.0 K/min heating rate under the flow of feed gases. Temperature was measured by using a thermocouple externally placed over the catalyst bed. 200 ml/min total flow rate was maintained for the feed which was composed of 5 vol. % CO, 2.5 vol. % $O_2$, and the balance $N_2$ unless otherwise indicated. The gas compositions were adjusted by using MKS type 1179A mass–flow controllers. The exit gases were sampled every 6 minutes via a 6-port valve and sent to a Gas Chromatograph (HP 4890) equipped with a CTR-I column and analyzed via a TCD. The conversions were determined from produced $CO_2$ amounts. Reproducibility of the light-off experiments was tested by performing at least two separate experiments for the Pt/$\gamma$-$Al_2O_3$ catalyst under stoichiometric conditions. In addition, the basic calculations for the mass transfer limitations showed that the external film mass transfer coefficient was high (~$10^4$) and effectiveness factor was approaching to 1.0 because the particle sizes were low ($\leq 10^{-4}$ m).

### 2.4. Isothermal CO Oxidation Reactions

The reaction orders were determined under isothermal conditions. The temperatures were adjusted such that the CO conversions remained less than 20 % a rough approximation for a differential reactor. While keeping the temperature and composition of the one of the reactants constant, the composition of the other reactant was changed. In order to keep reaction conditions consistent with the non-isothermal experiments, the composition of the CO was changed from 3-6 % by volume while keeping the $O_2$ at 2.5 % by volume. On the other hand, the composition of the $O_2$ was changed from 2-3 % by volume while keeping the CO at 5 % by volume. As a result, the reaction stoichiometry has spanned the whole range of lean-rich conditions. Experimental conditions such as total feed flow rate and catalyst loading were kept constant at 200 ml/min and 0.1 gram.

## 3. Results

### 3.1. Catalyst Characterization

The results of BET surface areas and platinum dispersion measurements via hydrogen chemisorption are shown in Table 4. The BET results revealed that the surface area of $Pt/CeO_2(C)$ (64.6 $m^2/g$) was much higher than that of $Pt/CeO_2(A)$ (2.7 $m^2/g$) or $Pt/CeO_2(B)$ (16.2 $m^2/g$). A general trend observed in this study is that the Pt dispersions

were higher when $\gamma$-$Al_2O_3$ was used as a support. However, it was not possible to measure the metal dispersions by strong hydrogen chemisorption when the catalysts were prepared from $CeCl_3.XH_2O$. This was attributed to the presence of residual chlorine ions from both oxide and metal precursors. To understand the effects of chlorine coming from precursors, all catalysts were washed for further dispersion analyses. It was observed that, for all catalysts washing improved their metal dispersion values.

### 3.2. Steady State Non – Isothermal CO Oxidation Reactions

The performances of the prepared catalysts on CO oxidation reaction were tested under the conditions described in experimental part. In order to be sure that the supports do not show any activity under the reaction conditions, pure supports were examined in terms of their CO oxidation reaction performances under stoichiometric conditions. The results are presented in Table 5 in terms of temperatures required to achieve 5%, 50% and 99% conversions ($T_5$, $T_{50}$, and $T_{99}$). It is clearly seen that pure supports require much higher temperatures to light-off. Therefore their contribution to the overall conversions could easily be neglected.

The light off curves of the 1 % Pt/$\gamma$-$Al_2O_3$ 1 % Pt/$CeO_2$(A)/$\gamma$-$Al_2O_3$, 1 % Pt /$CeO_2$(B)/$\gamma$-$Al_2O_3$ 1 % Pt/$CeO_2$(C)/$\gamma$-$Al_2O_3$ catalysts prior to hot water elutriation under stoichiometric conditions are presented in Fig. 1. Similarly, the light off curves of the 1 % Pt/$\gamma$-$Al_2O_3$, 1 % Pt /$CeO_2$(B)/$\gamma$-$Al_2O_3$, and 1 % Pt/$CeO_2$(C)/$\gamma$-$Al_2O_3$ catalysts after hot water elutriation under stoichiometric conditions are presented in Fig. 2. On the other hand, the performances of all the catalysts before and after hot water elutriation under

stoichiometric reaction conditions are given in terms of their light off, 50% conversion and 99% conversion values in Table 6.

When comparing the catalysts prepared from pure oxides, it was observed that $Pt/CeO_2(A)$ is a better catalyst than $Pt/\gamma\text{-}Al_2O_3$ in terms of CO oxidation temperatures. When the catalyst changed from $Pt/\gamma\text{-}Al_2O_3$ to $Pt/CeO_2(A)$ the reaction onset temperature decreased to from 477 to 423 K (see Table 6). On the other hand, $Pt/CeO_2(A)/\gamma\text{-}Al_2O_3$ catalyst did not show any activity superior to the $Pt/\gamma\text{-}Al_2O_3$ catalyst as shown in Table 6. Actually, the reaction onset temperature of the $Pt/CeO_2(A)/\gamma\text{-}Al_2O_3$ catalyst was slightly higher than the $Pt/\gamma\text{-}Al_2O_3$ catalyst. This was attributed to a simple dilution effect of $CeO_2$. The net effect observed on $Pt/CeO_2(A)\text{-}\gamma Al_2O_3$ was a right shift of the light-off curves, i.e. higher temperatures were required to achieve the same conversion under the same reaction conditions. This effect was interpreted as a dilution effect of ceria. When ceria weight was excluded, the net weight of the catalyst was 10% lower than $Pt/Al_2O_3$ thus the space-time of the reactive mixture was respectively lower. When the light off curves were adjusted with respect to the space times of $Pt/\gamma\text{-}Al_2O_3$ as described by Uner and Kaya [20], the light off curves were shifted to left and the temperatures were similar to that of pure $Pt/\gamma\text{-}Al_2O_3$ (Table 6). These results were interpreted as evidence for Pt selectively going on $\gamma\text{-}Al_2O_3$ and the mixed oxide supported catalyst behaved as if it were pure $Pt/\gamma\text{-}Al_2O_3$. This conclusion was further supported by the measured orders and activation energies over this particular catalyst. The reaction orders and activation energies resembled closely that of pure $Pt/\gamma\text{-}Al_2O_3$ further indicating that the Pt selectively went on $\gamma\text{-}Al_2O_3$ over the mechanical mixture of the oxide catalysts. Another observation for these catalysts was that, the residual chlorine coming from Platinum precursor did not have much effect on

catalyst performances towards CO oxidation under the imposed reaction conditions, although it had a negative effect on their metal dispersion values.

Before the mixed oxide catalyst supports prepared from $CeCl_3.XH_2O$ were discussed, it is worthwhile to mention the performance of the pure oxide catalyst prepared from $CeCl_3.XH_2O$. The light-off test results of washed and unwashed $Pt/CeO_2(B)$ catalyst are shown in Table 6 in the form of $T_5$, $T_{50}$, $T_{99}$ values. For this catalyst, the reaction onset temperature was measured as 486 K, a value higher than the corresponding alumina supported catalyst. However, the metal dispersion value of $Pt/CeO_2(B)$ catalyst improved from ~0% to ~50% and the reaction onset temperatures and $T_{50}$ values were decreased to 345 K and 358 K respectively after chlorine removal by washing.

The mixed oxide catalysts were prepared by sonicating the aqueous mixture of cerium salt and alumina. The use of an ultrasonic bath during the support preparation period increased the surface area and the activity of the $Pt/CeO_2(B)/\gamma\text{-}Al_2O_3$ catalyst. The reaction onset and $T_{50}$ values of the un-washed catalyst was 458 K and 498 K respectively while on the washed catalysts these values decreased to 390 K and 415 K. However, the activity of the washed $Pt/CeO_2(B)/\gamma\text{-}Al_2O_3$ catalyst was still worse than activity of the $Pt/CeO_2(B)$ catalyst.

Among all the catalysts $Pt/CeO_2(C)$ showed the best performance. Both its washed and un-washed reaction onset and $T_{50}$ values were the lowest. Similarly $Pt/CeO_2(C)/\gamma\text{-}Al_2O_3$ catalyst had the best performance towards CO oxidation reaction among the catalysts containing $\gamma\text{-}Al_2O_3$ (see Table 6). These catalysts were strongly affected by the residual chlorine coming from platinum precursor as indicated by the change in their dispersion values upon washing. The $T_{50}$ value of the $Pt/CeO_2(C)$

catalyst decreased around 15 K while that of the $Pt/CeO_2(C)$ /$\gamma$-$Al_2O_3$ catalyst decreased around 30 K upon chlorine removal by washing.

### 3.3. Steady State Isothermal CO Oxidation Reactions

Isothermal CO oxidation reactions experiments were conducted for all catalysts. First, experiments were performed with the $Pt/CeO_2(A)$ catalyst over a wide range of CO and $O_2$ partial pressures. The gas phase composition of CO was changed from 2 to 6 % by volume while keeping the $O_2$ at 3 % by volume level to determine the reaction orders with respect to CO. Similarly, CO was kept at 3 % while the $O_2$ was changed from 2 to 6 % by volume for determining the reaction orders with respect to oxygen. To determine the reaction orders, ln(rate) vs $\ln(P_{CO})$ or $\ln(Po_2)$ plots were drawn. For the simplicity of the calculations the reactor was operated at conversion levels less than 20 % and differential reactor assumptions were accepted. Because the reaction orders with respect to $P_{CO}$ and $Po_2$ were remained constant over a wide pressure range over $Pt/CeO_2$ catalyst, the range of $P_{CO}$ and $Po_2$ was narrowed for other catalysts. Thus, the CO composition was changed from 3 to 6 % while the $O_2$ was kept at 2.5 % by volume and the CO was kept at 5 % while the $O_2$ was changed from 2 to 3 % by volume. The reaction orders and the order measurement temperatures ($T_{iso}$) were presented in Table 6.

The results shown in Table 6 exhibit the following general trends: First of all over $\gamma$-$Al_2O_3$ supported Pt catalysts the reaction orders were determined as almost first order with respect to $O_2$ partial pressure and almost negative second order with respect

to CO partial pressure. This trend was not influenced by the presence of residual chlorine ions. Furthermore, when the mixed oxide support was prepared as a mechanical mixture of $CeO_2$(A) and $\gamma$-$Al_2O_3$ the measured reaction orders were almost similar to that of pure $\gamma$-$Al_2O_3$ supported platinum catalyst. Second trend observed was the consistency in the reaction orders of Pt supported over $CeO_2$ or $CeO_2/\gamma$-$Al_2O_3$ prepared via an incipient wetness technique. On these catalysts the reaction orders were measured as approximately zeroth order with respect to $O_2$ partial pressure and negative first order with respect to CO. Again, on these catalysts the reaction order did not change upon chlorine elimination indicating that the presence of chlorine did not alter the reaction mechanism.

### 3.4. Apparent Activation Energies

Apparent activation energies of the catalysts were calculated from by drawing the ln(rate) vs 1/T plots. The ln(rate) vs 1/T data were directly obtained from the light - off results of the catalysts. Again to assume the reactor as a differential reactor the conversion values was kept below 25 %. The apparent activation energies determined as such were shown in Table 6.

## 4. Discussion

### 4.1. Reaction mechanisms

In this study the performances of the $Pt/\gamma\text{-}Al_2O_3$, $Pt/CeO_2$ and $Pt/CeO_2/\gamma\text{-}Al_2O_3$ powder catalysts on CO oxidation reaction with and without chlorine were investigated. It was observed that when the support changed from $\gamma\text{-}Al_2O_3$ to $CeO_2$ (A,B,C) both reaction onset temperature and $T_{50}$ decreased consistent with the literature. The main reason of this change is due to a change in reaction mechanism, which is evident from the reaction orders and activation energies: The reaction orders for oxygen and CO was found as approximately +1 and –2 for $Pt/\gamma\text{-}Al_2O_3$ catalyst while those for $Pt/CeO_2$ catalyst were found as 0 and -1.

Given the reaction orders, a model was developed for $Pt/\gamma\text{-}Al_2O_3$ with the following assumptions:

i) The surface is poisoned by the adsorbed CO atoms, i.e., CO coverage is nearly one.

ii) The rate limiting step is the dissociative adsorption of oxygen.

The surface reactions were depicted as follows:

1. $CO + * \rightarrow CO*$
2. $O_2 + 2* \rightarrow 2O*$
3. $CO* + O* \rightarrow CO_2 + 2*$

As a result of the first assumption, the vacant site coverage could be written as

$\theta_v = 1 - \theta_{CO}$

and the second assumption leads to

rate= $k_2P_{O2}\theta_v^2$

Given that the first step proceeds under pseudo-equilibrium conditions

$\theta_{CO} = K_1P_{CO}/(1+K_1P_{CO})$

such that the reaction rate takes the following form:

rate=$k_2P_{O2}/(1+K_1P_{CO})^2$

here $k_i$ and $K_i$ are the rate and equilibrium constants of the $i^{th}$ step, respectively. $\theta_i$ indicate the fractional surface coverage of the $i^{th}$ species.

With these assumptions, and under the conditions that $K_1P_{CO} >>1$ a rate expression which is negative second order in terms of CO partial pressures and first order in terms of oxygen partial pressure could be obtained.

On the other hand, over the $Pt/CeO_2$ catalysts, the experimental reaction orders still indicated a CO poisoned mechanism while the reaction was almost zero order with respect to $O_2$ partial pressures. Probably over the $Pt/CeO_2$ catalyst reaction proceeds through the adsorbed CO and oxygen adatoms which are first dissociatively adsorbed on ceria surface and than reverse spilled over the platinum surface where, the reverse spill over oxygen adatom to platinum surface is the rate-determining step and CO is the most abundant surface species. Generally it is accepted that the CO oxidation reaction over platinum catalyst in the presence of ceria proceeded at the platinum-ceria interface between the adsorbed CO on platinum surface and oxygen adatom from ceria[27].

Again if we examined these sequence of steps mechanistically the assumptions are

i) The Pt surface is poisoned by the adsorbed CO atoms, i.e., CO coverage over Pt is nearly one.

ii) The rate limiting step is the oxygen exchange at the ceria and Pt interface.

iii) even in the absence of gas phase oxygen, ceria surface is oxidized, therefore the surface coverage of oxygen over ceria can be taken as independent of the gas phase oxygen partial pressure.

The surface reactions were depicted as follows:

1. $CO + * \rightarrow CO_*$
2. $O_2 + 2\otimes \rightarrow 2O_\otimes$
3. $O_\otimes + * \rightarrow O_* + \otimes$
4. $CO_* + O_* \rightarrow CO_2 + 2*$

Where * denotes a catalytic site on the Pt surface and $\otimes$ denotes a site over ceria surface.

As a result of the first assumption, the vacant site coverage over Pt could be written as

$\theta_v = 1 - \theta_{CO}$

and the second assumption leads to

rate= $k_2 \theta_{O\otimes} \theta_v$

The third assumption renders the surface coverage of oxygen over ceria almost constant such that rate= $k_2' \theta_v$, where $k_2' = k_2 \theta_{O\otimes}$.

Given that the first step proceeds under pseudo equilibrium conditions

$\theta_{CO} = K_1 P_{CO}/(1+K_1 P_{CO})$

such that the reaction rate takes the following form:

rate=$k_2' /(1+K_1 P_{CO})$

thus substantiating the measured reaction orders in this study.

### 4.2. Effect of chlorine on the catalytic activities

It was found that the presence of the chlorine greatly diminishes the activity of catalysts except $Pt/CeO_2(A)$ and $Pt/\gamma\text{-}Al_2O_3$ catalysts towards the CO oxidation reaction. For these two catalysts, the dispersion measurements by hydrogen chemisorption reveal not much difference between washed and unwashed catalysts. Therefore, it is fair to conclude that the amount of residual chlorine on these catalysts is not significant to alter the reaction. The chlorine originated from precursor was apparently removed during the catalyst calcination[28]. The residual chlorine was removed by washing the catalysts with a de-ionized water at temperatures around 95 °C as in the study of Wu et al. [13]. Wu et al. [13] reported that the residual chlorine could be removed completely from the $Ru/SiO_2$ catalyst just by washing with distilled hot water. In a different study Cant et al. [14] claimed that during the reduction or catalyst preparation period, steam is needed for removal of chlorine deposited on alumina support. In fact, the activity improvement observed on catalysts except $Pt/CeO_2(A)$ and $Pt/\gamma\text{-}Al_2O_3$ catalysts after washing indicated that the residual chlorine diminished the activity of the catalysts.

In this study it is also observed that washing had different effects on the metal dispersion values of the catalysts. For example, although washing highly improved the metal dispersion of the $Pt/CeO_2(B)$ and $Pt/CeO_2(C)$ catalysts, it had weaker effect on $Pt/CeO_2(B)/\gamma\text{-}Al_2O_3$ catalyst dispersions. Differences between the metal dispersion values of catalysts might be due to different effects of presence of chlorine. Salasc [21] suggested that because of the presence of the chlorine, on the $Pt/CeO_2/\gamma\text{-}Al_2O_3$ catalysts there are less sites able to chemisorb hydrogen leading to the formation of hydroxyl species on the surface and the hydrogen spillover is strongly inhibited. However, this

effect can be eliminated probably with hot water elutriation. On the other hand, the interactions between the supported platinum and the chlorine might be stronger as stated by Lieske et al. [15] and Zhou et al. [16]. They pointed out that chlorine can be strongly bonded to the support and then the platinum oxide crystallites can interact with it to form oxychloroplatinum complexes such as $PtO_xCl_y$, which have greater mobility. It is possible that the highly mobile oxychloroplatinum complexes caused the segregation of the platinum particles on $\gamma$-$Al_2O_3$ surface (leading to less metal dispersion value) after repeated treatments. For the $Pt/CeO_2(B)/\gamma$-$Al_2O_3$ catalyst most of the residual chlorine was coming form $CeCl_3.XH_2O$ but the for $Pt/CeO_2(C)/\gamma$-$Al_2O_3$ catalyst platinum precursor was the only residual chlorine source. It is possible that the source and amount of the residual chlorine can affect the catalysts in different ways.

As a result, it can be said that the presence of the chlorine in the catalysts reduces both the adsorption rate and capacity of a metal surface, which could be partially eliminated just by washing the catalysts with hot de-ionized water. Also, presence of the chlorine greatly diminishes the activity of the catalysts except for $Pt/CeO_2(A)$ and $Pt/\gamma$-$Al_2O_3$ catalysts.

Furthermore, the removal of chlorine did not seem to influence neither the reaction orders nor the activation energies of the catalysts to an appreciable extent as can be seen from Table 6. The largest difference in the measured activation energies between washed and unwashed catalysts occurred ($Pt/CeO_2$ (C)/$\gamma$-$Al_2O_3$, $Pt/CeO_2$ (B)/$\gamma$-$Al_2O_3$) when the measurement temperatures varied largely in order to maintain isokinetic conditions. Although highly speculative at this stage, it is important to note the fact that over the majority of the catalysts studied here the lack of change of the orders and the activation energies in the presence of chlorine can be attributed to the

fact that chlorine prefers to occupy the catalyst sites that are not directly important for the CO oxidation reaction. The site blocking effect is still apparent, though, through the dispersions measured via hydrogen chemisorption. The decrease in the reaction rates in the presence of chlorine without an appreciable change in the activation energies or reaction orders can be attributed to a decrease in the Arrhenius pre-exponential factor. On a fundamental level, the pre-exponential factor contains information about the sticking coefficients, entropy changes due to adsorption, reaction or desorption and the number and geometry of the surface sites. It seems that the presence of chlorine do not influence the reaction via electron transfer mechanisms, which should have reflected itself in the apparent activation energies, but it influences the overall reaction via a site blocking mechanism.

## 5. Conclusions

In this study the performances of the $Pt/\gamma\text{-}Al_2O_3$, $Pt/CeO_2$ and $Pt/CeO_2/\gamma\text{-}Al_2O_3$ powder catalysts on CO oxidation reaction were investigated. It was found that $Pt/CeO_2$ was a better catalyst than $Pt/\gamma\text{-}Al_2O_3$ in terms of CO oxidation reaction. It was observed that when the support changed from $\gamma\text{-}Al_2O_3$ to $CeO_2$ reaction onset temperature, $T_{50}$ and apparent activation energies decreased in accordance with the literature. It was also found that, while the activation energy of $Pt/\gamma\text{-}Al_2O_3$ catalyst under stoichiometric conditions was around 110.0 kJ/mol that of $Pt/CeO_2$catalysts were around 60 kJ/mol. This was attributed to the change in reaction mechanism over $Pt/CeO_2$ catalyst, which was proven by isothermal experiments. Reaction orders of CO and $O_2$ was found approximately as –2.0 and +1.0 respectively over the $Pt/\gamma\text{-}Al_2O_3$ catalyst. However over

the $Pt/CeO_2$ catalysts the orders of CO and $O_2$ was found as -1 and 0. It was observed that presence of the residual chlorine decreased metal dispersion value of all catalysts except $Pt/\gamma\text{-}Al_2O_3$. Similarly, activities of the catalysts except $Pt/\gamma\text{-}Al_2O_3$ and $Pt/CeO_2(A)$ towards the CO oxidation reaction was decreased in the presence of chlorine. Those negative effects of the residual chlorine could be partially removed by just hot water elutriation. $Pt/CeO_2(C)$ was the best catalyst among all $Pt/CeO_2$ catalysts and $Pt/CeO_2(C)/\gamma\text{-}Al_2O_3$ showed the best performance among all $Pt/CeO_2/\gamma\text{-}Al_2O_3$ catalysts.

## 6. Acknowledgements

The financial support for this project was provided by the Middle East Technical University Research Fund Projects under contract AFP-2000-03-04-04 and by Turkish Scientific and Technical Research Council, TUBITAK, under research contract no MISAG 188. Supplemantary funds were provided by TUBITAK Researh Infrastructure Support Funds under grant no MISAG A-54. The authors also gratefully acknowledge Hilal Demir's assistance during dispersion measurements.

## 7. References


1. J. R. Gonzalez-Velasco, M. A. Gutierrez-Ortiz, J.L. Marc, J. A. Botas, M.P. Gonzalez-Marcos, G. Blanchard, Appl. Catal. B-Environmental 25 (2000) 19.

2. J.R. Gonzalez-Velasco, M.A. Gutierrez-Ortiz, J.L. Marc, J.A. Botas, M.P. Gonzalez-Marcos, G. Blanchard, Appl. Catal. B- Environmental 22 (2000) 167.

3. R. Di Monte, P. Fornasiero, J. Kaspar, P. Rumori, G. Gubitosa, M. Graziani, Appl. Catal. B- Environmental 24 (2000) 157.

4. P. Fornasiero, G. Balducci, R. Di Monte, J. Kaspar, V. Sergo, G. Gubitosa, A. Ferrero, M. Graziani, J. Catal. 164 (1996) 173.

5. C.E. Hori, H. Permana, K.Y.S. Ng, A. Brenner, K. More, K.M. Rahmoeller, D. Belton, Appl. Catal. B- Environmental 16 (1998) 105.

6. A. Martinez-Arias, R. Cataluna, J.C. Conesa, and J.Soria, J. Phys. Chem. B 102 (1998) 809.

7. C. Serre, F. Garin, G. Belot, G. Maire, J. Catal. 141 (1993) 1.

8. S. H. Oh, J. Catal. 124 (1990) 477.

9. C. Serre, F. Garin, G. Belot, G. Maire, J. Catal 141 (1993) 9.

10. H. C. Yao, Y. F.Y. Yao, J. Catal. 86 (1984) 254.

11. R. M. Heck, R.J. Farrauto, Catalytic Air Pollution Control: Commercial technology, Van Nostrand Reinhold, New York, 1995.

12. W.P. Dow, T.J. Huang, Appl. Catal. A-General 141 (1996) 17.

13. X. Wu, B. C. Gerstein, T. S. King, J. Catal. 135 (1992) 68.

14. N. W. Cant, D. E. Angove, M. J. Patterson, Catal. Today 44 (1998) 93.

15. H. Lieske, G. Lietz, H. Spindler, J. Völter, J. Catal. 81 (1983) 8.

16. Y. Zhou, M. C. Wood, N. Winograd, J. Catal. 146 (1994) 82.

17. D.O. Uner, M. Pruski, B. C. Gerstein, T.S. King, J. Catal. 146 (1994) 530.

18. J. G. Nunan, H. J. Robota, M. J. Cohn, S. A. Bradley, J. Catal. 133 (1992) 309.

19. U. Oran MS Thesis, Middle East Technical University, Ankara, 2001.

20. D. Uner, S. Kaya, Stud. Surf. Sci. Catal. 133 (2001) 453.

21. S. Salasc, V. Perrichon, M. Primet, M. Chevrier, E. Mathis, N. Moral, Catal. Today 50 (1999) 227.

22. C. Hardacre, R. M. Ormerod, R. M. Lambert, Chem. Phys. Lett. 206 (1993) 171.

23. G. S. Zafiris, R. J. Gorte, J. Catal. 140 (1993) 418.

24. H. Muraki, S Matunaga, H. Shinjoh, M. S. Wainwright, D. L. Trimm, J. Chem. Tech. Biotechnol. 52 (1991) 415.

25. M. J. Kahlich, H. A. Gasteiger, R. J. Behm, J. Catal. 171 (1997) 93.

26. D. Uner, N.A. Tapan, I. Ozen, M. Uner, App. Catal. A-General, 251 (2003), 225.

27. C. Li, Y.X. Chen, W.Z. Li, Q. Xin, Stud. Surf. Sci. Catal. 77(1993) 217.

28. F.J. Gracia, J.T. Miller, A.J. Kropf, E.E. Wolf, J.Catal, 209(2002) 341.

## List of Tables



## List of Figures

**Table 1.**

| Catalyst | Activation | $T_{50}$ (K) | $CeO_2$ (wt %) | T range (K) | Ref. |
|---|---|---|---|---|---|
| $Pt/CeO_2/\gamma\text{-}Al_2O_3$ | Oxidizing | 748 | 23 | 423-773 | [16] |
| | Reducing | 493 | | | |
| $Pt/CeO_2/\gamma\text{-}Al_2O_3$ | Oxidizing | 618 | 20 | | |
| | Reducing | 548 | | | |
| $Pt/\gamma\text{-}Al_2O_3$ | - | 593 | - | | |
| $Pt/\gamma\text{-}Al_2O_3$ | 10% $O_2/N_2$ at 623 K 30 min | 473 | - | 423-523 | [20] |
| $Pt/\gamma\text{-}Al_2O_3$ | - | 443 | N/A | N/A | [21] |
| | - | 440 | | | |
| | - | 448 | | | |
| | - | 468 | | | |
| | - | 495 | | | |
| $Pt/\gamma\text{-}Al_2O_3$ | Reduction in 4% $H_2$ in Ar | 473 | - | N/A | [22] |
| $Pt/CeO_2/\gamma\text{-}Al_2O_3$ | | 373 | 20 | | |
| $Pt/CeO_2/\gamma\text{-}Al_2O_3$ | - | 568 | 24 | N/A | [23] |
| | Lean | 518 | | | |
| | Rich | 398 | | | |
| $Pt/\gamma\text{-}Al_2O_3$[1] | - | 555 | - | | |
| | Rich | 518 | - | | |
| $Pt/CeO_2$[1] | - | 628 | 100 | | |
| $Pt/\gamma\text{-}Al_2O_3$ | 3% $O_2/N_2$ at 673 K 1h | 563 | - | N/A | [24] |
| $Pt/CeO_2/\gamma\text{-}Al_2O_3$ | | 443 | 10 | | |
| $Pt/\gamma\text{-}Al_2O_3$ | 1.5 % CO/He at 973 K | 476 | - | N/A | [25] |
| | 5% $O_2$/He at 973 K | 499 | - | | |
| $Pt/CeO_2/\gamma\text{-}Al_2O_3$ | 1.5 % CO/He at 973 K | 357 | 14.5 | | |
| $Pt/CeO_2/\gamma\text{-}Al_2O_3$ | 5% $O_2$/He at 973 K | 477 | | | |
| $Pt/\gamma\text{-}Al_2O_3$ | 0.5% CO, 0.5% $O_2$ in $N_2$ | 483 | - | | |
| | 1.0% CO, 0.25% $O_2$ in $N_2$ | 500[1] | - | | |
| $Pt/CeO_2/\gamma\text{-}Al_2O_3$ | 0.5% CO, 0.5% $O_2$ in $N_2$ | 499 | 14.5 | | |
| | 0.5% CO, 0.5% $O_2$ in $N_2$ | 487[1] | | | |
| | 1.0% CO, 0.25% $O_2$ in $N_2$ | 426 | | | |
| | 1.0% CO, 0.25% $O_2$ in $N_2$ | 434[1] | | | |

[1] Activity was measured in terms of $T_{25}$ (Temperature required for the 25 % conversion).

**Table 2.**

Rate = $k.P_{CO}^{m}.Po_2^{n}$

| Catalyst | T range (K) | $E_a$ (kJ/mol) | m | n | Ref. |
|---|---|---|---|---|---|
| Pt/γ-$Al_2O_3$ | 436-503 | 112 | -1 | 1 | [13] |
| Pt//$RhCeO_2$/γ-$Al_2O_3$ | | N/A | -0.3 | 0.5 | |
| Pt/γ-$Al_2O_3$ | 373-433 | | -1 | 1 | [14] |
| Pt (100) | 425-725 | 138 if T≥500K | -1 | 1 | [15] |
| | | 54 if T≤ 473 K | -0.6 to 0 | 1 | |
| Pt-wire | ≤ 473 | 126 | -1 | 1 | [16] |
| Pt/γ-$Al_2O_3$ | | 92 - 125 | -0.6 to -1 | 0.7 to 1 | |
| Pt/$CeO_2$/γ-$Al_2O_3$ | | 50 - 117 | -0.6 to 1 | 0 to 0.9 | |
| Pt (111) | 323-430 | 69-36 | 0 | 1 | [17] |
| Pt/α-$Al_2O_3$ (0001) | 560-680 | 125-172 | -1 | 1 | [18] |
| Pt/γ-$Al_2O_3$ | ≤ 473 | 55.2 | -1.5 | 1 | [19] |
| Pt/γ-$Al_2O_3$ | 423-523 | 71 | -0.4 | 0.8 | [20] |

**Table 3.**

| Catalyst | Descriptions |
|---|---|
| Pt/ $\gamma$-$Al_2O_3$ | $\gamma$-$Al_2O_3$ powder obtained from Johnson-Matthey used as recieved. |
| Pt/ $CeO_2$ **(A)** | $CeO_2$(A) powder obtained from Johnson-Matthey used as recieved. |
| Pt/$CeO_2$ **(A)**/$\gamma$-$Al_2O_3$ | $CeO_2$(A)/$\gamma$-$Al_2O_3$ support prepared from the mechanical mixture of these pure powders. The mechanical mixture of oxides was obtained by wet mixing pure oxides with subsequent drying and calcination at 600 C for 4 hours. |
| Pt/ $CeO_2$ **(B)** | $CeO_2$(B) support obtained from the calcination of $CeCl_3.XH_2O$ at 600°C for four hours. |
| Pt/$CeO_2$ **(B)**/$\gamma$-$Al_2O_3$ | $CeO_2$(B-2)/$\gamma$-$Al_2O_3$ support prepared via an incipient wetness impregnation of aqueous solution of $CeCl_3.XH_2O$ and $\gamma$-$Al_2O_3$ in an ultrasonic bath following drying at 120°C and calcination at 600°C. |
| Pt/ $CeO_2$ **(C)** | $CeO_2$(C) support prepared by calcination of $Ce(C_2H_3O_2)_3.1.5H_2O$ at 600°C for four hours. |
| Pt/$CeO_2$ **(C)**/$\gamma$-$Al_2O_3$ | $CeO_2$(C)/$\gamma$-$Al_2O_3$ support prepared via an incipient wetness impregnation of aqueous solution of $Ce(C_2H_3O_2)_3.1.5H_2O$ and $\gamma$-$Al_2O_3$ following drying at 120°C and calcination at 600°C. |

**Table 4.**

| Catalyst | Surface area ($m^2/g$) | % Dispersion | |
|---|---|---|---|
| | | Before hot water elutriation | After hot water elutriation |
| Pt/ $\gamma$-$Al_2O_3$ | 66.2 | 50 | 55 |
| Pt/ $CeO_2$ (A) | 2.7 | 10 | 26 |
| Pt/$CeO_2$ (A)/$\gamma$-$Al_2O_3$ | 43.5 | 70 | NA |
| Pt/ $CeO_2$ (B) | 16.2 | ~ 0 | 50 |
| Pt/$CeO_2$ (B)/$\gamma$-$Al_2O_3$ | N/A | ~ 0 | 10 |
| Pt/ $CeO_2$ (C) | 64.6 | 17 | 59 |
| Pt/$CeO_2$ (C)/$\gamma$-$Al_2O_3$ | 52.5 | 7 | 54 |

NA : Hot water elutriation did not applied.

**Table 5.**

| Catalyst | Hot water elutriation | $T_5$ (K) | $T_{50}$ (K) | $T_{99}$ (K) |
|---|---|---|---|---|
| $CeO_2$(A) | No | 600 | 628 | 677 |
| $CeO_2$(B) | Yes | 640 | 710 | 743 |
| $\gamma$-$Al_2O_3$ | No | 600 | 650 | 673 |

$T_5$: The temperature at which 5% conversion is achieved

$T_{50}$: The temperature at which 50 % conversion is achieved

$T_{99}$: The temperature at which 99 % conversion is achieved

**Table 6.**

| Catalyst | Hot water elutriation | Dispersion (%) | $T_5$ (K) | $T_{50}$ (K) | $T_{99}$ (K) | Ea (kJ/mol) | $T_{iso}$ (K) | m | n |
|---|---|---|---|---|---|---|---|---|---|
| Pt/ $\gamma$-$Al_2O_3$ | No | 55 | 477 | 506 | 510 | 110 | 488 | -2.0 | +0.9 |
| Pt/$CeO_2$(A)/$Al_2O_3$ | No | 70 | 487 | 513 | 517 | 132 | 496 | -1.9 | +0.9 |
| Pt/$CeO_2$ (B)/$\gamma$-$Al_2O_3$ | Yes | 10 | 390 | 415 | 429 | 68 | 406 | -1.1 | 0.1 |
| | No | 0 | 458 | 498 | 509 | 80 | 479 | -0.9 | 0.2 |
| Pt/$CeO_2$ (C)/$\gamma$-$Al_2O_3$ | Yes | 54 | 367 | 392 | 409 | 42 | 382 | -1.3 | 0.1 |
| | No | 7 | 400 | 425 | 435 | 62 | 413 | -1.2 | 0.1 |
| Pt/$CeO_2$ (A) | Yes | 26 | 423 | 444 | 447 | 88 | 430 | -1.1 | 0.2 |
| | No | 10 | 419 | 446 | 452 | 85 | 427 | -1.2 | 0.2 |
| Pt/$CeO_2$ (B) | Yes | 50 | 345 | 358 | 366 | 61 | 350 | -1.1 | 0.2 |
| | No | 0 | 486 | 502 | 513 | 67 | 491 | -1.3 | 0.1 |
| Pt/$CeO_2$ (C) | Yes | 59 | 329 | 332 | 337 | 62 | 330 | -1.1 | -0.2 |
| | No | 17 | 338 | 345 | 352 | 50 | 340 | -1.0 | -0.1 |

m=Order of CO

n=Order of $O_2$

$T_5$: The temperature at which 5% conversion is achieved

$T_{50}$: The temperature at which 50 % conversion is achieved

$T_{99}$: The temperature at which 99 % conversion is achieved

$T_{iso}$: The temperature at which the reaction order measurements were performed

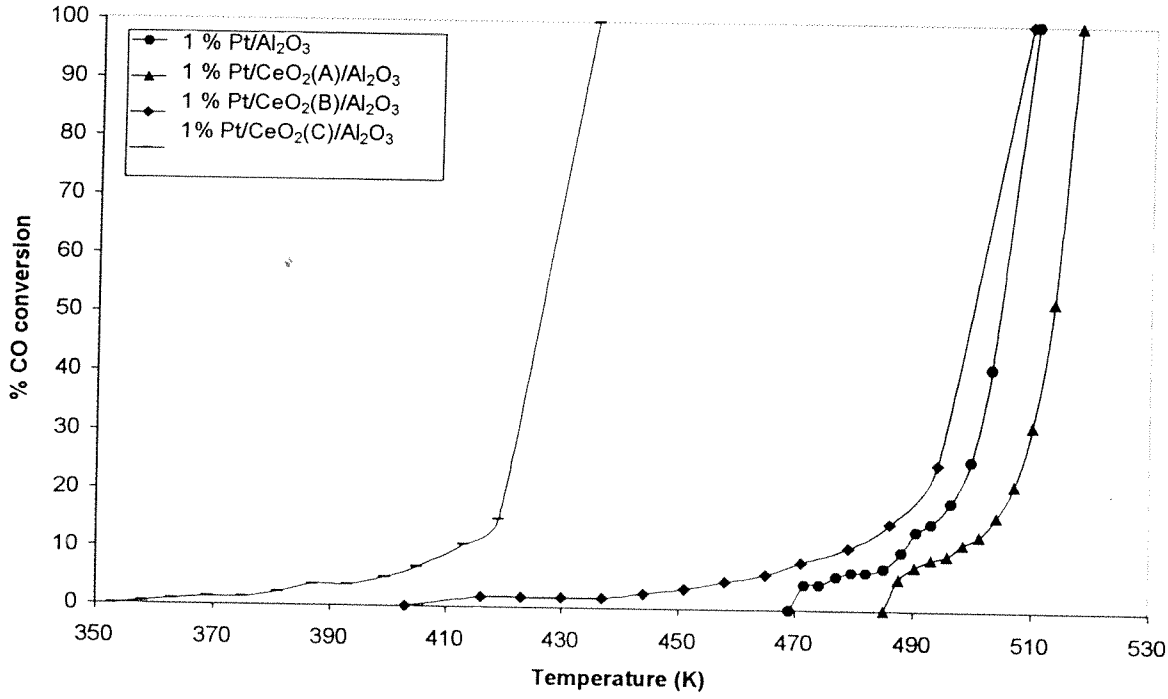
1 % Pt/Al2O3
1 % Pt/CeO2(A)/Al2O3
1 % Pt/CeO2(B)/Al2O3
1% Pt/CeO2(C)/Al2O3
% CO conversion
Temperature (K)
0
10
20
30
40
50
60
70
80
90
100
350
370
390
410
430
450
470
490
510
530

**Figure 1.**

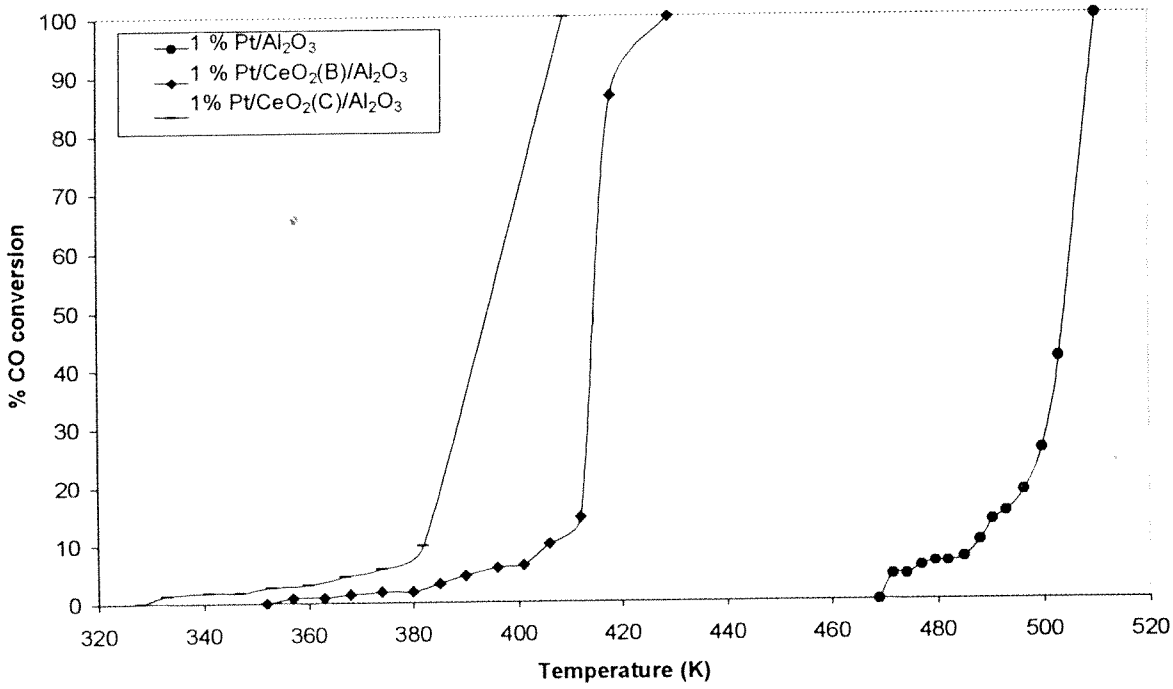
1 % Pt/Al2O3
1 % Pt/CeO2(B)/Al2O3
1% Pt/CeO2(C)/Al2O3
% CO conversion
Temperature (K)
0
10
20
30
40
50
60
70
80
90
100
320
340
360
380
400
420
440
460
480
500
520

**Figure 2.**

**CO Oxidation on Alumina Supported Pd-Pt mono- and bi-metallic Catalysts: Temperature Hysteresis**

S. Kaya, and D. Uner*

Department of Chemical Engineering

Middle East Technical University, Ankara, Turkey

**Running title:** CO oxidation on Pt-Pd Bimetallic catalysts

Corresponding author:

Deniz Uner

Address:

E-mail: uner@metu.edu.tr

Phone: +90 312 210 4383

Fax: +90 312 210 1264

**Abstract**

CO oxidation reaction was studied over $\gamma$-$Al_2O_3$ supported monometallic and bimetallic palladium- platinum catalysts at Pd:Pt atomic ratios: 1:3, 1:1, 3:1. Two different sets of catalysts were prepared by sequential and co-impregnation methods depending on the palladium precursor used. The catalyst performance tests were done using a synthetic gas mixture consisting of CO, $O_2$, and $N_2$ in the temperature range 373 and 523 K. The light-off experiments were performed in successive heating-cooling cycles. Severe temperature hysteresis behavior was observed on all catalysts. This was attributed to the CO island formation on the metal surface At low temperatures (below 423 K), the reaction followed Langmuir-Hinshelwood type of kinetics; negative order dependence in terms of CO and positive order dependence in terms of $O_2$ were determined. Co-impregnated catalysts behaved like monometallic Pd catalyst conforming that Pd atoms segregated to the surface.

Keywords: CO oxidation, bimetallic catalysts, palladium, platinum, surface segregation, reaction hysteresis.

## 1. Introduction

Bi-metallic catalysts are frequently used in industry due to their superior performances. It is known that chemical properties of the metal catalysts such as activity, selectivity, thermal stability, or resistance to poisoning could be modified by using a second metal (1). Synergistic effect result when the compound catalysts performance exceeds the sum of the performances of the individual components. For example, rather than individual Pd and Pt catalysts, bimetallic Pd-Pt catalysts are used for some hydrogenation reactions in the presence of sulfur due to improved sulfur resistance as a result of alloying (2-6).

The surface composition of alloys, and especially the composition of the outermost surface layer, is generally different from the bulk due to segregation processes (1). The surface composition of bimetallic alloys is generally considered to be determined by the following parameters (7): (i) temperature, (ii) metal surface free energies, (iii) heat of mixing, (iv) metal atomic sizes, and (v) presence of adsorbates. Formation of alloys can change electronic structure of the metals, accompanied by a change in bond strength of adsorbed species. Furthermore, alloying may suppress competitive reactions or prevent deposition of non-reactive species on the surface by changing the active ensemble sizes (8). If the mixing is exothermic the metals tend to form alloys. Depending on their extent of exothermic mixing behavior, one can talk about strong or weak alloying. Park and Lee (9) estimated heat of mixing of Pd and Pt as -0.03 eV/atom, supporting slightly exhothermic behavior upon mixing. Therefore, it can be considered that Pd-Pt system may form weak alloys at all compositions or individual components may preserve their identity. Surface tensions of pure components, mixing properties of the systems (such as heat of mixing or free energy of mixing) and values for the molar surface areas have helped researchers to predict surface fractions of the atoms. Surface tension of a pure metal is correlated with its heat of sublimation. Thus, in any mixture, the component that has the lowest pure component heat of vaporization or heat of

sublimation will be enriched in the surface region (10). It is energetically favorable to break the weakest bonds; hence the component that has the lowest bulk bond strength will segregate to the surface (10).

The experimental values for the heat of vaporization of liquid Pd (see Table 1) are lower than those of Pt (7, 11, and 12). In addition, experimental and theoretical evidence pointed to surface enrichment of Pd in Pd-Pt bimetallics. Range of melting temperatures of the metals that form the alloy can also give information about surface segregation process. Generally, the metal with lower melting point segregates to the surface. In accordance with these, it is expected that palladium should segregate to the surface because its melting temperature and heat of vaporization values are lower compared to that of Pt. As a result, in bimetallic catalyst systems, palladium should be lower coordinated than platinum. Harada *et al.* (13) reported that in the case of the Pt-Pd clusters prepared under nitrogen, the coordination numbers of Pd and Pt atoms around a Pd atom were determined as 3.8±0.7 and 0.9±0.2, respectively. Because palladium was found as in oxide form in oxidizing atmosphere, further decrease in coordination numbers of Pd around Pd atoms was also observed. Hansen *et al.* (14) measured surface concentration profile for the three low-index surfaces of Pt-Pd (1:1) random alloys at 500, 1000, and 1500 K by EXAFS technique. The results showed that in all cases Pd segregated to the surface. Therefore, at temperatures higher than 500 K, all of these faces will be covered by Pd atoms.

Differences in the adsorption energies of CO and $O_2$ on palladium and platinum surfaces can result in adsorption induced surface segregation. Van den Oetelaar *et al.* (7) discussed the role of adsorbates/adsorbents, cluster size, and metal-support interaction in the surface segregation process in supported nanoclusters in general and demonstrated the influence of these parameters on surface segregation in the Pd-Pt catalysts in particular. The Pd surface concentration increased with increasing temperature until above 973 K and

eventually slightly decreased. Heats of $O_2$ and CO adsorption on supported and unsupported palladium and platinum catalysts are given in Table 2 and 3, respectively. The heat of adsorption of $O_2$ and CO on supported and unsupported Pd and Pt are nearly the same so chemisorption-induced surface segregation is not expected in the Pd-Pt system due to adsorption of $O_2$ and CO, during a CO oxidation reaction.

The oxide-forming properties of the constituents are different for Pd and Pt which may result in enhanced Pd surface segregation in Pd-Pt alloys. Meusel *et al.* (24) found that starting at temperatures below 300 K the Pd particles rapidly incorporated large amounts of oxygen, finally reaching stoichiometries of PdO>0.5. Their STM data showed that neither the overall particle shape nor the dispersion was affected by the oxygen and CO treatment. Ciuparu *et al.* (25) stated that the most probable state was a metallic Pd superficial layer on a PdO core. Only the surface layers of relatively large alumina supported PdO particles were reduced by the flowing CO at room temperature, while small particles were completely reduced. After CO adsorption at room temperature on the pre-oxidized alumina supported Pd catalyst, there were two different populations of particles; small completely reduced Pd particles and larger PdO particles covered by reduced metallic layers. When temperature was increased, the mobility of bulk oxygen has increased, reached the surface and oxidized adsorbed CO molecules. In another study done by Zheng and Altman (26) over Pd(111) surface, Pd-O bond strength was measured to be between chemisorbed oxygen and bulk PdO. Navarro *et al.* (27) reported two TPR peaks at about 295 K and 356 K in Pd /$SiO_2$-$Al_2O_3$ one due to reduction of PdO and the other due to desorption of hydrogen from the decomposition of a bulk palladium hydride, respectively. Interaction between supported Pt surfaces and oxygen was not important compared to palladium surfaces, however, interaction of oxygen with Pt single crystal surfaces has been found as the reason of kinetic oscillations (28, 29).

In this study, the objective was to investigate the performance of bimetallic Pd-Pt catalysts towards CO oxidation reaction. The measured reaction orders and activation energies are used to propose a plausible mechanism for the same reaction.

## 2. Experimental

### 2.1 Catalyst preparation

The incipient wetness technique was used to prepare alumina impregnated monometallic and bimetallic palladium and platinum catalysts. 1 wt % of Pd, Pt or Pd-Pt were loaded onto the gamma-alumina ($\gamma$-$Al_2O_3$) supports by impregnating the supports with sufficient precious metal precursor solution to bring about incipient wetness (~1-2 ml solution/g support). For bimetallic catalysts Pd-Pt atomic ratios were selected as 1:3, 1:1 and 3:1. Two series of bimetallic catalysts were prepared differing in their Pd precursor and metal loading procedure. The first series was prepared via co-impregnation of Pd and Pt from $Pt(NH_3)_4Cl_2.H_2O$ (Johnson Matthey) and $PdCl_2$ (Johnson Matthey). The second series were prepared by sequential impregnation of $Pt(NH_3)_4Cl_2.H_2O$ (Johnson Matthey) $Pd(NO_3)_2$ (Johnson Matthey) since mixed aqueous solutions of $Pt(NH_3)_4Cl_2.H_2O$ and $Pd(NO_3)_2$ salts resulted in precipitation. The catalysts were dried at room temperature for 6 hours and at 393 K for 12 hours. Finally the catalysts were calcined at 723 K for 4 h. Part of these catalysts were used as such, and the other part was washed with hot distilled water (~350 K) until it is free of $Cl^-$ ions tested by $AgNO_3$ solution then again calcined at 673 K for 4 h (30).

### 2.2 Catalysts characterization

In this study active metal dispersions were determined by strong hydrogen amounts at 298 K measured by volumetric chemisorption methods (31). The adsorption experiments were performed in a manifold described elsewhere (32). Prior to reduction, about 2 g of catalyst was heated up to a temperature of 423 K and kept at that temperature for 30 min under vacuum ($10^{-4}$ Torr). The samples were reduced under stastic hydrogen at 623 K for 2 hours, during this period, the surface was exposed to hydrogen three times and after each 20-25 min.

exposure the gas in the manifold was replenished. The dispersions were calculated assuming a strong hydrogen stoichiometry of H/Pd=1 or H/Pt=1.

2.3 Activity measurements

CO oxidation activities over the prepared catalysts were conducted in a horizontal fixed-bed reactor made of quartz tube (13 mm ID) under atmospheric pressure. 100 mg catalyst diluted with 900 mg $\gamma$-$Al_2O_3$ was placed in the reactor. The catalyst bed was supported by quartz wool at both ends. A thermocouple was placed externally with one end touching the catalyst zone, in order to measure the bed temperature. The quartz reactor was placed inside a temperature controlled tubular oven. The temperature of the oven was increased from room temperature to the reaction temperature (approximately 350 K) then the catalysts were conditioned with a gas mixture 2.5 % CO, 5 % $O_2$ and $N_2$ for 30 minutes. Inlet gas compositions were controlled by MKS 1179A mass flow controllers and the analysis of the product gases was carried out using on-line gas chromatograph (HP 4890) equipped with a thermal conductivity detector (TCD). The total gas flow rate through the reactor was maintained constant at 200 ml/min. Effect of bimetallic interaction on CO oxidation reaction was first studied by dynamic light-off experiments. Two sets of data were collected which will be denoted as heating mode and cooling mode experiments. During the heating mode experiments, the catalyst bed was heated at a rate of 1 K/min and CO consumption and $CO_2$ formation rates were monitored with the gas chromatograph until 100 % CO conversion was obtained. At this stage the heating ramp was stopped and the tubular oven was cooled naturally while the conversion of CO to $CO_2$ was followed as well. The second set of data will be referred to as cooling mode. The reaction orders with respect to carbon monoxide and oxygen were measured at the temperatures where CO conversion was below 5 % so that differential reactor assumption was valid.

## 3. Results and Discussion

### *3.1 Characterization of monometallic and bimetallic Pd and Pt catalysts*

Active site characterizations of all catalysts were performed by volumetric hydrogen chemisorption technique, at ambient temperature. It is well known that palladium and hydrogen can form a β-hydride species so the dispersion measurements are based on the data collected below 10-12 Torr hydrogen pressures. In this pressure range the spillover effect is also minimized. Below 10 Torr, it was assumed that hydrogen molecules were only chemisorbed to the metals. Active metal dispersions of monometallic and bimetallic catalysts were calculated assuming H/M (M: Pd or Pt) stoichiometry equal to one. For bimetallic catalysts, calculated dispersions are based on weighed averages of the atomic masses of palladium and platinum metals. The dispersion values of all monometallic and bimetallic catalysts are given in Table 4 and 5. Total hydrogen adsorption isotherms of washed catalyst samples prepared by both sequential and co-impregnation technique up to 100 Torr showed that Pd:Pt (1:3) catalysts have the lowest hydrogen adsorption capacities. The decrease of metal dispersions upon washing was observed especially for bimetallic catalysts. This decrease was attributed to sintering of particles during the second calcination after washing.

### *3.2 Non-isothermal CO oxidation performances on alumina supported monometallic and bimetallic palladium-platinum catalysts*

CO oxidation reactions on both monometallic and bimetallic catalysts were investigated in two parts. In the first part unwashed catalysts were tested under lean, stoichiometric, and rich gas environment by increasing the reactor temperature. In the second part, CO oxidation reaction performances were compared for the washed catalysts and the reaction hysteresis during heating and cooling mode were studied.

*Unwashed catalysts*

CO oxidation performances of bimetallic catalysts reside in between the monometallic palladium and platinum catalysts for the sequentially impregnated series. As seen in Figure 1, increasing palladium weight fraction from zero to one resulted in gradual increase in the reaction performances. However, for co-impregnated catalyst group, reaction taking place on the bimetallic catalysts showed similar performances with monometallic palladium (Figure 2). The other important result to be mentioned is the difference in the light-off performances of monometallic palladium prepared from two different palladium precursors. Light-off temperature ($T_{50}$, the temperature at which 50 % CO conversion is attained) of 1 % $Pd/Al_2O_3$ catalyst prepared from $Pd(NO_3)_2$ precursor is 40 K lower than that of palladium catalyst prepared from $PdCl_2$ precursor, which could be due to a poisoning effect of the $Cl^-$ remained on the surface from the catalyst precursor.

Bimetallic catalysts in co-impregnated catalyst group behaved like monometallic palladium catalyst due to the segregation of palladium to the surface. According to the light off behaviors up to 30 % conversion, it was obvious that all bimetallic Pd-Pt catalysts and monometallic palladium followed the identical light-off trend in nearly the same temperature interval. On the other hand, the results presented in Figure 1 indicate that palladium and platinum metals in sequentially impregnated bimetallic catalysts can be found as separate entities on the support surface.

*Washed catalysts*

CO oxidation performances of sequentially impregnated and co-impregnated catalysts after washing under stoichiometric feed gas compositions are shown in Figure 3 and 4. In

sequentially impregnated catalyst group, monometallic palladium catalyst showed the best oxidation activity. Its $T_{50}$ value is 40 K lower than that of monometallic platinum catalyst. Performances of bimetallic catalysts did not change after washing and again resided between monometallic catalysts depending on the palladium fraction. As seen in these figures, there exists no synergistic catalyst performance of the bimetallic catalysts, towards CO oxidation reaction.

In co-impregnated catalyst group, the light-off performances of all catalysts are almost the same. More precisely, it can be said that after washing the performance gap between monometallic catalysts became narrower and the performances of bimetallic Pd-Pt catalyst were identical with monometallic palladium. For this group no synergy was observed either. All co-impregnated catalysts showed similar light-off performances up to 20 % conversion.

Washing did not result in improvement in the light-off performance of the sequentially impregnated catalyst group excluding monometallic platinum catalyst. After washing, reaction onset temperature and $T_{50}$ value on 1% $Pt/\gamma$-$Al_2O_3$ catalyst decreased by 50 K and 25 K respectively. Despite reaction onset temperatures of the remaining bimetallic catalysts enhanced at least 40 K, washing had no effect on sequentially impregnated catalysts. On the contrary, for co-impregnated catalyst group, both reaction onset temperature and $T_{50}$ values enhanced after washing. With increasing palladium fraction, light-off temperatures of washed and unwashed samples got closer. Since, both palladium and platinum catalysts were prepared from chlorine containing metal salts, removal of residual chlorine apparently improved the performance of the catalyst. Irregular behaviors of sequentially impregnated catalysts were difficult to explain but we concluded that Pd-Pt interactions in this group seemed to be different in comparison to co-impregnation method. Furthermore, the dispersions of the catalysts have decreased upon washing indicating particle sintering. The irregularities in the catalyst performances can also be attributed to the decrease in the particle dispersions as

measured by hydrogen chemisorption method. There was 60 K improvement in the onset performance of monometallic platinum and palladium (from palladium chloride) catalysts after removing residual chlorine. Monteiro *et al.* (33) clearly demonstrated that the position of IR CO absorption frequencies depended on the nature of Pd precursors. In addition to the two infrared absorption peaks of CO (linear and bridged), there exists a third small peak related to bridge-bonded CO on the catalyst prepared from $Pd(NO_3)_2$ precursor. The authors suggested that highly dispersed metal particles obtained by using palladium chloride precursor were the most active sites in CO oxidation.

3.3 Temperature hysteresis

Oxidation performances of the catalysts were studied while increasing the reaction temperature and the heating was stopped when 100 % CO conversion was attained. The conversions were monitored during the reactor cooling, and a hysteresis behavior was observed on all of the catalysts. This hysteresis behavior was studied under three different feed gas compositions, namely oxygen excess, CO excess and stoichiometric gas mixtures. As seen in Figure 5 (a) and (b), CO-rich feed gas composition gave the worst activity performance. Similar results were obtained during cooling mode; especially on 1 % Pd/$\gamma$-$Al_2O_3$ catalyst (from $Pd(NO_3)_2$ solution) 100 % conversion was sustained below 373 K. The activities of the palladium were the same under CO-lean and stoichiometric feed gas compositions. In addition, similar to the heating mode within a narrow temperature range there exist sudden conversion change (drop) during cooling mode. Although the difference of $T_{50}$ values between heating and cooling mode under rich conditions was 70 K, it was almost 90 K under CO-lean conditions.

The evidence in this study supported the existence of CO islands on the surface of the platinum and palladium that change in the light-off behavior during in one heating-cooling

cycle. Up to 30-40 % conversion, the reaction rate was slow and reaction might proceed at the peripherals of the CO islands. An additional mechanism has been suggested in which CO islands nucleate and grow in size until they reach a critical size (34) which is the 30-40 % conversion level depending on the catalyst used. At this point, the adsorbed oxygen region between the CO islands becomes compressed, which changes the kinetics of that layer and provides feedback to return the system to the initial CO free state. These islands of CO block a portion of the active sites and change in size during the reaction. Also, the sharp increase in conversion value within a narrow temperature range can be another explanation of critical CO level. Passing this level leads to a jump in the reaction rate. In addition to that, the size of the CO islands may be related to the amount of chlorine on the platinum and palladium particles. The mechanism that drives the change in island size is still unclear due to the differences between light-off behaviors up to 30-40 % conversion levels on washed and unwashed catalysts.

It has to be pointed out that the sudden increase and decrease in the reaction rate should indeed be related to a sudden change in the CO coverage. The effect is mainly connected to decrease or increase in the CO coverage (during heating and cooling mode, respectively). In both bimetallic catalyst groups, due to palladium surface segregation process all cooling mode light of performances of bimetallic catalysts are similar to monometallic palladium activity. Another interesting result was obtained when the bimetallic catalysts were subjected to successive heating-cooling cycles. Narrowed hysteresis loop may also be attributed to surface temperature assisted segregation of palladium because similar behavior was not observed for monometallic samples. As seen in the Figure 6, a clear change in the light-off behavior after first heating-cooling cycle can correspond to surface segregation of Pd. This behavior did not repeat, second and third light-off curves (heating-cooling) overlapped. In addition, it was obvious that the reaction proceeds with its exothermicity after

all surface CO was burned out. When 40 % conversion levels were passed, externally measured reactor temperature immediately increased 10-20 K above the furnace set point temperature.

*3.4 Reaction mechanisms, apparent activation energies and orders*

Apparent activation energies of CO oxidation reaction on monometallic and bimetallic palladium-platinum catalysts (washed) were calculated from the slope of the ln (rate) vs. 1/T graphs, rate was in terms of moles of CO reacted/site.s and T was in K. The ln (rate) vs. 1/T data was obtained directly from light-off curves below 10 % conversion.

For sequentially and co-impregnated impregnated catalyst groups apparent activation energies and reaction orders with respect to CO and $O_2$ were presented in Table 6 and Table 7 respectively. Carbon monoxide and oxygen orders were estimated at constant temperature over a narrow range of carbon monoxide and oxygen partial pressures assuming power law type rate expression. CO orders were measured by changing CO amounts in the gas phase in the 2-6 % range wile maintaining $O_2$ at 2.5% levels. On the other hand $O_2$ orders were measured by keeping CO levels at 4% and changing $O_2$ values in 1-5% range. On sequentially impregnated catalysts, CO orders estimated in isokinetic region on all catalysts were close to −1, except for monometallic palladium catalysts. On mono-metallic palladium catalyst (preparedfrom $Pd(NO_3)_2$ precursor) CO order was -0.47. In a previous study the abundance of bridge bonded CO was noted(33). Following these lines, the coverage of a bridge bonded CO can be estimated as(38)

$$\theta_{CO}=(KP_{CO})^{1/2}/(1+KP_{CO})^{1/2}$$

Under the condition that this CO is the poisoning species, one can estimate the vacant site concentration as $\theta_v=1/(1+KP_{CO})^{1/2}$ suggesting that the bridge bonded CO species is involved in the reaction from the approximate negative half orders measured in this study.

With increasing palladium weight fraction a decrease in oxygen order from 1.84 to 1.16 was observed. Similar to the sequentially impregnated catalysts, on co-impregnated catalysts CO orders were estimated as close to -1 indicating surface poisoning by CO. The reaction order with respect to oxygen on monometallic platinum catalyst was quite higher than the other catalysts in both catalyst groups.

*Isothermal reaction rate change*

Starting from O-rich conditions the steady-state reaction rate increases with increasing CO fraction, until a critical $CO/O_2$ ratio is reached at which the system switches to a CO-rich steady-state in both monometallic palladium and platinum surfaces (Figure 9 (a) and (b)). This point at which the CO poisoning becomes dominant is connected with a steep drop in reaction rate. Below the critical pressure, the surface is fairly covered by oxygen $\theta_O \cdot \theta_{CO}$ becomes predominant above the critical pressure, and oxygen adatoms decrease to negligible amounts, i.e., from $\theta_O > \theta_{CO}$ to $\theta_O << \theta_{CO}$ with increasing CO pressure. This change was attributed to a change of the rate-determining step from CO adsorption to $O_2$ adsorption. Thus, the former region of $\theta_O > \theta_{CO}$ provides a stage suitable for the examination of site preference, one in which oxygen is more reactive toward CO when different kinds of oxygen are on the surface.

Similarities in the reaction rates at 423, 433, and 443 K on the Pd catalyst after the rate maximum can be explained by Pd-O interaction (Figure 9 (b)). Ertl *et al.* (35) suggested that starting from a low CO pressure value, the catalytic activity of the surface will first be low due to filling of the subsurface oxygen reservoir, but as CO pressure is approaching the rate maximum the depletion of subsurface oxygen will lead to an increase in the catalytic activity. Beyond the rate maximum (stoichiometric point), the formation of CO ad-layer will lead to a depletion of subsurface oxygen as oxygen atoms located in the near-surface region will

segregate to the surface and react off with chemisorbed CO. At low CO pressures the formation of subsurface oxygen will become dominant. Pfefferle *et al.* (36) stated that after CO adsorption at room temperature on the pre-oxidized alumina supported Pd catalyst, there were two different populations of particles; small completely reduced Pd particles and larger PdO particles covered by reduced metallic layers. When temperature was increased, the mobility of bulk oxygen must have increased, which has reached the surface and oxidized adsorbed CO molecules. Under the assumption that subsurface oxygen decreases adsorption of CO, the reduced residence time on the surface will only lead to low CO coverages high temperatures, where the desorption rate of CO is high. Beyond rate maximum $O_2$ adsorption becomes the limiting step as a CO ad-layer already exists on the surface. CO adsorption will dominate over oxygen adsorption leading to the formation of a CO ad-layer on the surface.

## 4. **Conclusions**

CO oxidation reaction was studied over mono- and bi-metallic Pd-Pt catalysts. The bimetallic catalysts were prepared by sequential impregnation and co-impregnation methods. The reaction results indicate intimate contact between Pd and Pt for co-impregnated catalysts. Furthermore, Pd segregated to the surface on these catalysts. On the other hand, intimate interaction between Pd and Pt was not established for sequentially impregnated catalysts. Measured reaction orders and activation energies did not indicate any significant synergy due to the alloy formation neither for the sequentially nor for co-impregnated catalysts.

**Acknowledgement**

The financial support for this project was provided by TUBITAK under research grant MISAG-188 and MISAG A-54. Additional support was provided by Middle East Technical University through Research Fund Projects.

**References**


1. Rousset, J. L., Renouprez, A. J., and Cadrot , A. M., *Phys. Rev. B* **58**, 2150 (1998)
2. Rousset, J. L., Cadrot, A. M., Cadete Santos Aries, F. J. and Renouprez, A., *J. Chem. Phys.* **102**, 8574 (1995)
3. Blomsma, E., Martens, J. A., and Jacobs, P. A., *J. Catal.* **165**, 241 (1997)
4. Renouprez, A., Rousset, J. L., Cadrot, A. M., Soldo, Y., and Stievano, L., *J. of Alloys and Comp.* **328**, 50 (2001)
5. Guillon, E., Lynch, J., Uzio, D., Didillon, B., *Catal. Today* **65**, 201 (2001)
6. Especel, C. M., Bazin, D., Guerin, M., Marecot, P., and Barbier, J., *React. Kinet. Catal Lett.*, **69**, 209 (2000)
7. van den Oetelaar, L. C. A., Nooij, O. W., Oerlemans, S., van der Gon, A. W. D., Brongersma, H. H., Lefferts, L., Roosenbrand, A. G., and van Veen, J. A. R., *J. Phys. Chem. B* **102**, 3445 (1998)
8. Toollenaar, F. J. C. M., Stoop, F., and Ponec, V., *J. Catal.* **82**, 1 (1983)
9. Park, B., and Lee, H., *J. Mater. Res.* **14**, 281 (1999)
10. King, T. S., in "Surface Segregation and Related Phenomena", (P. A. Dowben and A. Miller, eds.), CRC Press, 1990
11. Kuijers, F. J., Tieman, B. M., and Ponec, V., *Surf. Sci.* **75**, 657 (1978)
12. Overbury, S. H., Bertrand, P. A., and Somorjai, G. A., *Chem. Rev.* **75**, 547 (1976)
13. Harada, M., Asakura, K., Ueki, Y., and Toshima, N., *J. Phys. Chem.* **96**, 9730 (1992)
14. Hansen, P. L., Molenbroek, A. M., and Ruban, A. V., *J. Phys. Chem.* **101,** 1861 (1997)
15. Bourane, A. and Bianchi, D., *J. Catal.* **202**, 34 (2001)
16. Yeo, Y. Y., Vattuone, L., and King, D. A., *J. Chem. Phys.* **106**, 392 (1997)
17. Chou, P., and Vannice, M. A., *J. Catal*, **105**, 342 (1987)
18. Conrad, H., Ertl, G., Kuppers, J., E. E. Latta, *Surf. Sci.* **65**, 245 (1977)

19. Ertl, G., and Koch, J., *Phys. Chem. N. F.* **69**, 323 (1970)

20. Vannice, M. A., Hasselbring, L. C., and Sen, B., *J. Catal.* **97**, 66 (1986)

21. Shigeishi, and R. A., King D. A., *Surf. Sci.* **58**, 379 (1976)

22. Chou, P., Vannice, M. A., *J. Catal.* **104**, 17 (1987)

23. Tracy, J. C., and Palmberg, P. W., *J. Chem. Phys.* **51**, 4852 (1969)

24. Meusel, I., Hoffmann, J., Hartmann, J., Heemeier, M., Bäumer, M., Libuda, J., and Freund, H. J., *Catal. Lett.* **71**, 5 (2001)

25. Ciuparu, D., Bensalem, A., and Pfefferle, L., *Appl. Catal. B: Environmental* **26**, 241 (2000)

26. Zheng, G., and Altman, E. I., *Surf. Sci.* **462**, 151 (2000)

27. Navarro, R. M., Pawelec, B., Trejo, J. M., Mariscal, R., and Fierro, J. L. G., *J. Catal.* **189,** 184 (2000)

28. Khan, K.M., *Physica A* **278**, 526 (2000)

29. Dicke, J., Rotermund, H. H., Lauterbach, J., *Surf. Sci.* **454–456**, 352 (2000)

30. Uner, D. O., Pruski, M., and King, T. S., *J. Catal.* **156**, 60 (1995)

31. Wu, X., Gerstein, B. C., and King, T. S., *J. Catal.* **135**, 68 (1992)

32. Uner, D., Tapan, N. A., Ozen, I., and Uner, M., *App. Cat. A.: General*, **251**, 225 (2003).

33. Monteiro, R. S., Dieguez, L. C., and Schmal, M., *Catal. Today* **65**, 77 (2001)

34. Fanson, P. T., Delgass, W. N., and Lauterbach, J., *J. Catal.* **204**, 35 (2001)

35. Conrad, H., Ertl, G., E. and Latta, E., *Surf. Sci.* **41**, 435 (1974)

36. Ciuparu, D., Bensalem, A., Pfefferle, L., *Appl. Catal. B: Environmental* **26**, 241 (2000)

37. Table of Periodic Properties of Elements Sargent-Welch Scientific Company, Skokie, IL, 1979.

38. Uner, D.O., *J. Catal.*, **178**, 382 (1998)

**List of Tables**

**List of Figures**

Figure 9. Change in the rate of the reaction with increasing partial pressure of CO. (a) 1 % $Pt/\gamma\text{-}Al_2O_3$ and (b) 1 % $Pd/\gamma\text{-}Al_2O_3$. Feed gas composition: 2.5 % $O_2$, balance $N_2$. $V_{total}$ =200 ml/min. Dashed lines show stoichiometric point.

Table 1

| Property | Palladium | Platinum |
|---|---|---|
| Atomic number | 46 | 78 |
| Atomic weight (g/mole) | 106.4 | 195.09 |
| Melting point ($K_s$) | 1825 | 2045 |
| Boiling point (K) | 3237 | 4100 |
| Heat of vaporization (kJ/mol) | 357 | 510 |
| Heat of fusion (kJ/mol) | 17.60 | 19.80 |

Table 2

| Catalyst | Method | $-\Delta H_{ad}$ (kJ/mole) | Ref. |
|---|---|---|---|
| 2.9 % $Pt/Al_2O_3$ | IR | ~30 | 15 |
| Pt(111) | Calorimetric | 308±32 | 16 |
| 0.98 %$Pd/SiO_2$-$Al_2O_3$ | DSC | 236.1 | 17 |
| | | 231.1 | |
| 1.80 %$Pd/Al_2O_3$ | | 253.3±14.7 | |
| 0.32 %$Pd/Al_2O_3$ | | 255.0 | |
| 0.36 %$Pd/Al_2O_3$ | | 216.0 | |
| | | 336.2 | |
| 0.54 %$Pd/Al_2O_3$ | | 261.5 | |
| 2.33 %$Pd/Al_2O_3$ | | 199.3±38.1 | |
| | | 167.5±4.2 | |
| Pd(111) | TPD | 230.3 | 18 |
| Pd(100) | Isosteric[1] | 251.2 | 19 |

[1] Maximum values based on work function change

Table 3

| Catalyst | Method | $-\Delta H_{ad}$ (kJ/mole) | Ref. |
|---|---|---|---|
| 2.1 % $Pt/\eta$-$Al_2O_3$ | TPD | 99.2±2.9 | 20 |
| Pt(111) | LEED | 135 | 21 |
| Pt(111) | Calorimetric | 180±19 (T= 300 K) | 16 |
| 1.80 %$Pd/Al_2O_3$ | DSC | 85.0 | 22 |
| 0.32 %$Pd/Al_2O_3$ | | 136.1 | |
| 0.36 %$Pd/Al_2O_3$ | | 98.4 | |
| | | 149.9 | |
| 0.54 %$Pd/Al_2O_3$ | | 141.1 | |
| 2.33 %$Pd/Al_2O_3$ | | 97.6 | |
| | | 82.1 | |
| Pd(100) | UHV[1] | 149.5 | 23 |

[1] Maximum values based on work function change

Table 4

| | | Dispersion, % | | μmole of Surf atom/g cat. |
|---|---|---|---|---|
| Catalyst | Pd:Pt | (unwashed) | (washed) | (washed) |
| 1 % $Pt/\gamma\text{-}Al_2O_3$ | 0:1 | 70.4 | 60.8 | 31.2 |
| 1 % $Pd\text{-}Pt/\gamma\text{-}Al_2O_3$ | 1:3 | 62 | 42.5 | 26.3 |
| 1 % $Pd\text{-}Pt/\gamma\text{-}Al_2O_3$ | 1:1 | N/A | 38.3 | 27.8 |
| 1 % $Pd\text{-}Pt/\gamma\text{-}Al_2O_3$ | 3:1 | 40.7 | 44.6 | 37.2 |
| 1 % $Pd/\gamma\text{-}Al_2O_3$ | 1:0 | 34.3 | 32.9 | 31.0 |

Table 5

| | | Dispersion, % | | μmole of Surf atom/g cat. |
|---|---|---|---|---|
| Catalyst | Pd:Pt | (unwashed) | (washed) | (washed) |
| 1 % $Pt/\gamma\text{-}Al_2O_3$ | 0:1 | 70.4 | 60.8 | 31.2 |
| 1 % $Pd\text{-}Pt/\gamma\text{-}Al_2O_3$ | 1:3 | 57.8 | 39.6 | 18.3 |
| 1 % $Pd\text{-}Pt/\gamma\text{-}Al_2O_3$ | 1:1 | 52.3 | 38.3 | 27.8 |
| 1 % $Pd\text{-}Pt/\gamma\text{-}Al_2O_3$ | 3:1 | 49.1 | 23.5 | 19.6 |
| 1 % $Pd/\gamma\text{-}Al_2O_3$ | 1:0 | 47.9 | 27.9 | 26.2 |

Table 6

| Catalyst | Pd:Pt | Activation energy measurement Temperature range (K) | $E_a$ (kJ/mole) | CO order measurement Temperatures (K) | CO orders | $O_2$ order measurement Temperatures (K) | $O_2$ orders |
|---|---|---|---|---|---|---|---|
| $Pt/\gamma\text{-}Al_2O_3$ | 0:1 | 420-465 | 57.0 | 448 | -0.81 | 455 | 1.84 |
| $Pd\text{-}Pt/\gamma\text{-}Al_2O_3$ | 1:3 | 425-465 | 56.7 | 458 | -0.74 | 458 | 1.46 |
| $Pd\text{-}Pt/\gamma\text{-}Al_2O_3$ | 1:1 | 425-470 | 59.6 | 450 | -0.86 | 450 | 1.31 |
| $Pd\text{-}Pt/\gamma\text{-}Al_2O_3$ | 3:1 | 420-470 | 50.2 | 453 | -0.89 | 443 | 1.16 |
| $Pd/\gamma\text{-}Al_2O_3$ | 1:0 | 425-470 | 74.0 | 423 | -0.47 | 423 | 1.23 |

Table 7

| Catalyst | Pd:Pt | Activation energy measurement Temperature range (K) | $E_a$ (kJ/mole) | Reaction order measurement Temperatures (K) | CO orders | $O_2$ orders |
|---|---|---|---|---|---|---|
| $Pt/\gamma\text{-}Al_2O_3$ | 0:1 | 420-465 | 57.0 | 448 | -0.81 | 1.84 |
| $Pd\text{-}Pt/\gamma\text{-}Al_2O_3$ | 1:3 | 425-465 | 47.1 | 440 | -1.35 | 1.21 |
| $Pd\text{-}Pt/\gamma\text{-}Al_2O_3$ | 1:1 | 445-470 | 51.2 | 445 | -0.59 | 1.35 |
| $Pd\text{-}Pt/\gamma\text{-}Al_2O_3$ | 3:1 | 425-480 | 67.9 | 450 | -0.94 | 1.35 |
| $Pd/\gamma\text{-}Al_2O_3$ | 1:0 | 425-480 | 58.7 | 445 | -0.93 | 0.84 |

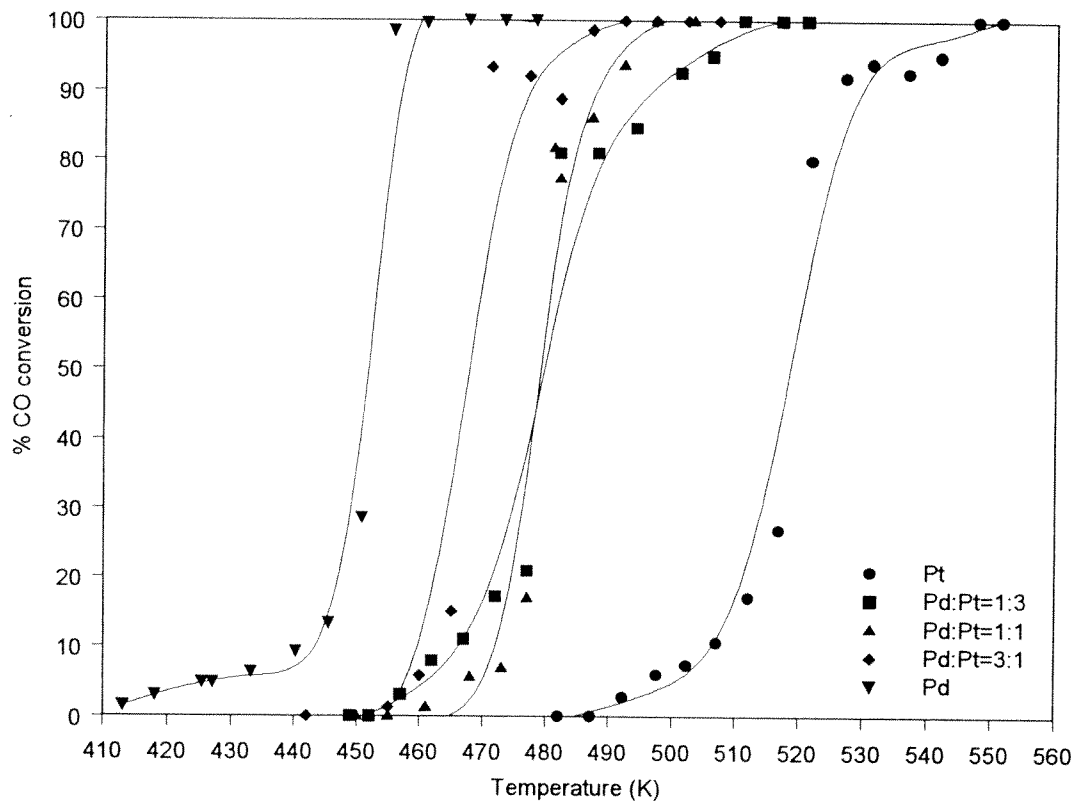


Figure 1

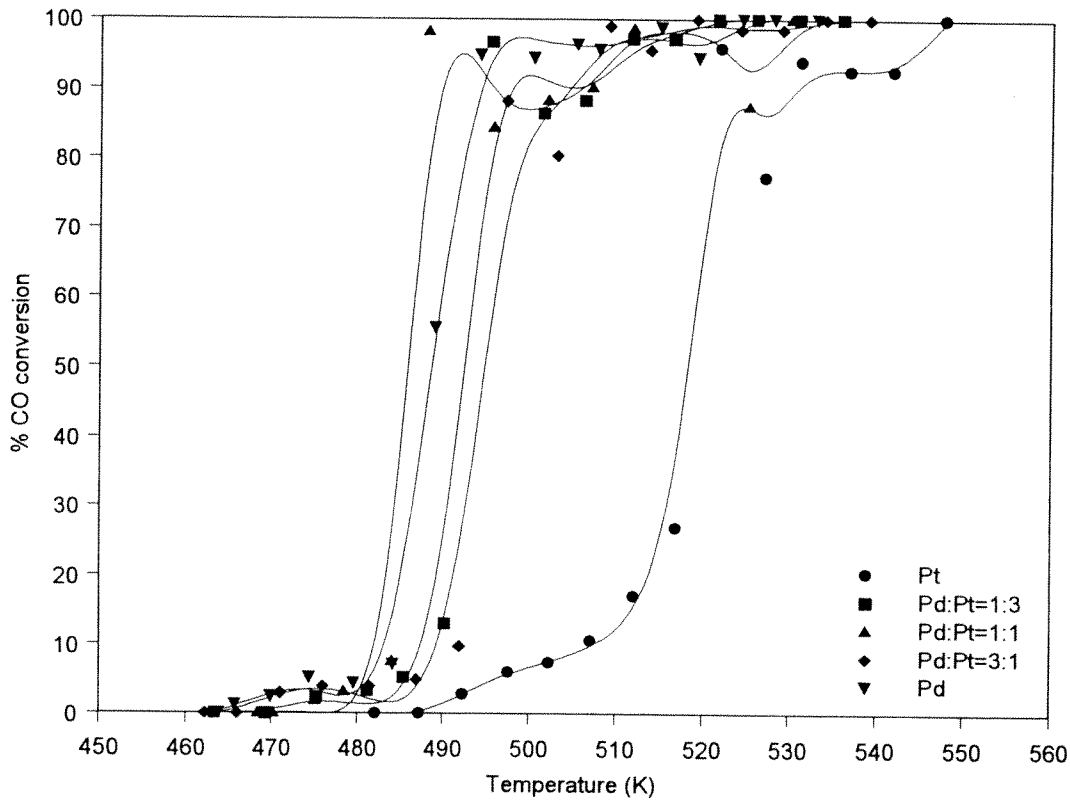
100
90
80
70
60
50
40
30
20
10
0
% CO conversion
450
460
470
480
490
500
510
520
530
540
550
560
Temperature (K)
Pt
Pd:Pt=1:3
Pd:Pt=1:1
Pd:Pt=3:1
Pd

Figure 2

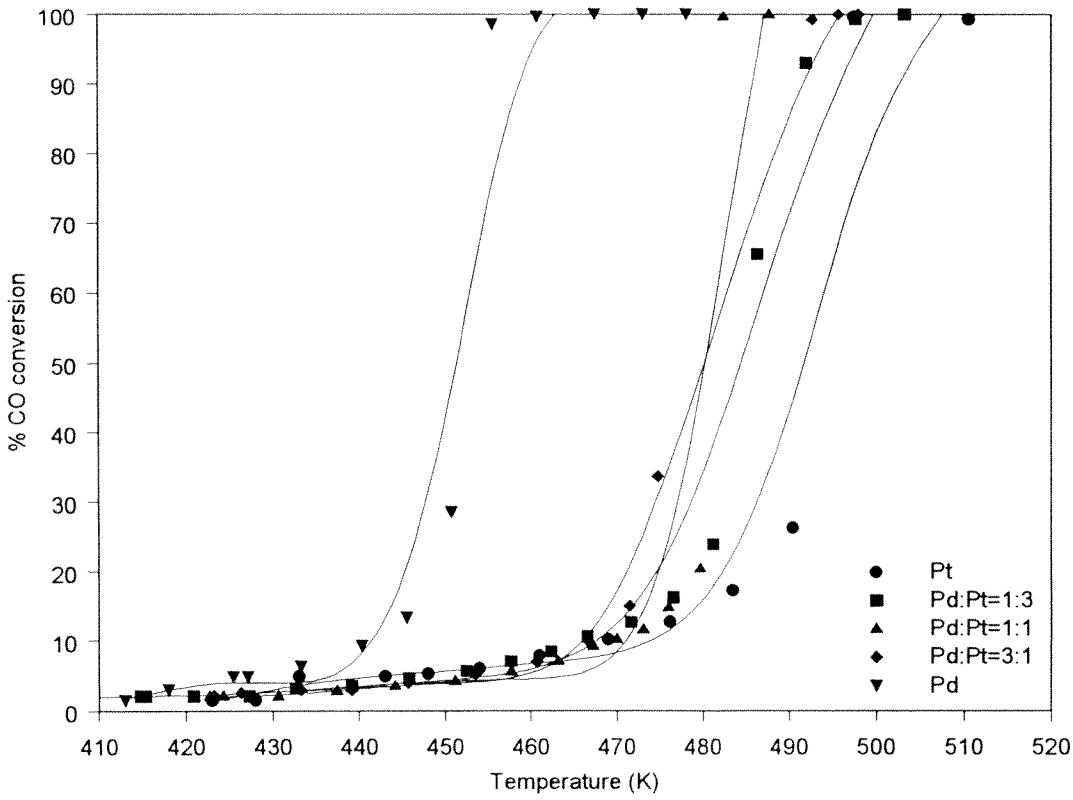
100
90
80
70
60
50
40
30
20
10
0
% CO conversion
410
420
430
440
450
460
470
480
490
500
510
520
Temperature (K)
Pt
Pd:Pt=1:3
Pd:Pt=1:1
Pd:Pt=3:1
Pd

Figure 3

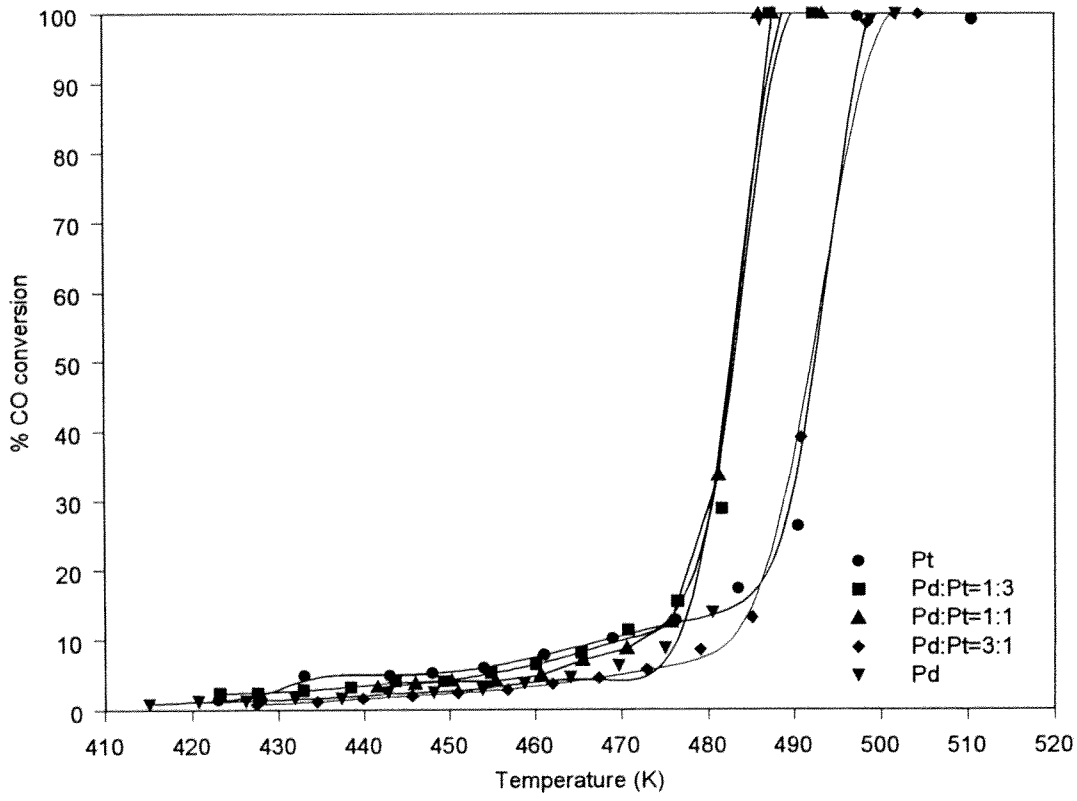
100
90
80
70
60
50
40
30
20
10
0
% CO conversion
410
420
430
440
450
460
470
480
490
500
510
520
Temperature (K)
Pt
Pd:Pt=1:3
Pd:Pt=1:1
Pd:Pt=3:1
Pd

Figure 4

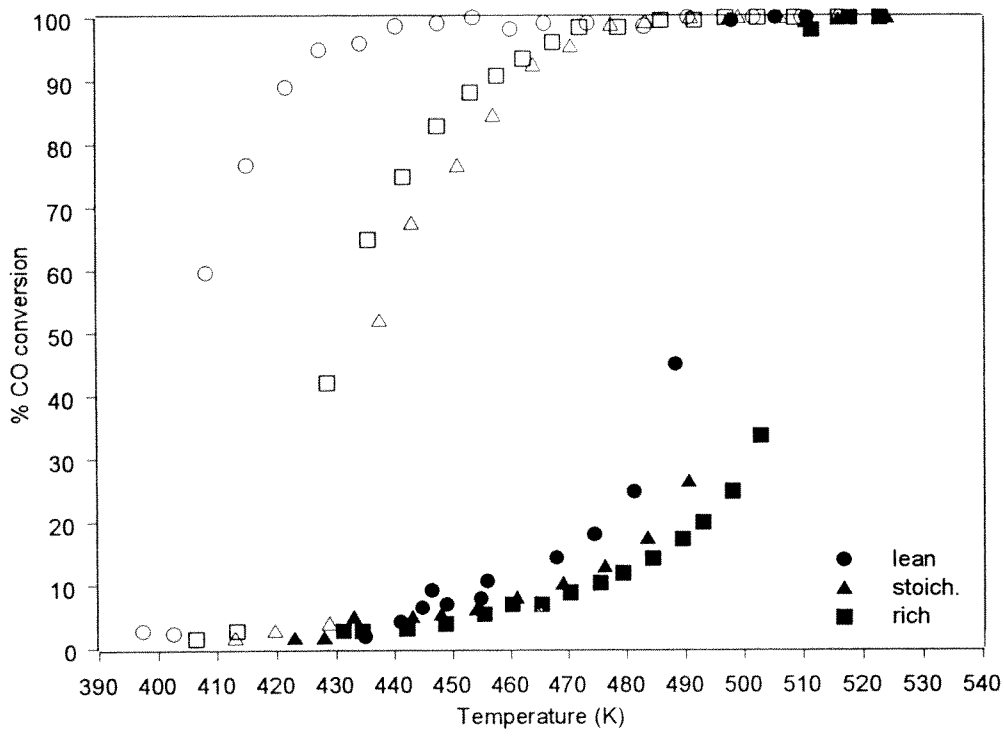
% CO conversion
Temperature (K)
lean
stoich.
rich
0
10
20
30
40
50
60
70
80
90
100
390
400
410
420
430
440
450
460
470
480
490
500
510
520
530
540

Figure 5(a)

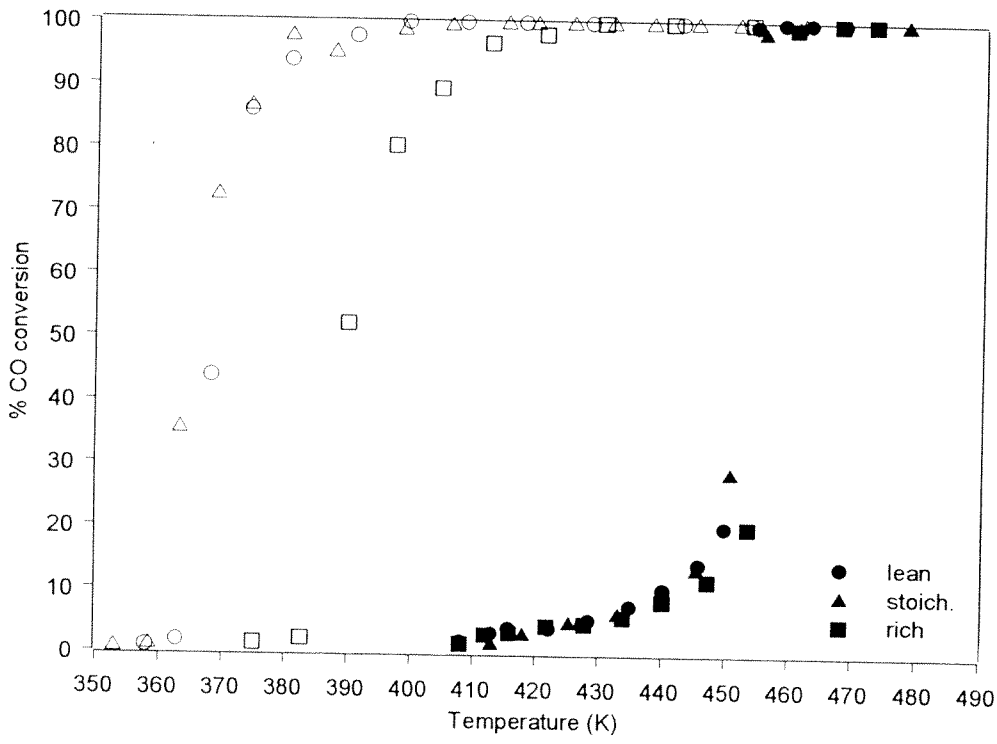
100
90
80
70
60
50
40
30
20
10
0
% CO conversion
350
360
370
380
390
400
410
420
430
440
450
460
470
480
490
Temperature (K)
lean
stoich.
rich

Figure 5(b)

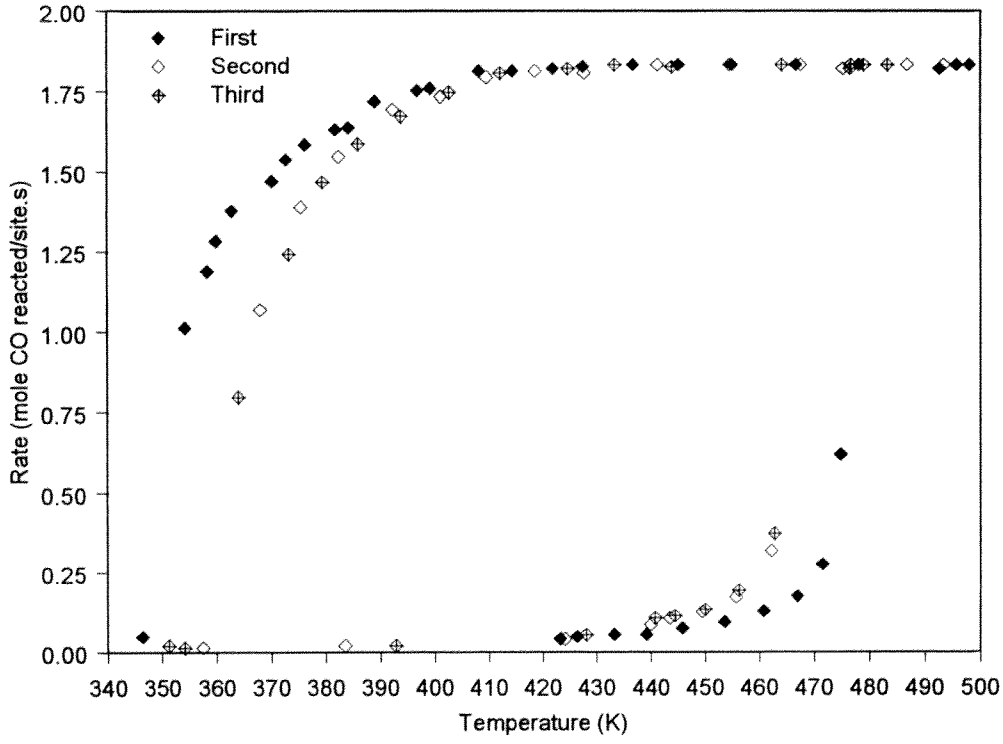
First
Second
Third
Rate (mole CO reacted/site.s)
Temperature (K)
2.00
1.75
1.50
1.25
1.00
0.75
0.50
0.25
0.00
340 350 360 370 380 390 400 410 420 430 440 450 460 470 480 490 500

Figure 6

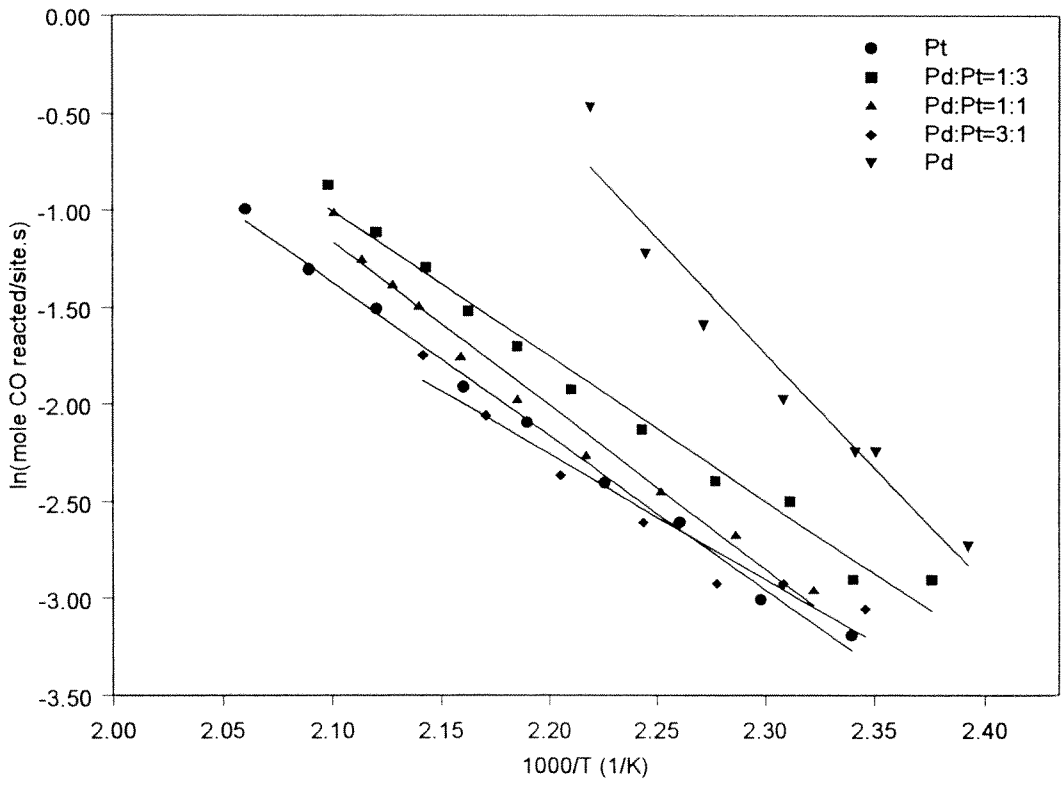
0.00
-0.50
-1.00
-1.50
-2.00
-2.50
-3.00
-3.50
ln(mole CO reacted/site.s)
2.00
2.05
2.10
2.15
2.20
2.25
2.30
2.35
2.40
1000/T (1/K)
Pt
Pd:Pt=1:3
Pd:Pt=1:1
Pd:Pt=3:1
Pd

Figure 7

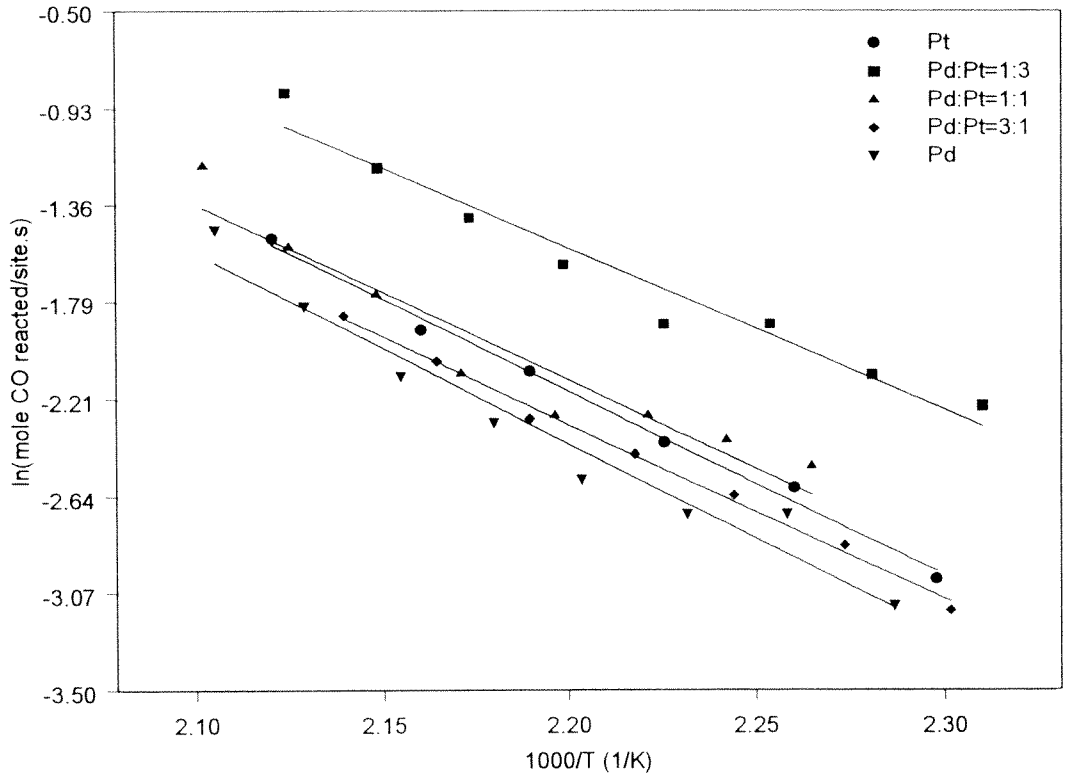
-0.50
-0.93
-1.36
-1.79
-2.21
-2.64
-3.07
-3.50
ln(mole CO reacted/site.s)
2.10
2.15
2.20
2.25
2.30
1000/T (1/K)
Pt
Pd:Pt=1:3
Pd:Pt=1:1
Pd:Pt=3:1
Pd

Figure 8

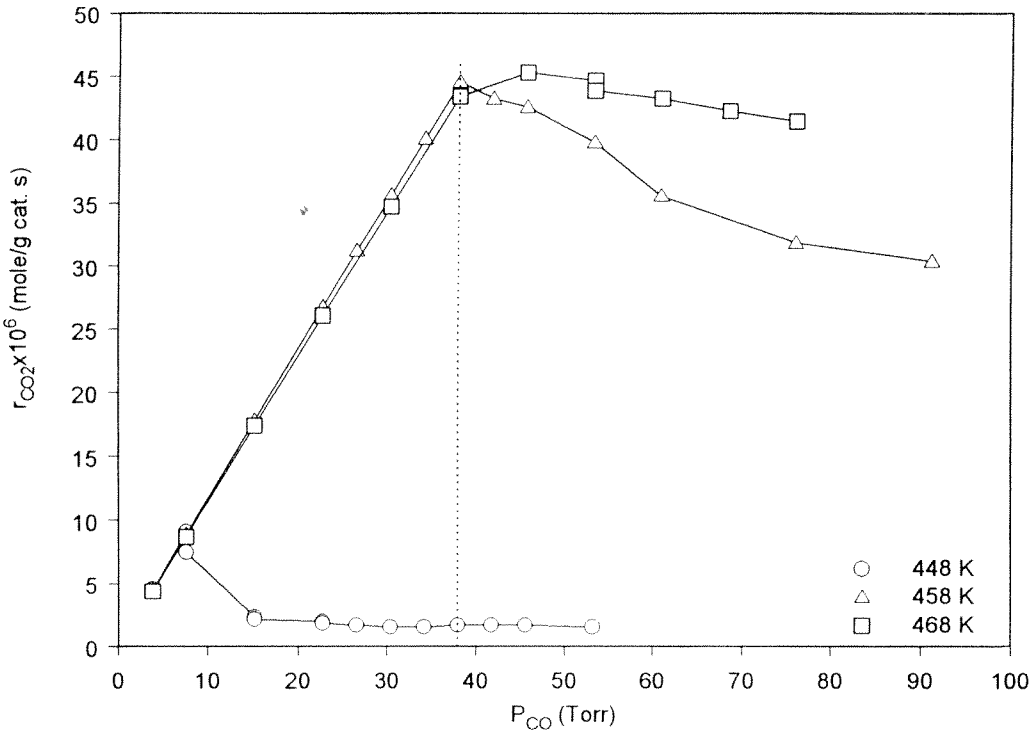
50
45
40
35
30
25
20
15
10
5
0
0
10
20
30
40
50
60
70
80
90
100
$r_{CO2}x10^6$ (mole/g cat. s)
$P_{CO}$ (Torr)
448 K
458 K
468 K

Figure 9(a)

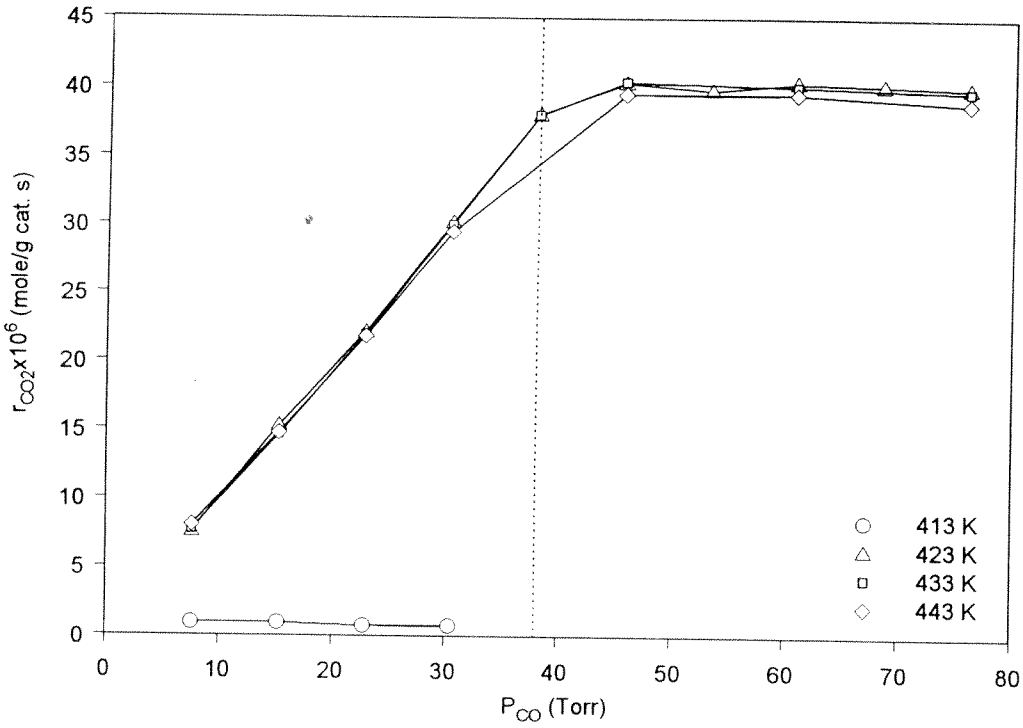
45
40
35
30
25
20
15
10
5
0
0
10
20
30
40
50
60
70
80
$r_{CO2}x10^6$ (mole/g cat. s)
$P_{CO}$ (Torr)
413 K
423 K
433 K
443 K

Figure 9(b)

Available online at www.sciencedirect.com
SCIENCE DIRECT®
ELSEVIER
Applied Catalysis A: General 251 (2003) 225–234
APPLIED CATALYSIS A: GENERAL
www.elsevier.com/locate/apcata

# Oxygen adsorption on $Pt/TiO_2$ catalysts

D. Uner*, N.A. Tapan[1], İ. Özen[2], M. Üner

*Chemical Engineering, Middle East Technical University, Inonu Bulvari, Ankara 06531, Turkey*

Received 25 October 2002; received in revised form 14 April 2003; accepted 15 April 2003

**Abstract**

Oxygen adsorption over $Pt/TiO_2$ surfaces were investigated as a function of metal loading. Oxygen adsorption over pure $TiO_2$ was molecular at all pressure ranges investigated. On the other hand, differential heats of adsorption measured by adsorption calorimetry indicated that oxygen adsorption was dissociative over $Pt/TiO_2$ surfaces until the Pt surface was saturated with oxygen. The saturation coverage of atomic oxygen on Pt was determined as approximately one from adsorption calorimetry. The initial heat of oxygen adsorption was determined as ~375 kJ/mol over 0.5 wt.% $Pt/TiO_2$. The differential heats of oxygen adsorption at coverages less than one monolayer of Pt surface was ~200 kJ/mol consistent with the oxygen adsorption heats over Pt single crystals reported in the literature. As the pressure increased after the saturation of Pt surface, oxygen adsorption continued in a manner similar to oxygen adsorption over pure $TiO_2$. Isosteric heats of oxygen adsorption over pure and $Pt/TiO_2$ samples at coverages >5 μmol/g catalyst were determined to be around 10 kJ/mol. The amounts of oxygen adsorption over $Pt/TiO_2$ surfaces depended strongly on the pretreatment conditions. Most favorable oxygen adsorption was observed over calcined/reduced samples.


*Keywords:* Oxygen adsorption; Spillover; Pt; $TiO_2$; Heat of adsorption

## 1. Introduction

$Pt/TiO_2$ systems are used both as catalysts and solid-state gas sensors. These systems are exploited as photo-catalysts due to the proper band gap of $TiO_2$ for excitation by electromagnetic radiation in the UV frequencies. Furthermore, the semiconductor nature of $TiO_2$ makes it a good alternative for the solid-state gas sensor for oxygen, hydrogen, and some combustion gases. In both photo-catalysis and sensor applications, interaction of $TiO_2$ surface with oxygen is necessary, and in both systems, the presence of Pt is known to improve the performance, mostly argued as due to the spillover phenomenon.

Spillover is a widely recognized fact since the 60s in the field of catalysis [1–3]. Spillover phenomenon is also observed and exploited in the field of solid-state gas sensors as well [4–7]. Among the many definitions of spillover, two are quoted here: "Spillover is the mobility of sorbed species from one phase on which it is easily adsorbed onto another phase where it does not directly adsorb" [8] or "Spillover is the transport or overflow of active species sorbed or formed on a first surface onto an other surface that does not under

* Corresponding author. Tel.: +90-312-210-4383; fax: +90-312-210-264.
*E-mail address:* uner@metu.edu.tr (D. Uner).
[1] Present address: Chemical and Environmental Engineering, Illinois Institute of Technology, 10 West 33rd Street, Chicago, IL 60616, USA.
[2] Present address: Materials Science and Engineering Program, Faculty of Engineering and Natural Sciences (FENS), Sabancy University, Orhanli, Tuzla, 81474 Istanbul, Turkey.

0926-860X/$ – see front matter © 2003 Elsevier B.V. All rights reserved.
doi:10.1016/S0926-860X(03)00317-X

Table 1
Adsorption and desorption rate parameters of oxygen over Pt and $TiO_2$ surfaces

| Surface | Adsorption mode of oxygen | Saturation coverage (ml) | Sticking Coefficient ($S_0$) | $E_{a,des}$ (kJ/mol) | $\Delta H_{ads}$ (kJ/mol) | Reference |
|---|---|---|---|---|---|---|
| Pt(1 1 1) | Dissociative | | 0.064 | | 339 ± 32 | [14] |
| Pt(1 1 0) | Dissociative | 0.35 | 0.34 | | 332 ± 10 | [15] |
| Pt(1 1 1) | | 0.25 | 0.06 | 213.4, 175.7 | | [16] |
| Pt(S)-[9(1 1 1) × (1 1 1)] | | 0.5 | 0.06 | 205, 171.5 | | [17] |
| Pt(1 1 1) | Molecular | 0.6 | | | 37 ± 2 | [18] |
| Pt(1 1 1) | Dissociative | 0.4 | | | 470 ± 10 | [18] |
| Pt(1 1 1) | | 0.25 | 0.048 ± 0.006 | | | [19] |
| Pt(1 1 1) | | 0.25 | | | | [20] |
| Pt(1 1 1) | Molecular, peroxo | | | | 40.5 | [21] |
| Polycristalline Pt | | 0.75 | | | | [22] |
| Pt(1 1 1) | Molecular | | 0.12 | | | [23] |
| $TiO_2$(1 1 0) | Molecular | | $8 \times 10^{-5}$ | 94 | | [24] |
| $TiO_2$(1 1 0) | Molecular | | 0.5–0.6 | 108 | | [25] |

the same conditions sorb or form the active species" [3].

Most of the oxides are poor adsorbents for stable molecules such as $O_2$ or $H_2$. However, when a metal capable of braking O–O or H–H bond is present, the dissociated molecules can migrate from the metal to the support surface, and the sorption capacity of the oxides towards these dissociated molecules are almost proportional to the surface area of the oxide. Therefore, the presence of a metal can improve the sorption capacity of an oxide by orders of magnitude via the spillover mechanism. In the solid-state gas sensors, the chemical sensation is based on the capacity of the surface to interact with the adsorbate and to the extent of the electron transfer processes between the adsorbate and the primary conducting phase. Therefore, if the surface concentration of the adsorbate is higher at a given gas phase pressure, the sensitivity of the material will improve. In the field of catalysis, spilled-over species can increase the reaction rate by several mechanisms. For $Pt/TiO_2$ photo-catalysts, for example, oxygen spilled over from Pt to $TiO_2$ may enhance the rate of the photo-oxidation reaction taking place over the oxide surface [9–13].

In Table 1, the adsorption heats, the desorption activation energies, saturation coverages, and initial sticking coefficients of oxygen over various surfaces of Pt and $TiO_2$ are reviewed. The data presented in Table 1 indicate that over Pt surfaces, oxygen can adsorb both molecularly and dissociatively, while the dissociative adsorption yielding almost a factor of 10 higher heats of adsorption. Over $TiO_2$ surfaces, it has been reported that dissociative oxygen adsorption requires oxygen vacancy sites and the coverage of oxygen is reported to be proportional to the oxygen vacancy concentration, in the order of $10^{14}$ sites/cm$^2$ [25]. There were no direct measurement data on heat of adsorption of oxygen over pure $TiO_2$ surfaces in the literature to the extend of the authors' knowledge: the data presented in Table 1 for the desorption activation energies of molecular oxygen over $TiO_2$ surfaces were reported based on the Redhead analysis of the Thermal Desorption Spectra [24,25]. This method requires assumptions for the desorption process order and desorption process frequency factor for activation energy determinations, and therefore the results are prone to errors of such assumptions.

In this study, the objective was to determine oxygen and hydrogen adsorption characteristics of pure and Pt containing $TiO_2$ powders. This was accomplished by measuring adsorption isotherms of powders at different metal loadings which was subjected to numerous catalyst pretreatment procedures. The differential adsorption heats were measured directly for oxygen adsorption on Pt sites. On the other hand, isosteric heats of adsorption on $TiO_2$ were determined from the adsorption isotherms measured at room temperature and at 0 °C.

## 2. Materials and methods

### 2.1. Sample preparation

All of the samples were prepared by incipient wetness impregnation of Pt from a solution of tetraammine platinum(II) chloride hydride (Johnson Matthey) on dried Degussa P25 $TiO_2$ support (50 $m^2$/g BET surface area). The impregnation solution was prepared by dissolving an appropriate amount of $PtCl_2(NH_3)_4 \cdot H_2O$ salt in distilled water. Approximately 2 ml of solution per gram of support was needed to bring about incipient wetness. The slurries obtained after impregnation were dried overnight at room temperature and at 400 K for 2 h. The catalysts prepared as such were reduced in hydrogen at 723 K prior to the adsorption measurements. In order to eliminate the effect of residual chlorine, the catalysts were either reduced or calcined in air at 723 K, washed in hot water until all of the chlorine ions were removed [28], dried and reduced for adsorption tests. The hot water elutriation continued until the filtrate solution did not show any turbidity after the addition of $AgNO_3$ solution.

### 2.2. Adsorption measurements

Adsorption measurements were conducted on a home built adsorption apparatus based on the design of Wu et al. [26]: a multiport high-vacuum Pyrex glass manifold with a volume of 166 $cm^3$ in connection with a turbo molecular pump (Varian Turbo V70D) backed by a mechanical pump (Varian SD-40). In order to minimize hydrocarbon impurities in the manifold, high-vacuum greaseless, bakeable stopcocks with Teflon plugs and FETFE O-ring seals (Ace Glass) were employed to manipulate gas storage and/or dosage. The manifold was capable of a vacuum better than $10^{-6}$ Torr (1 Torr = 133.3 Pa) after bake-out. A cold cathode gauge (Varian 524-2) monitored pressures below $10^{-3}$ Torr. Pressures from $10^{-4}$ to $10^{3}$ Torr were measured by two capacitance absolute pressure gauges (Varian CeramiCel). Catalyst samples were held in a Pyrex cell, a small heating mantle connected to a Variac was used to adjust the temperature in the cell. The schematics of the adsorption manifold and peripherals is given in Fig. 1.

All catalyst samples were treated inside the Pyrex cell. Approximately 1 g of sample was loaded into the cell, which was then attached to one of the sample ports of the manifold. The catalysts were reduced in situ according to the following recipe. Approximately 100 Torr of helium was dosed in the manifold, the temperature of the heating mantle surrounding the cell was raised to 423 K for about 30 min to remove the residual water on the sample. The sample was then evacuated, 100 Torr of $H_2$ was dosed on the sample and the temperature was gradually raised to 623 K. At this temperature the sample was evacuated, fresh hydrogen at 750 Torr was dosed for 30 min. Evacuation and fresh hydrogen dose for 30 min was repeated until the catalyst was exposed to hydrogen atmosphere at 623 K for at least 2 h. After the reduction process, the catalyst was cooled down to room temperature during final evacuation.

Pure hydrogen and oxygen gases (99.99%) were used in the experiments. Hydrogen and oxygen adsorption experiments were performed at room temperature, 263, 273, and 330 K. The total oxygen and hydrogen adsorption isotherms were measured in the 0–800 Torr pressure range.

### 2.3. Microcalorimetry

Heat of adsorption measurements were conducted on Setaram C-80 Tian-Calvet calorimeter coupled to the multiport high-vacuum Pyrex glass manifold, described in Section 2.2. Home-made Pyrex sample and the reference cells for the calorimeter are shown in Fig. 1. The sample and the reference cells were connected to each other and to the vacuum manifold by a Pyrex tee. Stainless Steel bellows were used to connect the sample and the reference cells to the tee. All of the connections were made of stainless steel Cajon Ultra Torr unions. Thermal insulation of the home-made cells were followed from the original design of the sample cells of Setaram: in order to avoid convective currents surrounding the sample cells, three aluminum rings were placed around the sample tube as shown in Fig. 1. The aluminum rings were supported by concentric glass tubes placed outside the sample tube.

Approximately 1 g of pre-reduced and pre-calcined sample was loaded into the sample cell, which was then attached to one end of the tee connection and inserted into the sample port of the microcalorimeter. The other end of the tee connection was attached to an empty sample cell inserted into the reference

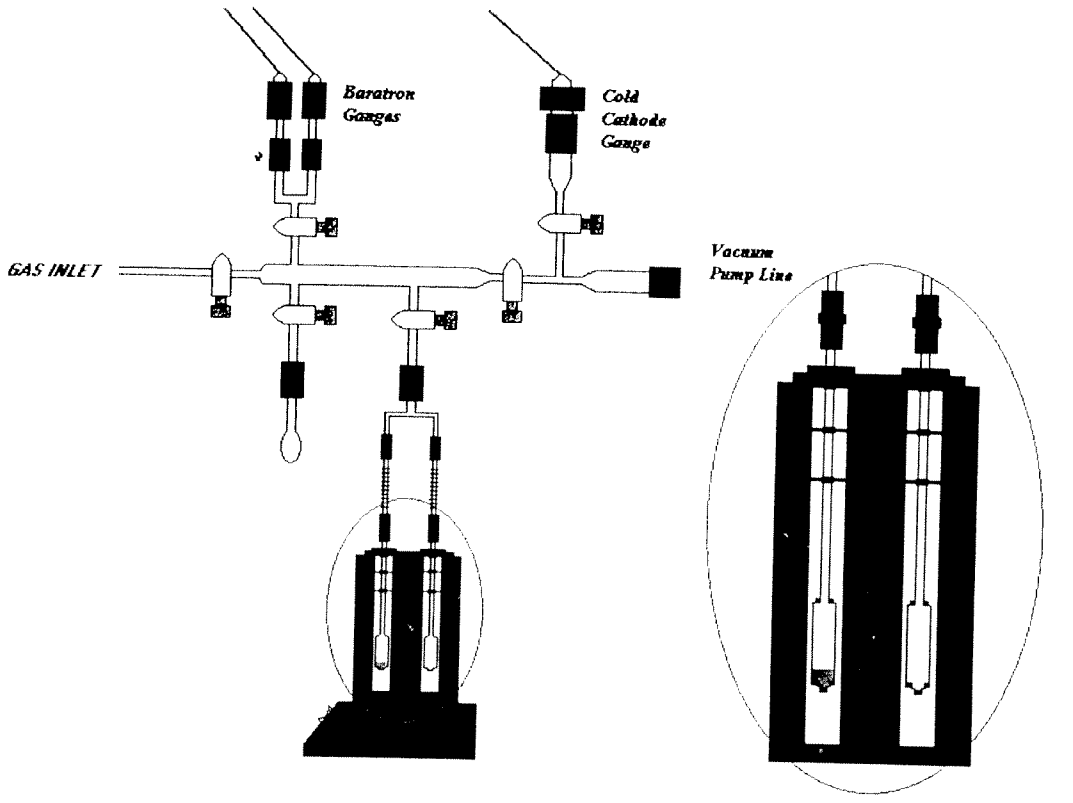


Fig. 1. The schematic drawing of the adsorption manifold and the sample-reference cell configuration for the microcalorimeter.

port of the microcalorimeter. The reduction procedure described above was followed except the high pressure $H_2$ dosing temperature reduced to 523 K due to the maximum allowable temperature limit of the microcalorimeter. After the reduction process the catalyst was cooled down to 303 K during final evacuation. Differential heats of adsorption were measured by introducing small amounts of gas into the sorption chamber. The amount adsorbed and the heat evolution data were recorded up to the point where there was no heat signal detected upon incremental gas dosing.

## 3. Results and discussion

### 3.1. Dispersion measurements

The dispersion measurements were based on the procedure described by Uner et al. [27]. The catalysts were reduced in situ as described in Section 2. Total and weak adsorption isotherms were measured up to a maximum hydrogen pressure of ~30 Torr. The strong hydrogen amounts were deduced from the difference between the zero pressure adsorption amounts. The strong hydrogen adsorption amounts, and the dispersion values obtained for 1:1 $H:Pt_{surface}$ stoichiometry for Pt loaded $TiO_2$ catalysts are presented in Table 2. As seen in Table 2, percent dispersions were anomalously high for the low loading ratios (0.001 and 0.01 wt.% Pt). This is suspected to be due to the presence of an irreversible component of the spilled over hydrogen over the support surface [27]. But excluding very low loading ratios it can be said that increase in Pt loading from 0.1 to 1.83% increased the active metal site density and dispersion. The increase in dispersion with increasing metal loading may contradict the general understanding of supported metal catalysis. However, when the metals are supported on $TiO_2$, one must consider the possibility of decoration

Table 2
The metal dispersions, isosteric heats of oxygen adsorption over pure and Pt containing $TiO_2$ as a function of metal loading

| Pt (wt.%) | Pt loading (μmol Pt/g catalyst) | Strong H (μmol H/g catalyst) | Strong H/Pt | $O_2$ coverage (μmol/g catalyst) | $\Delta H_{iso}$ (kJ/mol) |
|---|---|---|---|---|---|
| 0 | 0 | N/A | N/A | 10 | 7.3 |
| 0 | 0 | N/A | N/A | 20 | 13.7 |
| 0.001 | 0.05 | 0.33 | 6.43 | 5 | 9.7 |
| 0.01 | 0.51 | 1.18 | 2.31 | 18 | 11.2 |
| 0.1 | 5.12 | 0.20 | 0.03 | 10 | 7.3 |
| 0.5 | 25.60 | 0.01 | 0.00 | 5 | 13.3 |
| 1.83 | 93.80 | 11.53 | 0.12 | 5 | 6.9 |

The oxygen coverages indicate the coverage at which the isosteric heats are calculated.

of the metal particles by the $TiO_x$ moieties during the catalyst preparation procedure. If $TiO_x$ moieties prefer the low coordination edge and corner sites, they can block a relatively higher fraction of adsorption sites on smaller particles. Therefore, it is possible to measure lower values of apparent dispersions for low loading catalysts by hydrogen chemisorption. On the other hand, this sort of decoration is not possible for monodispersed catalysts, e.g. 0.001 or 0.01 wt.% catalysts in this study, therefore the site blocking effects were not observed on these catalysts.

### 3.2. Effect of metal loading on $H_2$ adsorption

Due to the known spillover behavior of hydrogen, spillover characteristics of the samples were investigated with respect to hydrogen gas. Hydrogen gas adsorption was studied in the pressure range 8–800 Torr. The adsorbed gas was allowed to reach equilibrium for 30–150 min before the adsorption data were collected. The isotherms collected at room temperature and at 273 K are shown in Fig. 2 as a function of metal loading. The lowest loaded sample

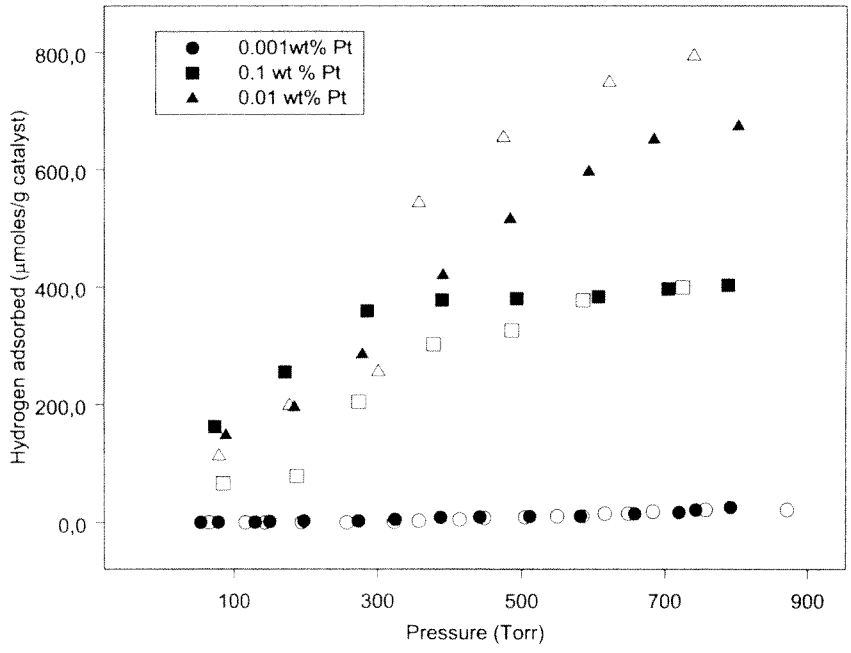


Fig. 2. Room temperature hydrogen adsorption studies over $Pt/TiO_2$ catalysts. The open symbols correspond to the isotherms measured at 273 K, the dark symbols correspond to the isotherms measured at room temperature.

(0.001 wt.% Pt) did not exhibit much hydrogen adsorption beyond the potential uptake of pure $TiO_2$. As the Pt loading increased, the hydrogen uptake has also increased. The unique behavior observed in the dispersion data was also observed here. The hydrogen uptake capacity of 0.01 wt.% catalyst was higher than that of 0.1 wt.% catalyst at elevated pressures. This effect could be attributed to the higher nominal dispersion of the low loading (0.01 wt.% Pt) catalyst thereby causing increased amounts of hydrogen spillover. One must bear in mind that the spillover process is surface diffusion limited [2] and the process may continue over several hours at such a slow rate that may not be observable within the sensitivity limits of pressure measurements in our experiments. The data presented in Fig. 2 contains the pseudo-equilibrium isotherm information of hydrogen adsorption over the metal surface, however, the equilibrium condition for the spilled over hydrogen may not have been established within that time frame. Thus, highly dispersed catalysts, having higher metal-oxide interfacial areas, can cause facile spillover process than their lower dispersed conterparts.

As to the nature of the spilled over hydrogen is concerned, the charge balance over the metal surface requires that atomic hydrogen must spillover to the support. The spilled over hydrogen may undergo chemical interactions with the support to form $H^+$ and $e^-$ pairs [29] which may result in formation of $Ti^{3+}$ ions [30].

### 3.3. Oxygen adsorption studies

In order to establish the oxygen adsorption capacity of pure $TiO_2$, a series of adsorption measurements were performed on (i) untreated $TiO_2$, i.e. $TiO_2$ was used as received; (ii) $TiO_2$ evacuated at 393 K for 1 h; and (iii) $TiO_2$ being subjected to incipient wetness treatment with distilled water, dried and evacuated. All of the catalysts were evacuated for 1 h before any adsorption measurements were performed. Room temperature oxygen adsorption isotherms of pure $TiO_2$ subjected to pretreatment conditions mentioned above are presented in Fig. 3. As seen in Fig. 3, incipient wetness treatment of $TiO_2$ with distilled water caused a decrease in the oxygen adsorption capacity of pure support. On the other hand, there was no observable difference between the oxygen adsorption isotherms of untreated support and support evacuated at 393 K. The loss of oxygen adsorption capacity as a result of incipient wetness treatment can be attributed to

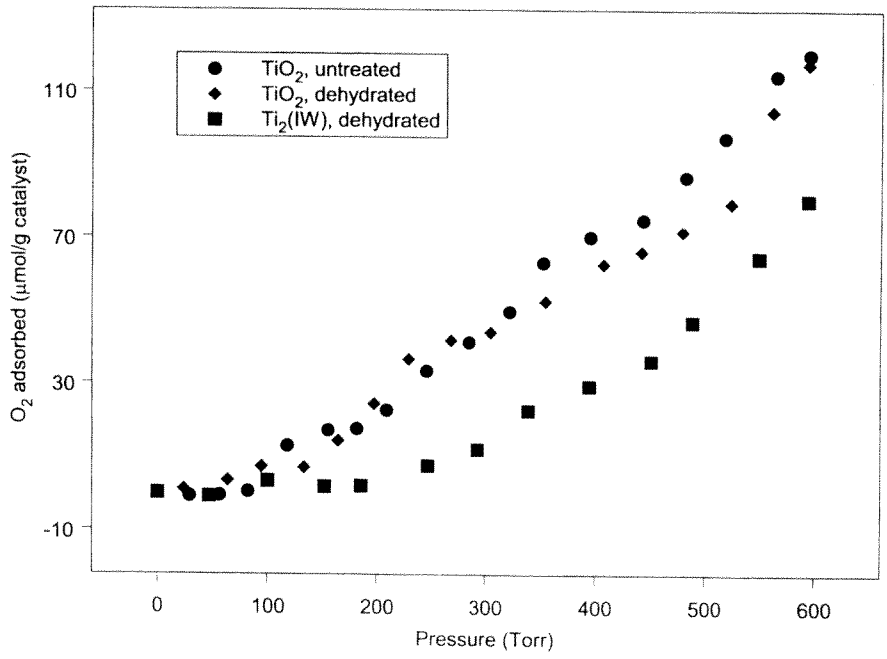


Fig. 3. Oxygen adsorption isotherms over $TiO_2$ at room temperature treated under different conditions.

Table 3
BET surface areas, strong hydrogen adsorption amounts, and zero coverage differential heats of adsorption of pure and Pt containing $TiO_2$

| Pt (wt.%) | BET surface area ($m^2$/g catalyst) | Pt loading (μmol Pt/g catalyst) | Strong H (μmol H/g catalyst) | Strong H/Pt | $O_2$ saturation coverage over Pt (μmol/g catalyst) | Zero coverage heat of adsorption (kJ/mol) |
|---|---|---|---|---|---|---|
| 0[a] | 45.9 | 0 | N/A | N/A | N/A | N/A |
| 0[b] | 45.2 | 0 | N/A | N/A | N/A | N/A |
| 0.5 | 44.5 | 51.30 | 0.86 | 0.03 | 1.5 | 320 |
| 1.0 | 44.5 | 51.30 | 6.36 | 0.12 | 3.0 | 380 |

[a] $TiO_2$ as received.
[b] $TiO_2$ was subjected to incipient wetness treatment with pure water and dried at 300 K.

hydroxilation of the oxygen adsorption sites which could not be restored during the further treatment of the sample. The highest amount of oxygen uptake measured on these catalysts was ~110 μmol/g catalyst over an untreated sample. The BET surface areas of the untreated $TiO_2$ and $TiO_2$ after an incipient wetness treatment with pure water and drying are given in Table 3. As can be seen from the data, there was no observable difference between the surface areas of either sample, a slight decrease in the surface area occurred upon incipient wetness treatment, coherent with a decrease in the oxygen adsorption capacity of the catalyst.

Because the Pt containing catalysts were prepared via incipient wetness impregnation, the adsorption capacities of all the catalysts investigated in this study were compared to that of $TiO_2$(IW). The effect of calcination and the order of reduction and calcination on the oxygen adsorption isotherms over 0.5 wt.% $Pt/TiO_2$ were investigated after the following steps: (i) the fresh catalyst was first reduced and then calcined; (ii) the fresh catalyst was reduced, calcined, and re-reduced; (iii) the catalyst was calcined only; (iv) the fresh catalyst was calcined and then reduced. After each of the treatments listed here, the oxygen adsorption capacities of the catalysts were measured and plotted in Fig. 4. It was observed that the order of reduction and calcination steps was important, the oxygen adsorption capacity of a calcined/reduced sample was higher than that of reduced/calcined sample.

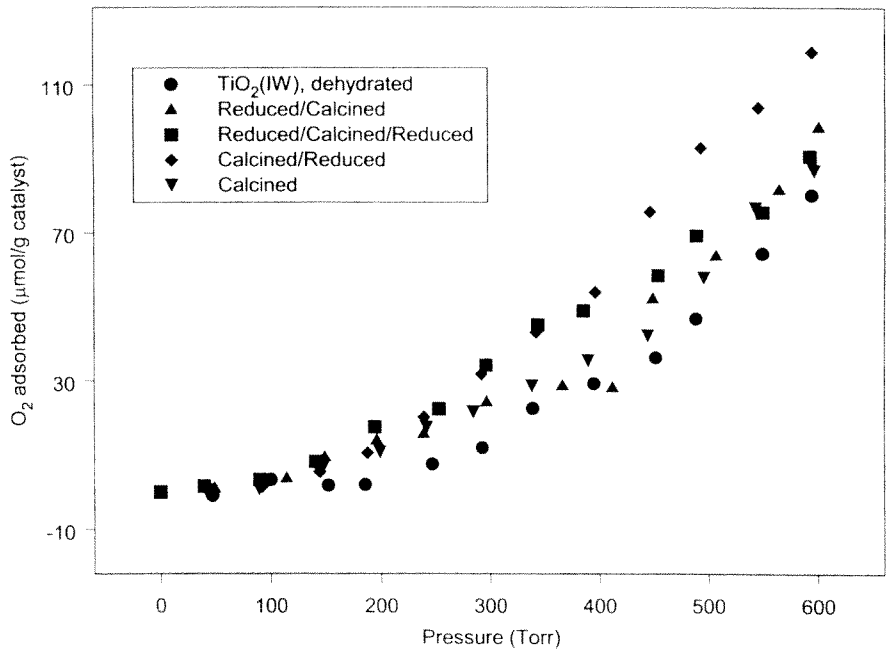


Fig. 4. Effect of reduction and/or calcination on room temperature oxygen adsorption isotherms over 0.5 wt.% $Pt/TiO_2$.

Furthermore, all of the samples exhibited higher oxygen coverages than $TiO_2$(IW). The excess amounts of adsorbed oxygen can be attributed to either spillover or direct oxygen adsorption over support surface due to the limited oxygen adsorption capacity of the metal particles. If the oxygen adsorption capacity of $Pt/TiO_2$ is compared to that of the untreated $TiO_2$, one may conclude that the presence of Pt assisted the restoration of oxygen adsorption sites, which were lost over $TiO_2$ surface during the incipient wetness treatment. On the other hand, if the oxygen adsorption capacity of $Pt/TiO_2$ is compared to $TiO_2$(IW) sample, one may conclude the presence of a spillover process. The adsorption process orders can clarify whether the excess oxygen is due to the direct adsorption of molecular oxygen over $TiO_2$ sites or due to the spillover of dissociated oxygen.

In order to determine the order of the oxygen adsorption process over pure $TiO_2$(IW), log($P$) was plotted against log(coverage) (not shown). Within the pressure range covered in this study, the log–log plot yielded straight lines with slopes equal to 1 indicating molecular adsorption of oxygen at room temperature and below over pure and Pt containing $TiO_2$ surfaces at pressures exceeding 10 Torr. Between the two hypotheses presented in the previous paragraph, direct adsorption of molecular oxygen over $TiO_2$ surface after the saturation of the metal particles seems more realistic given that the adsorption process order is one in that pressure zone. In order to provide a firm judgement about which of these processes prevail, surface spectroscopic evidence is still required.

The effect of metal loading on oxygen adsorption was monitored after reduction/calcination/re-reduction steps. It was observed that low loading catalysts (0.1 and 0.5 wt.% Pt) behaved similarly with higher oxygen uptakes while a high loading catalyst (1.0 wt.%) exhibited a behavior similar to that of $TiO_2$(IW) at elevated pressures (Fig. 5). The heat of adsorption data measured on these catalysts and low coverage behavior will be discussed in the next section.

### 3.4. Heats of adsorption

#### 3.4.1. Differential heats of adsorption

The direct measurement of the differential heats of adsorption was performed by adsorption calorimetry as described in the Section 2. There was no observable heat of adsorption within the sensitivity limits

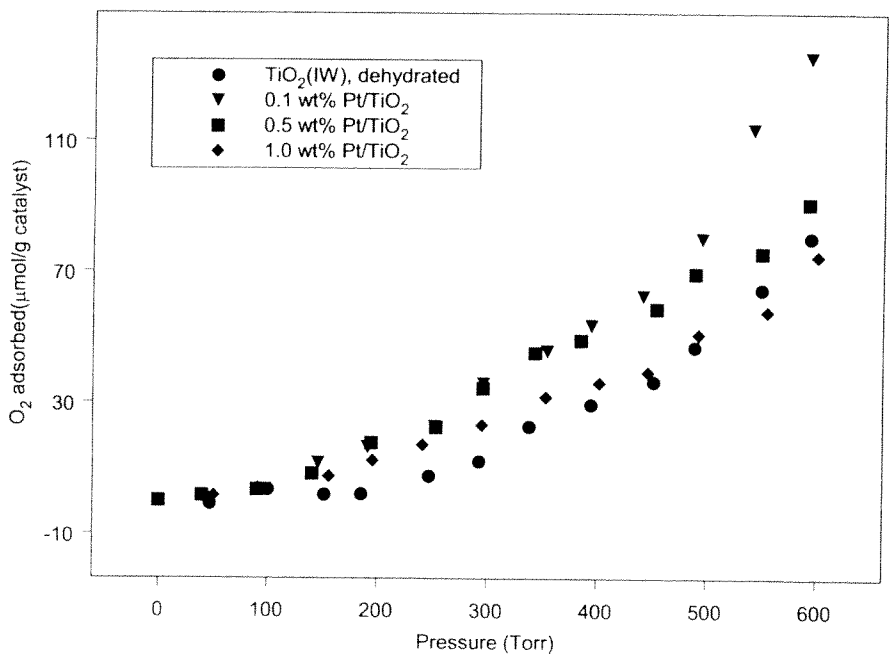


Fig. 5. Comparison of room temperature oxygen adsorption isotherms with respect to Pt loading over reduced/calcined/re-reduced samples.

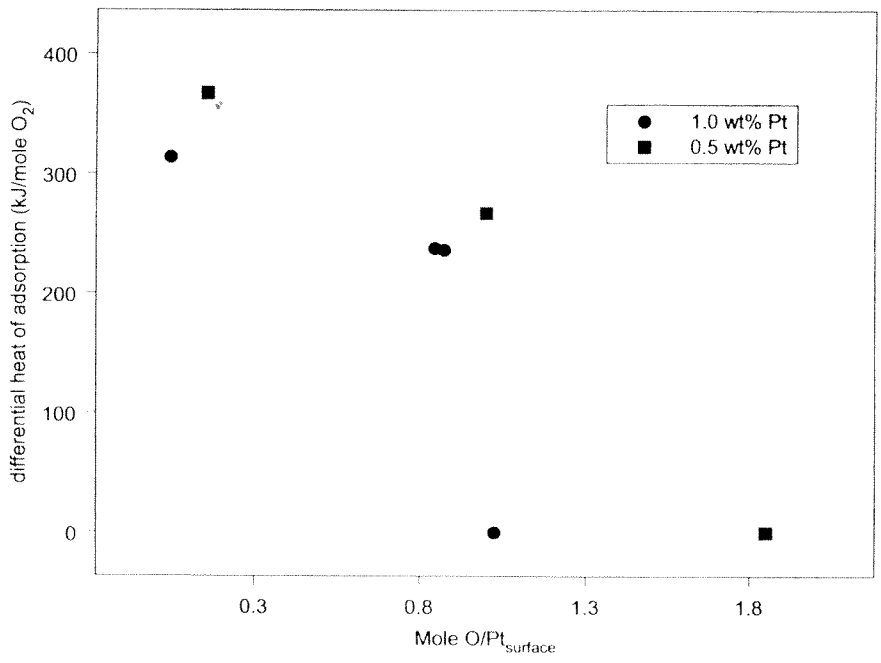


Fig. 6. Differential heats of oxygen adsorption on 0.5 and 1 wt.% $Pt/TiO_2$ measured at 30 °C.

of experimentation over pure $TiO_2$ surface. Similarly, measurements on low metal loading (0.1% or less) did not show any measurable adsorption heats. Due to the limitations associated with the present design of the gas manifold, the least amount of quantifiable adsorption was within 0.5 μmol range. Therefore, events occurred at lower coverages could not be quantified in terms of coverage and in terms of heat evolution per mole of gas adsorption. For low metal loadings, it is most probable that the highest heat evolving event, i.e. the dissociative adsorption of oxygen over Pt surface, occurred at this low coverage limit and thus could not be measured. The differential heats of oxygen adsorption on 0.5 and 1 wt.% $Pt/TiO_2$ as a function of surface coverage of Pt (mole O adsorbed/surface Pt) are presented in Fig. 6. The thermally tractable adsorption stopped at approximately 3 μmol $O_2$/g catalyst over 1 wt.% $Pt/TiO_2$ while on 0.5 wt.% $Pt/TiO_2$ the saturation occurred at approximately half of this coverage. When the adsorbed amounts were based on per surface Pt site determined by strong hydrogen chemisorption, it was observed that the surface of 1 wt.% catalyst is saturated at approximately one monolayer of Pt. The last experimental data point for surface saturation of 0.5 wt.% catalyst is recorded at a surface coverage of 1.8 mol O/surface Pt. However, this point can not be considered as the point of saturation, rather, it is due to the limitations of dosing smaller volumes of gas into the chamber. The saturation coverage of oxygen on both surfaces can be taken as approximately one, which is slightly higher than the reported oxygen saturation coverage for polycrystalline Pt [22]. It is important to note that while there was no measurable adsorption heat beyond the noise level of the instrument after this coverage, oxygen adsorption amounts could be quantified volumetrically up to 800 Torr.

The adsorption heats measured for the 0.5 wt.% catalyst were systematically higher than those over 1 wt.% catalyst. Lower Pt loading catalyst also has a lower dispersion (3.4%) as measured by volumetric hydrogen chemisorption, which indicated larger crystallites and therefore the presence of more low index planes than 1 wt.% Pt catalyst. The heats of adsorption data reported in the literature, compiled in Table 1, are for (1 1 1) or (1 1 0) planes of Pt, no data could be found for (1 0 0) planes. The difference in the heats of

adsorption on 0.5 and 1 wt.% catalysts may be due to the structure dependence of oxygen adsorption on different crystallographic planes [31]. However, the data presented here is not sufficient to provide conclusive evidence.

*3.4.2. Isosteric heat of adsorption of oxygen*

Isosteric heats of adsorption of oxygen were determined from oxygen adsorption isotherms measured at 0 °C and at room temperature. The isosteric heats were calculated at constant oxygen coverage by using Clasius–Clapeyron equation.

$$\ln\left(\frac{P_2}{P_1}\right) = -\frac{\Delta H_{\text{iso}}}{R}\left(\frac{1}{T_2} - \frac{1}{T_1}\right) \quad (1)$$

Isosteric heats of adsorption thus calculated are presented in Table 2. The coverage values are presented on the same table to indicate at which coverage the heat of adsorptions were calculated. It is important to note here that the isosteric heats of adsorption calculated as such are determined at coverages higher than the saturation coverage of Pt. The heat of adsorption data indicate that the high-energy sites (those of Pt) are saturated before 3 μmol/g catalyst for 1 wt.% Pt/$TiO_2$. All of the isosteric heats were calculated at coverages much higher than this value, therefore belong to oxygen adsorption over $TiO_2$ surface. The isosteric heats thus calculated are very low in comparison to the dissociative oxygen adsorption over $TiO_2$ surfaces, as presented in Table 1. The isosteric heats determined indicate that at the coverages studied here, oxygen interaction with $TiO_2$ surface is much weaker than its interaction with Pt surface.

## 4. Conclusions

Oxygen adsorption over pure and Pt containing $TiO_2$ samples indicated that oxygen adsorption at room temperature over pure $TiO_2$ is molecular while oxygen adsorption over Pt/$TiO_2$ is dissociative up to $O:Pt_{surface}$ stoichiometry of approximately one. While the experimental data collected in this study indicated that large amounts of atomic hydrogen spillover, no direct evidence could be found for oxygen spillover from Pt to $TiO_2$. The excess oxygen adsorbed over Pt/$TiO_2$ samples could be attributed to direct adsorption of molecular oxygen over $TiO_2$ surfaces.

## Acknowledgements

Financial support for this project was provided by TUBITAK under research Grants MISAG-96 and MISAG-188. The acquisition of the adsorption calorimeter was possible through a State Planning Organization Technology Research Grant No. AFP-03-04-DPT-98K122550. The authors acknowledge Mr. Isa Mbaraka for his assistance in dispersion measurements.

## References

[1] S. Khoobiar, J. Phys. Chem. 68 (1964) 411.
[2] M. Boudart, J.A. Robell, E.V. Ballou, J. Phys. Chem. 68 (1964) 2748.
[3] W.C. Conner, J.L. Falconer, Chem. Rev. 95 (1995) 759.
[4] V. Brynzari, G. Korotchenkov, S. Dimitriev, Sens. Actuators B: Chem. 61 (1999) 143.
[5] N. Barsan, U. Weimar, J. Electroceram. 7 (2001) 143.
[6] H. Nienhaus, Surf. Sci. Rep. 45 (2002) 3.
[7] A. Ruiz, J. Arbiol, A. Cierera, A. Cornet, J.R. Morante, Mater. Sci. Eng. C-Bio. Mater. Sens. Syst. S. 19 (2002) 105.
[8] S.J. Teichner, Stud. Surf. Sci. Catal. 77 (1993) 27.
[9] S. Ozbek, D.O. Uner, Stud. Surf. Sci. Catal. 126 (1999) 411.
[10] I. Ozen, D. Uner, Stud. Surf. Sci. Catal. 133 (2001) 445.
[11] J.L. Falconer, K.A. Magrini-Bair, J. Catal. 179 (1998) 171.
[12] D.S. Muggli, J.L. Falconer, J. Catal. 191 (2000) 318.
[13] A.L. Linsebigler, G.Q. Lu, J.T. Yates, Chem. Rev. 95 (1995) 735.
[14] D.A. King, Y.Y. Yeo, L. Vattunoe, J. Chem. Phys. 106 (1997) 392.
[15] D.A. King, Y.Y. Yeo, C.E. Wartnaby, J. Phys. Chem. 100 (1996) 12483.
[16] C.T. Campbell, G. Ertl, Surf. Sci. 107 (1981) 220.
[17] K. Schwaha, E. Bechtold, Surf. Sci. 65 (1977) 277.
[18] J.L. Gland, B.A. Sexton, G.B. Fisher, Surf. Sci. 95 (1980) 587.
[19] D.R. Monroe, R.P. Merrill, J. Catal. 65 (1980) 461.
[20] C. Puglia, A. Nilsson, Surf. Sci. 342 (1995) 119.
[21] B. Mullins, P.D. Nolan, J. Chem. Phys. 111 (1999) 3696.
[22] Y.Y. Tong, J.J. Van der Klink, J. Phys.-Condens. Mater. 7 (1995) 2447.
[23] H. Froitzheim, G. Hess, A. Cudok, Surf. Sci. 307–309 (1994) 761.
[24] W. Gopel, G. Rocker, R. Feierabend, Phys. Rev. B 28 (1983) 3427.
[25] M.A. Henderson, W.S. Epling, C.L. Perkins, C.H.F. Peden, U. Diebold, J. Phys. Chem. 103 (1999) 5328.
[26] X. Wu, B.C. Gerstein, T.S. King, J. Catal. 118 (1989) 238.
[27] D.O. Uner, M. Pruski, T.S. King, J. Catal. 156 (1995) 60.
[28] X. Wu, B.C. Gerstein, T.S. King, J. Catal. 135 (1992) 68.
[29] G.C. Mather, F.M.B. Marques, J.R. Frade, J. Eur. Ceram. Soc. 19 (1999) 887.
[30] J.C. Conesa, J. Soria, J. Phys. Chem. 86 (1982) 1392.
[31] C. Descorme, D. Duprez, Appl. Catal. A: Gen. 202 (2002) 231.

# Adsorption Calorimetry In Supported Catalyst Characterization: Adsorption Structure Sensitivity On Pt/$\gamma$-$Al_2O_3$

M. Uner and D. Uner[1]

Chemical Engineering, Middle East Technical University

Ankara 06531

Turkey

[1]uner@metu.edu.tr

**Abstract:**

In this study, the structure sensitivity of hydrogen, oxygen and carbon monoxide adsorption was investigated by changing the metal particle size of $Pt/Al_2O_3$ catalysts. 2 % $Pt/Al_2O_3$ catalysts were prepared by incipient wetness method; the particle size of the catalysts was manipulated by calcining at different temperatures. The dispersion values for the catalysts calcined in air at 683K, 723K, 773K and 823K were measured as 0.62, 0.28, 0.20 and 0.03 respectively. The differential heats of adsorption of hydrogen, carbon monoxide and oxygen were measured using a SETARAM C80 Tian-Calvet calorimeter. No structure dependency was observed for hydrogen, carbon monoxide or oxygen initial heats of adsorption. The adsorbate:metal stoichiometries at saturation systematically decreased with increasing particle size. Hydrogen chemisorption sites with low and intermediate heats were lost when the particle size increased. On the other hand, oxygen and carbon monoxide initial heats and adsorption site energy distributions did not change appreciably with the metal particle size.

**Introduction:**

Many catalytic reactions are structure sensitive, the rate depends on the detailed geometrical structure of the surface atoms of the catalyst. Structure sensitivity usually

manifests itself as a dependence of the rate per surface atom on the average size of the catalyst particles. The understanding is that the relative number of corner and edge sites increases dramatically with decreasing particle diameter, and these very low-coordinated surface atoms could have a substantially different ability to interact with the gas phase molecules. Norskov *et al.* (1) have demonstrated that the heat of adsorption of a species is directly related to the local structure of the catalysts, the step sites are more active unless poisoned, and they bind the adsorbates more strongly. The amount of heat evolved during the adsorption process, called the heat of adsorption, is closely related to the adsorbate-substrate bond strength. Furthermore, the differential heat of adsorption can be dependent on the surface coverage of the adsorbate due to the lateral adsorbate-adsorbate interactions or due to the surface heterogeneity.

The structure sensitivity of CO oxidation reaction is observed for gas phase catalytic reactions (2, 3) as well as in anodic oxidation studies (4). Both Zafiris and Gorte (2) and Gracia *et. al* (3) have measured lower activation energies for CO oxidation at lower dispersions. Zafiris and Gorte (2) have attributed the structure sensitivity of CO oxidation to higher desorption rates over larger particles promoted by the repulsive interactions due to the higher CO coverages on larger planes. The oxidation of CO to form $CO_2$ reaction proceeds via the combination of a chemisorbed CO molecule with a chemisorbed oxygen atom, the latter produced through the dissociative adsorption of $O_2$ on the Pt surface. Due to the poisoning effect of the CO adsorption on the Pt surface, amount of and bond strength of adsorbed oxygen on the surface gains more importance. The limited amount of data on oxygen adsorption compiled in a previous publication (5) is quoted in Table 1 for reference. The adsorption heats strongly depend on whether the adsorption is molecular or dissociative. Once dissociated, oxygen forms strong bonds with the surface exceeding 250 kJ/mol. However, the adsorption of oxygen over metal surfaces is hampered by the low sticking

coefficients on the surface. The dissociative sticking coefficient of oxygen was shown to increase exponentially with step concentration, adsorbed species at the steps are bound on the step edges, and dissociation almost exclusively takes place at the step sites (16 and references therein). The existence of the step sites was demonstrated to enhance the adsorption and dissociation of oxygen (16,17).

NMR studies combined with heat of adsorption measurements indicated that hydrogen adsorption over mono and bi-metallic $Ru/SiO_2$ catalysts is structure sensitive: hydrogen chemisorption is more facile over low coordination edge and corner sites (18-22). The structure sensitivity of hydrogen adsorption was reflected in the calorimetry data in terms of loss of sites with low and intermediate heats in the presence of Ag or Cu atoms. However, initial heats of adsorption were not influenced in the presence of Ag or Cu. The initial and integral heats of adsorption data presented in Table 2 for hydrogen over Pt do not change much with the particle size.

Structure sensitivity of CO adsorption was theoretically investigated by Hammer *et al.*(26). Their predictions on well-defined crystal planes indicated strong structure sensitivity in the adsorption energy from one structure to the other. The existence of the step sites is being demonstrated to enhance the adsorption of CO (25-27). Initial heats of CO adsorption on two different orientations of Pt single crystal surfaces are different beyond experimental errors (Table 3). But, the structure dependency of CO chemisorption is difficult to elucidate from the literature data collected over supported metal catalysts (Table 3).

Therefore, the objective of this study was to measure oxygen, hydrogen and CO adsorption heats to elucidate the energetic component of structure sensitivity of adsorption over $2\%Pt/Al_2O_3$ by changing the particle size. Calcination temperature was selected as the parameter to manipulate the particle size in order to avoid complications that may arise due to the preparative chemistry.

## 2. Materials and Methods:

**2. 1. Sample preparation:** All of the samples were prepared by incipient wetness impregnation of Pt from a solution of tetraammine platinum(II) chloride hydride (Johnson Matthey) on dried $\gamma$-$Al_2O_3$ (Johnson Matthey, 65 $m^2/g$ BET surface area). The impregnation solution was prepared by dissolving an appropriate amount of $PtCl_2(NH_3)_4.H_2O$ salt in distilled water. Approximately 2 ml of solution per gram of support was needed to bring about incipient wetness. The slurries obtained after impregnation were dried overnight at room temperature and at 400 K for two hours. The catalyst prepared as such was divided into four portions and each portion was calcined in air at a different temperature for four hours. The calcination temperatures were selected as 410, 450, 500 and 600 °C.

**2. 2. Adsorption Measurements:** Adsorption measurements were conducted on a home built adsorption apparatus explained in detail in a previous publication (5): a multi-port high-vacuum Pyrex glass manifold with a volume of 166 $cm^3$ in connection with a turbo molecular pump (Varian Turbo V70D) backed by a mechanical pump (Varian SD-40). In order to minimize hydrocarbon impurities in the manifold, high-vacuum greaseless, bakeable stopcocks with Teflon plugs and FETFE O-ring seals (Ace Glass) were employed to manipulate gas storage and/or dosage. The manifold was capable of a vacuum better than $10^{-6}$ Torr after bake-out. A cold cathode gauge (Varian 524-2) monitored pressures below $10^{-3}$ Torr. Pressures from $10^{-4}$ to $10^{3}$ Torr were measured by two capacitance absolute pressure gauges (Varian CeramiCel). Catalyst samples were held in a Pyrex cell, a small heating mantle connected to a Variac was used to adjust the temperature in the cell.

All catalyst samples were treated inside the Pyrex cell. Approximately 1 g of sample was loaded into the cell, which was then attached to one of the sample ports of the manifold. The catalysts were reduced *in-situ* according to the following recepie: Approximately 100 Torr of

helium was dosed in the manifold, the temperature of the heating mantle surrounding the cell was raised to 423 K for about 30 min to remove the residual water on the sample. The sample was then evacuated, 100 Torr of $H_2$ was dosed on the sample and the temperature was gradually raised to 623 K. At this temperature the sample was evacuated, fresh hydrogen at 750 Torr was dosed for 30 min. Evacuation and fresh hydrogen dose for 30 min was repeated until the catalyst was exposed to hydrogen atmosphere at 623 K for at least 2 hours. After the reduction process, the catalyst was cooled down to room temperature during final evacuation. The dispersion measurements were performed according to the method described by Uner et al (28). After collecting the total and weak hydrogen adsorption isotherms, the zero pressure values were obtained by extrapolating the data, the difference between the total and weak isotherm zero pressure values were reported as the strong hydrogen amounts. This value was used as the metal dispersions by assuming 1H:1Pt stoichiometry for the strongly bound hydrogen.

**2. 3. Microcalorimetry:** Heat of adsorption measurements were conducted on Setaram C-80 Tian-Calvet Calorimeter coupled to the multi-port high-vacuum Pyrex glass manifold, similar in design to the manifold described in section 2.2. In this manifold a Pfeifer turbo molecular pump station backed by a diaphragm pump was used. The pressure measurements was done by a Baratron gauge(Varian CeramiCel) in the range of $10^{-4}$-10 Torr. The details of the home made Pyrex sample and the reference cells for the calorimeter and the schematics of the set up are given in a previous publication (5). The sample and the reference cells were connected to each other and to the vacuum manifold by a Pyrex Tee. Stainless Steel bellows were used to connect the sample and the reference cells to the Tee. All of the connections were made of stainless steel Cajon Ultra Torr unions. Thermal insulation of the home made cells were followed from the original design of the sample cells of Setaram: in order to avoid

convective currents surrounding the sample cells, three aluminum rings were placed around the sample tube. The aluminum rings were supported by concentric glass tubes placed outside the sample tube.

Approximately 1 gr of pre-reduced and pre-calcined sample was loaded into the sample cell, which was then attached to one end of the tee connection and inserted into the sample port of the microcalorimeter. The other end of the tee connection was attached to an empty sample cell inserted into the reference port of the microcalorimeter. The reduction procedure described above was followed except the high pressure $H_2$ dosing temperature reduced to 543 K due to the maximum allowable temperature limit of the microcalorimeter. After the reduction process the catalyst was cooled down to 303 K during final evacuation. Differential heats of adsorption were measured by introducing small amounts of gas into the sorption chamber. The amount adsorbed and heat evolution data were recorded up to the point where there was no heat signal detected upon incremental gas dosing to the limit of the pressure measurement (10 Torr).

## 4. Results and discussion

The hydrogen adsorption amounts as measured by volumetric chemisorption are presented in Table 4 as a function of calcination temperature. It can be seen from the data presented in Table 4 that the catalyst particle sizes could be manipulated by changing the calcination temperature as measured by the strongly adsorbed hydrogen stiochiometries. On the same table the saturation coverages of all adsorbates as measured by calorimetry are also presented for comparison.

Hydrogen heat of adsorption data was plotted against hydrogen coverage Figure 1. The coverages were determined as the ratio of the hydrogen adsorption amounts to the total hydrogen amounts measured from chemisorption experiments. The heat of adsorption data was evaluated as per mol of atomic hydrogen adsorbed. The structure sensitivity of hydrogen

adsorption is evident from the data presented in Figure 1. As observed by Narayan and King (18) and Savargoankar *et al.* (19) over bimetallic catalysts, our catalysts have lost hydrogen adsorption sites with low and intermediate energies as the particle size increased, for the catalysts calcined at 450 and 500 °C. On the other hand, the heat of adsorption data of hydrogen over the catalyst calcined at 600 °C fall on the same curve as the data of the catalyst calcined at 410 °C. For the catalyst calcined at 600 °C, due to the low number of surface sites available for chemisorption, the sites with high initial heats could not be sampled. Narayan and King(18) and Savargoankar *et al.* (19) have attributed the sites with low and intermediate heats to planar surfaces over the catalyst particles. Our expectations of a catalyst calcined at 600 °C is to have mostly planar surfaces and the heats of adsorption of hydrogen values measured over these surfaces indicate that planar surfaces dominate over the catalyst calcined at 600 °C.

Oxygen adsorption data was also plotted in terms of dissociated oxygen coverages and heats per mol of atomic oxygen. The coverages were based on the saturation coverage over the catalyst as measured by calorimetry. It is important to note here that the differential heat of adsorption curve of oxygen over the catalyst calcined at 600 °C lies systematically above the differential heat of adsorption curve of the other catalysts. This can be interpreted as a particle size effect, over larger particles our group has measured higher heats over $Pt/TiO_2$ particles(5). CO adsorption heats shown in Figure 3 were also plotted against the fractional coverage, the coverage values were normalized to the saturation values as measured by calorimetry. Carbon monoxide adsorption heats do not exhibit any structure sensitivity; the heat of adsorption data for all catalysts fell on the same curve. The initial heats of adsorption and adsorption heats at saturation agree well with the literature data (Table 3) as well as the isosteric heats of adsorption measured by Dulaurent and Bianchi(29).

The number of moles of gas adsorbed at saturation per gram catalyst is plotted against the calcination temperature in Figure 4. The decrease in the adsorbed gas amounts is consistent with the decrease in metal dispersions (Table 4). The data in Figure 4 has some general characteristic trends. First of all, adsorbed oxygen amounts are consistently lower than that of carbon monoxide and hydrogen. Second, the decrease in adsorbed oxygen amounts with dispersion is not as pronounced as observed in hydrogen or carbon monoxide. Finally, on the catalyst calcined at 600 °C, the amount of hydrogen, oxygen and CO adsorbed approaches to similar values. Adsorbed hydrogen amounts are about twice as much as adsorbed CO or even larger for adsorbed oxygen amounts. This is believed to be due to a weakly bound hydrogen that exists on the metal surfaces at H:M stoichiometries greater than 1 (18).

In order to compare adsorption energetics, initial (open symbols) and integral (dark symbols) adsorption heats of oxygen, hydrogen and carbon monoxide were plotted in Figure 5 as a function of the amount of gas adsorbed at saturation. From Figure 5, one can deduce that neither initial nor integral heats of adsorption do not show a trend with changing metal particle size. It is important to note here that the oxygen adsorption heat data show a systematic decrease with decreasing particle size and the data point pertinent to the smallest particle size distribution catalyst show an increase in both initial and integral heats.

Finally, in order to demonstrate the relative change in the adsorbent-adsorbate relationships with the metal particle size, data in Figures 1-3 were replotted in figure 6 a and b. In Figure 6a the heats of adsorption of oxygen, carbon monoxide and hydrogen were plotted for the catalyst calcined at 410 °C, while in Figure 6 b the heats of adsorption of oxygen, carbon monoxide and hydrogen were plotted for the catalyst calcined at 600 °C. From Figure 6-a one can easily deduce that hydrogen adsorption sites have a broader site energy distribution, the intermediate and low adsorption sites are not observed for carbon monoxide and oxygen. Carbon monoxide and oxygen adsorption energetics follow similar

trends, which are not influenced by the metal particle size, while hydrogen adsorption site energy distribution is significantly altered by the particle size. On the other hand, over catalyst calcined at 600 °C CO and O heat of adsorption curves follow similar trends, energetically and for the coverages at which they saturate the surface, while hydrogen adsorption heats exhibit a drastic decrease from high initial heats of adsorption to a very low heats of adsorption, indicating that sites with intermediate heats are completely lost.

## 5. Conclusions:

The structure sensitivity of hydrogen, oxygen and carbon monoxide was studied by adsorption calorimetry. The structure sensitivity of hydrogen chemisorption was observed consistent with the previous studies. On the other hand, the changes in the metal particle size did not reflect itself consistently to the initial and integral heats of adsorption of CO and oxygen adsorption heats. CO and oxygen adsorption isotherms and heat of adsorption data resembled each other closely indicating that these molecules compete for the same kind of sites. The site energy distributions measured by adsorption calorimetry indicated that as the particle size decreased the site density of intermediate heats decreased.

## 6. Acknowledgement:

The financial support for this project is provided by TUBITAK under research contract no MISAG 188. The acquisition of the adsorption calorimeter was possible through a State Planning Organization Technology Research Grant no: AFP-03-04-DPT-98K122550.

## 7. References:

[1] J. K. Norskov, T. Bligaard, A, Logadottir, S. Bahn, L.B. Hansen, M. Bollinger, H. Bengaard, B. Hammer, Z. Slivancanin, M. Mavrikakis, Y. Xu, S. Dahl, CJ.H. Jakobsen, J. Catal., 209 (2002) 275-278.

[2] G. S. Zafiris, R. J. Gorte, J. Catal. 140 (1993) 418-423.

[3] F.J. Gracia, L. Bollmann, E.E. Wolf, J.T. Miller, A.J. Kropf, J.Catal, 220 (2003) 382-391.

[4] W. Akemann, K.A. Friedrich, U. Linke, U. Stimming, Surf. Sci, 402-404 (1998) 571-575.

[5] D. Uner, N. A. Tapan, I. Ozen, and M. Uner, App. Catal. A: General, 251 (2003) 225-234.

[6] Y.Y. Yeo, L. Vattunoe, and D.A. King, J. Chem. Phys., 106, (1997) 392-403.

[7] C.E. Wartnaby, A. Stuck, Y.Y. Yeo, and D.A. King, J. Phys. Chem. 100, (1996) 12483-12488.

[8] C.T. Campbell, G. Ertl, H. Kuipers, J. Segner, Surf. Sci., 107 (1981) 220-236.

[9] K. Schwaha, and E. Bechtold, Surf. Sci., 65, (1977) 277-286.

[10] J.L. Gland, B.A. Sexton, and G.B. Fisher, Surf. Sci., 95 (1980) 587-602.

[11] D.R. Monroe and R.P. Merrill J. Catal., 65 (1980) 461-469.

[12] C. Puglia, A. Nilsson, B. Hernnas, O. Karis, P. Bennich, N. Martensson, Surf. Sci. 342 (1995) 119-133.

[13] P.D. Nolan, B.R.Lutz, P.L. Tanaka, J.E. Davis, C.B. Mullins, *J.*Chem. Phys., 111, (1999) 3696-3704.

[14] Y.Y. Tong, J.J. Van der Klink, J. Phys.-Condens. Mat., 7 (1995) 2447-2459.

[15] A. Cudok, H. Froitzheim, G. Hess, Surf. Sci. 307-309 (1994) 761-767.

[16] H. Wang, R.G. Tobin, D.K. Lambert, C.L. Di Maggio, G.B. Fisher, Surf. Sci, 372 (1997) 267-278.

[17] Z. Slivancanin, B. Hammer, Surf. Sci, 515 (2002) 235-244.

[18] R.L. Narayan, T.S. King, Thermochimica Acta, 312 (1998) 105-114.

[19] N. Savargaonkar, R.L. Narayan, M. Pruski, D. O. Uner, T.S. King, J. Catal. 178 (1998) 26-33.

[20] N. Savargaonkar, D. Uner, M. Pruski, T. S. King, Langmuir, 18 (2002) 4005-4009.

[21] D.P. VanderWiel, M. Pruski, T.S. King, J. Catal., 188 (1999) 186-202.

[22] N. Kumar, T.S. King, R.D. Vigil, Chem. Eng. Sci., 55 (2000) 4973-4979.

[23] R.D. Cortright and J.A. Dumesic, J. Catal., 157 (1995) 576-583.

[24] S.B. Sharma, J.T. Miller, J.A. Dumesic, J. Catal., 148 (1994) 198-204.

[25] A.D. Karmazyn, V. Fiorin, S.J. Jenkins, D.A. King, Surf. Sci. 538 (2003) 171-183.

[26] B. Hammer, O.H. Nielsen, and J.K. Norskov, Catalysis Letters, 46 (1997) 31-35.

[27] J.-S. McEwen, S.H. Payne, H.J. Kreuzer, M. Kinne, R. Denecke, H.-P., Steinruck, Surf. Sci. 545 (2003) 47-69.

[28] D.O. Uner, M. Pruski, and T.S. King, J. Catal., 156 (1995)60-64.

[29] O. Dulaurent, D. Bianchi, App. Catal.A-General, 196 (2000) 271-280.

**List of Tables:**



**List of Figures:**

Table 1.

| Surface | Adsorption mode | Saturation coverage (ML) | Sticking coefficient, $S_0$ | $E_{a,\,des}$ (kJ/mol) | $\Delta H_{ads}$ (kJ/mol) | Reference |
|---|---|---|---|---|---|---|
| Pt(111) | dissociative | | 0.064 | | 339±32 | (6) |
| Pt(110) | dissociative | 0.35 | 0.34 | | 332±10 | (7) |
| Pt(111) | | 0.25 | 0.06 | 213.4 -175.7 | | (8) |
| Pt(S)-[9(111)x(111)] | | 0.5 | 0.06 | 205-171.5 | | (9) |
| Pt(111) | molecular | 0.6 | | | 37±2 | (9) |
| Pt(111) | dissociative | 0.4 | | | 470±10 | (10) |
| Pt(111) | | 0.25 | 0.048±0.006 | | | (11) |
| Pt(111) | | 0.25 | | | | (12) |
| Pt(111) | molecular peroxo | | | | 40.5 | (13) |
| Polycristalline Pt | | 0.75 | | | | (14) |
| Pt(111) | molecular | | 0.12 | | | (15) |

Table 2.

| Catalyst | % Pt | Initial heat of adsorption (kJ/mol) | Integral heat of adsorption (kJ/mol) | Saturation coverage (μmol/g catalyst) | Dispersion (mol H ads/mol Pt) | Reference |
|---|---|---|---|---|---|---|
| $Pt/SiO_2$ | 1.2 | 93 | 66 | 38.6 | 1.18 | (23) |
| Pt-$K/SiO_2$ | 1.2 | 95 | 67 | 46.0 | 1.31 | (23) |
| Pt-$Sn/SiO_2$ | 0.93 | 92 | 59 | 16.1 | 0.51 | (23) |
| Pt-Sn-$K//SiO_2$ | 0.93 | 97 | 52 | 26.0 | 0.89 | (23) |
| $Pt/SiO_2$ | 4.0 | 91 | 67 | 69 | 0.51 | (24) |
| $Pt/SiO_2$ | 7.0 | 92 | 68 | 94 | 0.63 | (24) |

Table 3.

| Catalyst | % Pt | Initial heat of adsorption (kJ/mol) | Integral heat of adsorption (kJ/mol) | Saturation coverage (μmol/g catalyst) | Dispersion (mol H ads/mol Pt) | Reference |
|---|---|---|---|---|---|---|
| $Pt/SiO_2$ | 1.2 | 144 | 104 | 48.7 | 1.18 | (23) |
| Pt-$K/SiO_2$ | 1.2 | 140 | 101 | 26.7 | 1.31 | (23) |
| Pt-$Sn/SiO_2$ | 0.93 | 135 | 83 | 19.6 | 0.51 | (23) |
| Pt-Sn-$K//SiO_2$ | 0.93 | 138 | 91 | 10.4 | 0.89 | (23) |
| $Pt/SiO_2$ | 4.0 | 140 | 105.1 | 130 | 0.51 | (24) |
| $Pt/SiO_2$ | 7.0 | 140 | 113.8 | 162 | 0.63 | (24) |
| Pt(221) | - | 185 | 170 | 1.5 ML[1] | - | (25) |
| Pt(111) | - | 180±8 | 119.5 | 1 ML[1] | - | (6) |

[1] ML: Monolayer

Table 4.

| | By calorimetry | | | By volumetric chemisorption | | |
|---|---|---|---|---|---|---|
| Calcination temperature (°C) | CO saturation coverages ($CO/Pt_{total}$) | O saturation coverages ($O/Pt_{total}$) | H saturation coverages ($H/Pt_{total}$) | Total hydrogen amounts ($H/Pt_{total}$) | Weak hydrogen amounts ($H/Pt_{weak}$) | Strong hydrogen amounts ($H/Pt_{strong}$) |
| 410 | 0.20 | 0.15 | >0.7 | 0.83 | 0.20 | 0.63 |
| 450 | 0.25 | 0.15 | >0.4 | 0.47 | 0.18 | 0.29 |
| 500 | 0.10 | 0.12 | 0.20 | 0.26 | 0.06 | 0.20 |
| 600 | 0.04 | 0.06 | 0.08 | 0.09 | 0.05 | 0.04 |

Figure 1.

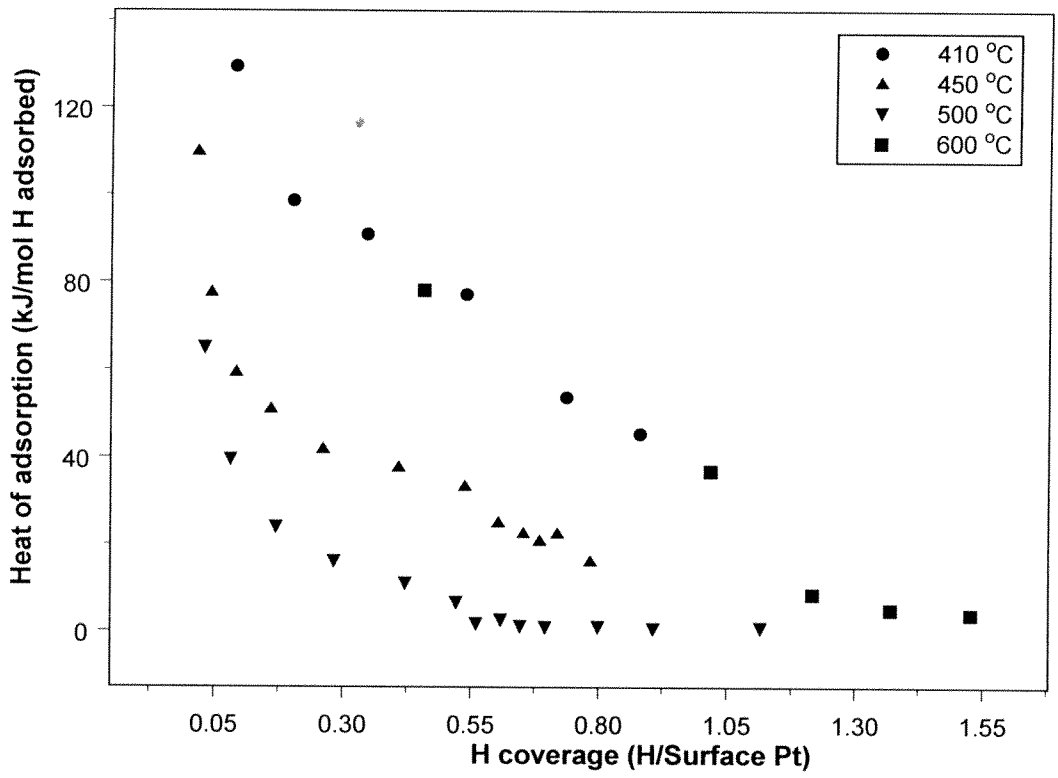
410 °C
450 °C
500 °C
600 °C
Heat of adsorption (kJ/mol H adsorbed)
120
80
40
0
0.05
0.30
0.55
0.80
1.05
1.30
1.55
H coverage (H/Surface Pt)

Figure 2.

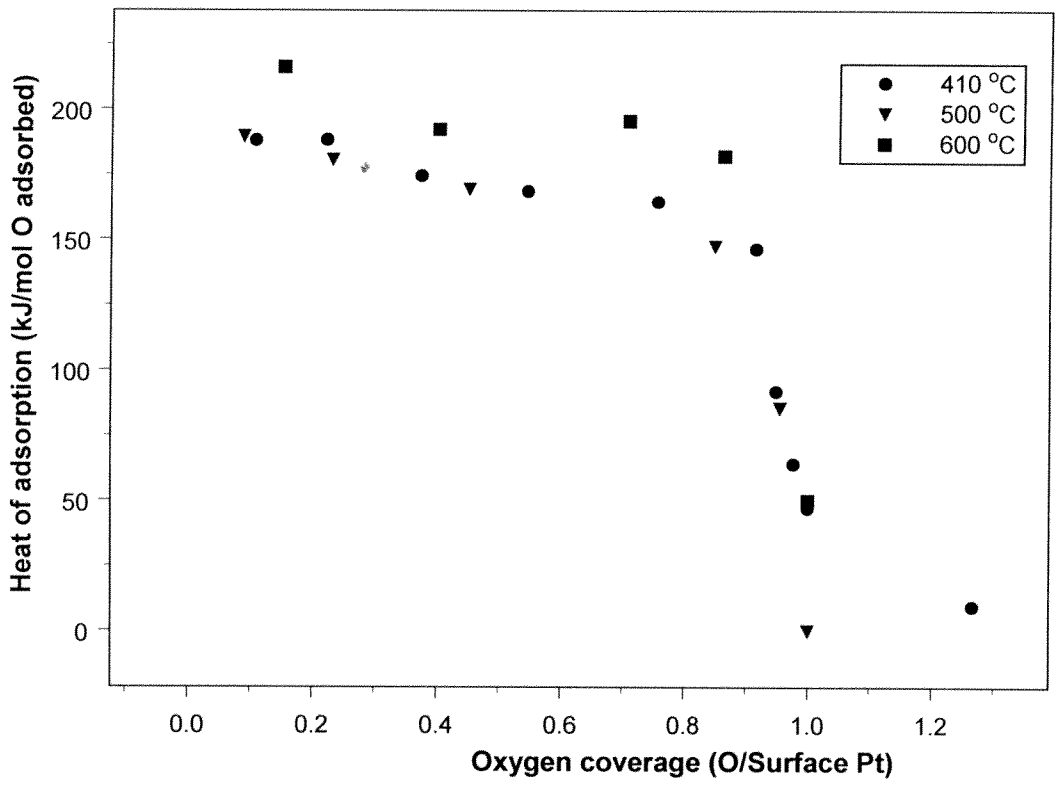
Heat of adsorption (kJ/mol O adsorbed)
200
150
100
50
0
0.0
0.2
0.4
0.6
0.8
1.0
1.2
Oxygen coverage (O/Surface Pt)
410 °C
500 °C
600 °C

Figure 3.

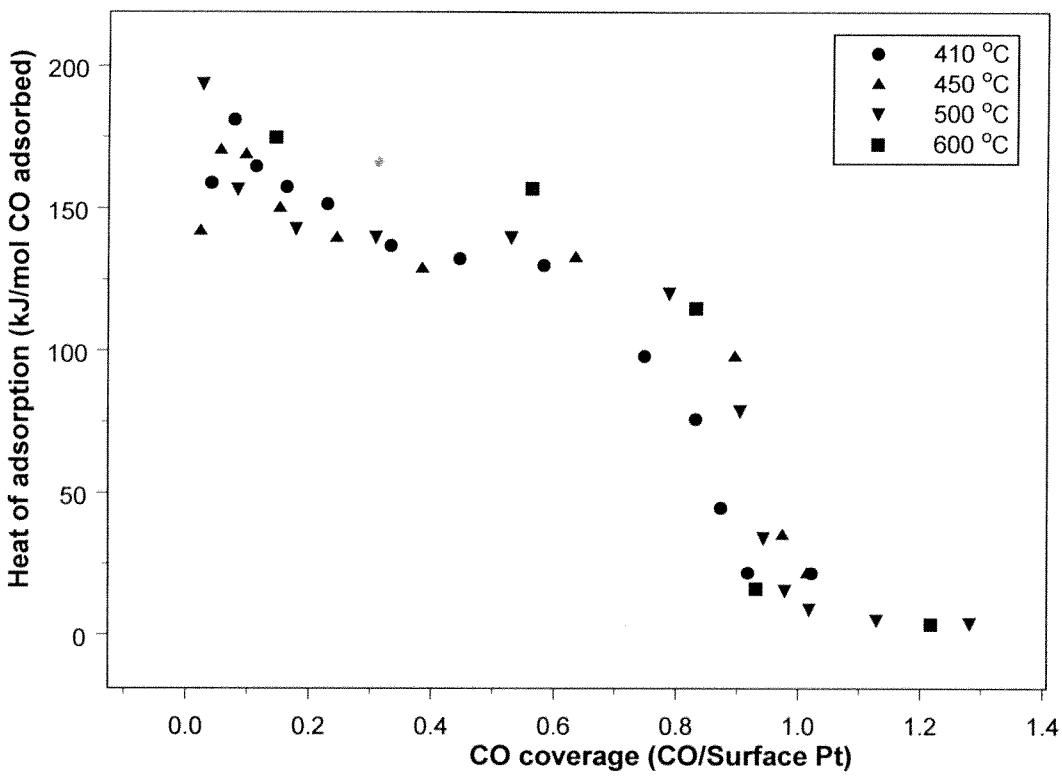
Heat of adsorption (kJ/mol CO adsorbed)
200
150
100
50
0
0.0
0.2
0.4
0.6
0.8
1.0
1.2
1.4
CO coverage (CO/Surface Pt)
410 °C
450 °C
500 °C
600 °C

Figure 4.

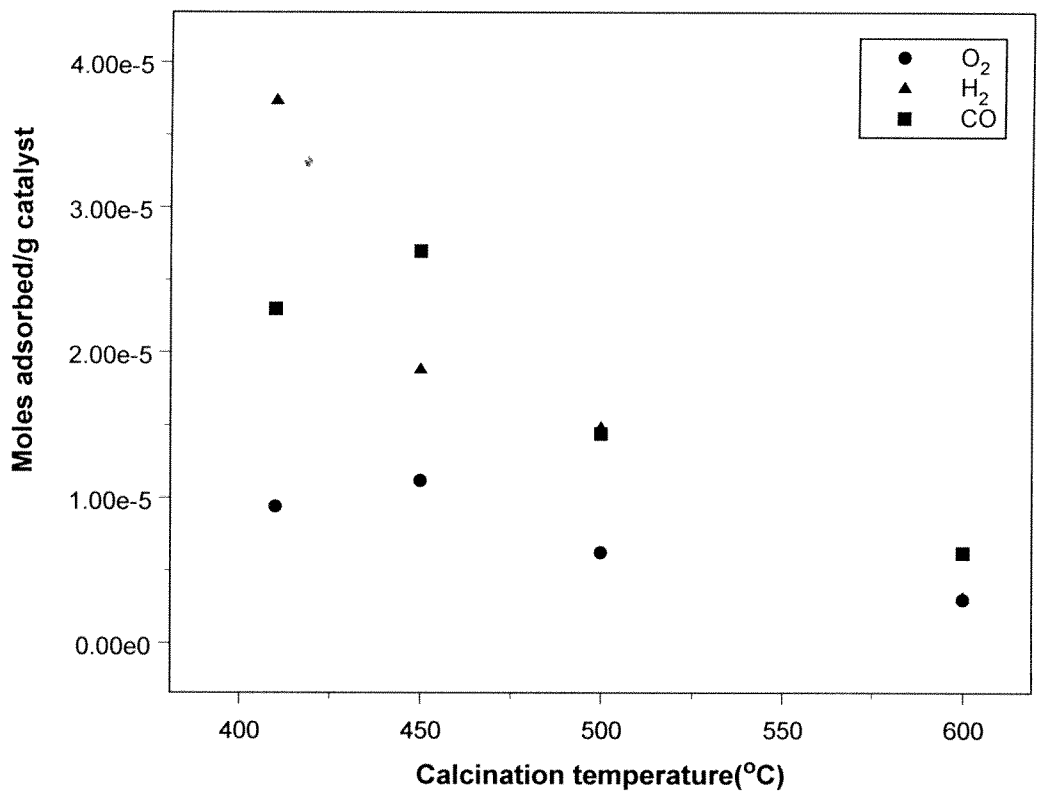
4.00e-5
3.00e-5
2.00e-5
1.00e-5
0.00e0
Moles adsorbed/g catalyst
400
450
500
550
600
Calcination temperature(°C)
O2
H2
CO

Figure 5.

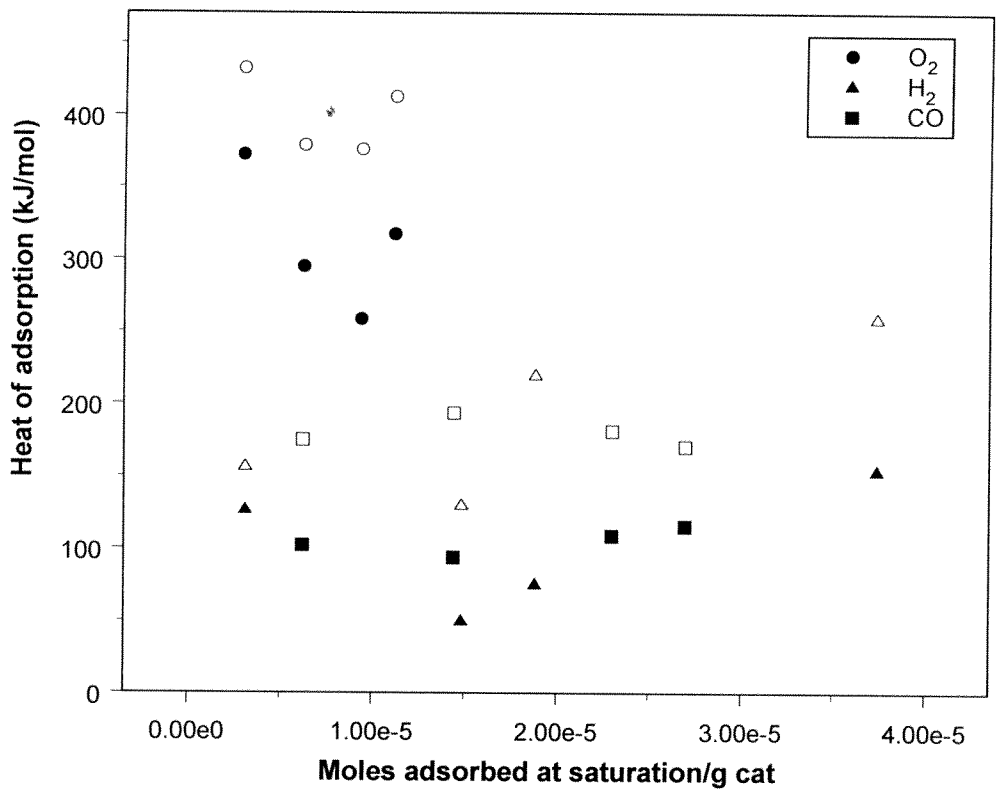
Heat of adsorption (kJ/mol)
400
300
200
100
0
0.00e0
1.00e-5
2.00e-5
3.00e-5
4.00e-5
Moles adsorbed at saturation/g cat
O2
H2
CO

Figure 6-a

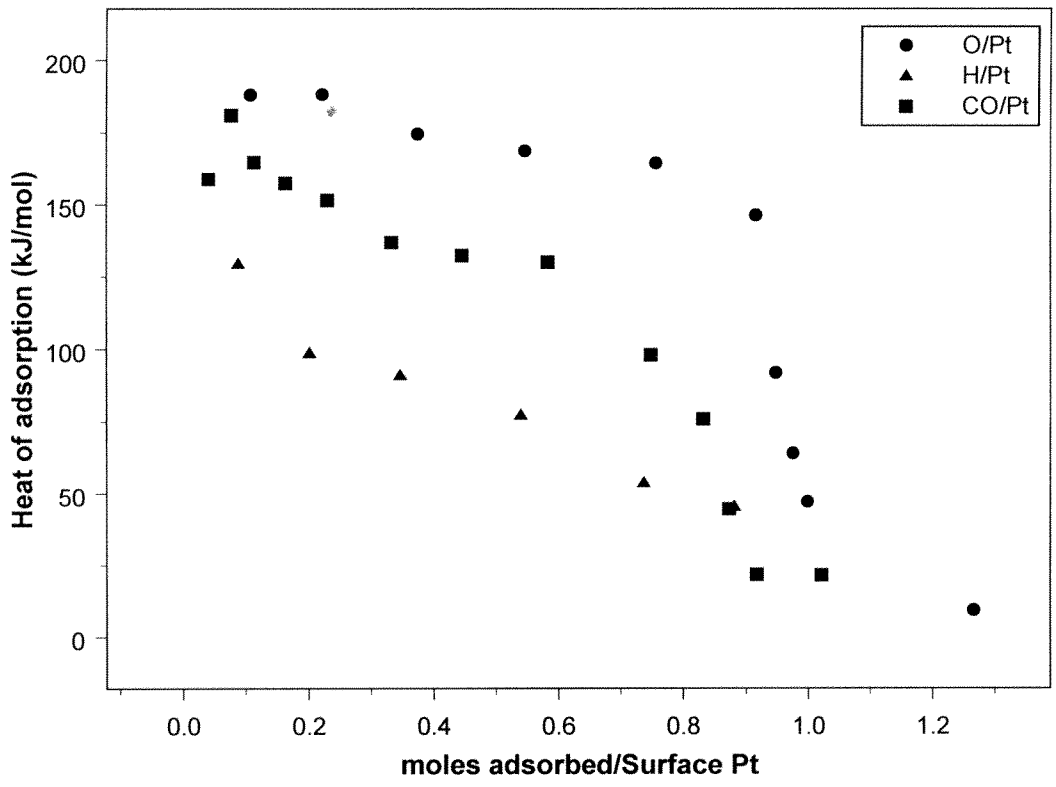
O/Pt
H/Pt
CO/Pt
Heat of adsorption (kJ/mol)
200
150
100
50
0
0.0
0.2
0.4
0.6
0.8
1.0
1.2
moles adsorbed/Surface Pt

Figure 6-b

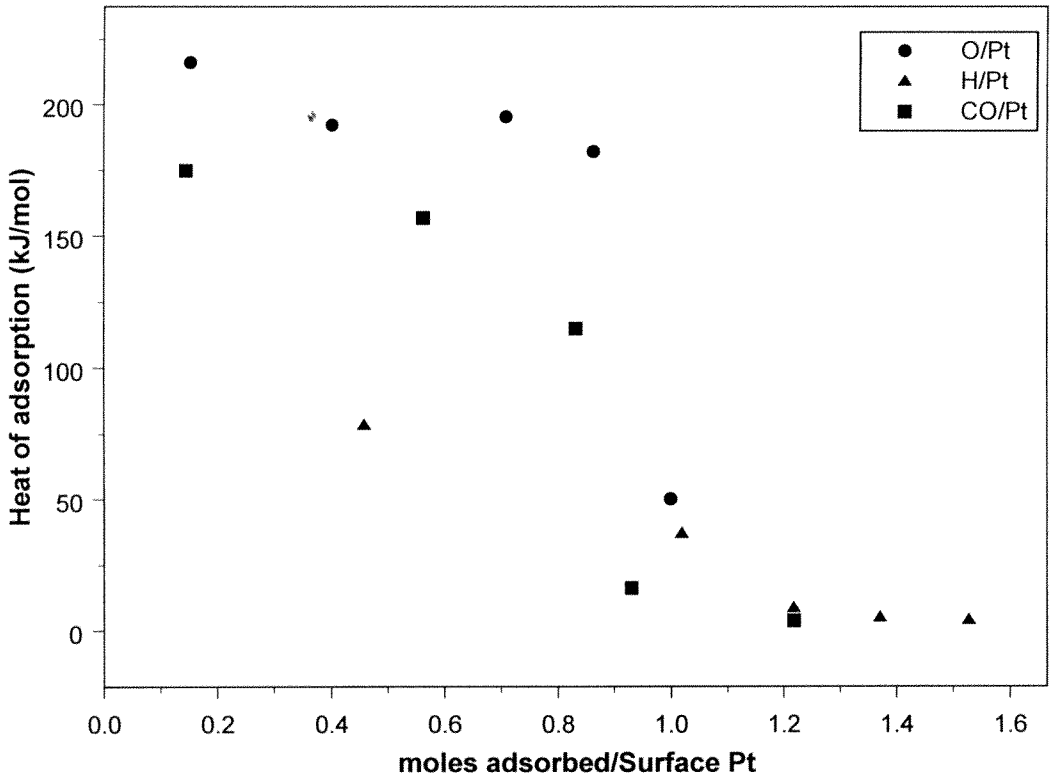
O/Pt
H/Pt
CO/Pt
Heat of adsorption (kJ/mol)
200
150
100
50
0
0.0
0.2
0.4
0.6
0.8
1.0
1.2
1.4
1.6
moles adsorbed/Surface Pt

## UYGULAMA NOTU

TÜBİTAK tarafından MİSAG 188 kodu ile desteklenen 'Emisyon kontrolünde kullanılan değerli metal katalizörler üzerinde CO oksitlenmesi reaksiyonu yapısal duyarlılık (Structure sensitivity) gösterir mi?' başlıklı projenin sonuçlarının hayta geçirilebilmesi için gerekli aşamalar aşağıda özetlenmiştir.

Bu çalışmada destekli metal katalizörler üzerinde elde edilen kökten bulgular katalizör tasarımı açısından son derece önemlidir. CO oksitlenmesi tepkimesinin yapısal duyarlılığı konusunda açık ve net bulgular elde edilmiştir. Bu sonuçlar hem emisyon kontrolü katalizörlerinde kullanılabilecek hem de PEM yakıt pillerinde kullanılabilecek seçici CO oksitlenmesi tepkimesinin gerçekleşebileceği katalizörleri tasarlamak amacı ile kullanılabilecektir. Ancak uygulamaya geçilebilmesi için pilot ölçek deneylerinin yapılabilmesi gerekmektedir. Buna ek olarak ülkemizde henüz ticari anlamda katalizör üreten bir kuruluş olmadığından elde edilen sonuçların ulusal katma değere dönüştürülmesi henüz mümkün değildir.

TÜBİTAK'ın koordinasyonunu üstlendiği VİZYON 2023 projesinde Kimya panelinin bulguları, kimya endüstrisinin gelişebilmesi için kendi teknolojisini ve kendi katalizörünü üretebilmesi konusuna parmak basmaktadır. Bu konuda TÜBITAK tarafından üstlenilmesi gereken görev güdümlü projeler kanalı ile halen dağınık bir biçimde gerçekleşen katalizör araştırmalarını daha odaklı ve daha sürekli hale getirebilmek olmalıdır. Bu konuda şimdiye kadar yürütülmüş ve yürütülmekte olan katalizör alışmalarında görev alan araştırmacıların endüstri kuruluş temsilcileri ile bir araya getirilerek yapılan çalışmaların uygulanabilirliği ve uygulamaya geçirebilmek amacı ile alınması gereken tedbirler açısından ortak görüşlerin oluşturulduğu bir çalışma kişisel görüşlerden çok daha verimli sonuçlar doğurabilecektir.

| **BİBLİYOGRAFİK BİLGİ FORMU** | |
|---|---|
| **1. Proje No:** MİSAG 188 | **2. Rapor Tarihi:** Aralık 2003 |
| **3. Projenin başlangıç ve bitiş tarihleri:** Ağustos 2001-Ağustos 2003 | |
| 4. **Projenin adı:** Emisyon kontrolünde kullanılan değerli metal katalizörler üzerinde CO oksitlenmesi reaksiyonu yapısal duyarlılık (Structure sensitivity) gösterir mi? | |
| **5. Proje Yürütücüsü ve Yardımcı araştırıcılar:** Doç. Dr. Deniz Üner<br>Murat Üner<br>Bora Atalık | |
| **6. Projenin yürütüldüğü Kuruluş ve adresi:** Kimya Mühendisliği Bölümü<br>Orta Doğu Teknik Üniversitesi<br>Ankara 06531 | |
| **7. Destekleyen Kuruluşların Adı ve Adresi:** | |
| **8. Öz:** Karbon monoksitin karbon dioksite oksitlenmesi tepkimesi oksijen molekülünün yüzeyde parçalanarak adsorplanması sonucunda oluşan oksijen atomu ile adsoplanmış karbon monoksit molekülünün etkileşimi ile gerçekleşir. Karbon monoksitin Pt üzerinde yol açtığı zehirleme etkisi yüzünden oksijen adsoplanması daha da önem kazanır. Bu çalışmanın amacı oksijen, hidrojen ve karbon monoksitin $Pt/\gamma\text{-}Al_2O_3$ üzerindeki adsorplanması ve yapısal duyarlılığını incelemektir. Metallerin parçacık büyüklüğü kalsinasyon sıcaklığı ve süresini yükselterek artırılmış ve bu şekilde katalizörlerin yapısı değiştirilmiştir. Bu şekilde aynı miktarda metal yüklenmiş fakat farklı parçacık büyüklüğünde dolayısı ile farklı kenar, köşe ve düzlem atom oranları içeren katalizörler hazırlanmıştır. Temiz yüzey adsorplanma ısıları ölçüldüğünde karbon monoksit ve oksijenin yapıya duyarlılık göstemedikleri, ancak hidrojenin temiz yüzey adsorplanma ısısının parçacık büyüklüğü ile ters orantılı olduğu belirlenmiştir. Bu sonuç hidrojenin CO veya $O_2$ den daha fazla yapısal duyarlılık gösterdiğinin bir işareti olarak alınmıştır. CO oksitlenmesi tepkimesinin yapısal duyarlılık gösterdiği ise reaksiyon deneyleri ile açığa çıkarılmıştır. Tepkimenin aktivasyon enerjisinin artan parçacık büyüklüğü ile sistematik olarak azaldığı ortaya çıkarılmıştır.<br><br>*Anahtar kelimeler:* Katalizör, Destekli metal katalizör, ikili metaller, karbon monoksit oksitlenmesi, seçici karbon monoksit oksitlenmesi, platin , adsorplanma ısısı, mikrokinetik analiz. | |
| **9. Proje ile ilgili yayın/tebliğlerle ilgili bilgiler:**<br>4 uluslararası tebliğ ve 3 uluslararası makale hazırlandı ve/veya yayınlandı. Bir uluslararası makale yayına hazırlanıyor. | |
| **10. Bilim Dalı:**<br>Doçentlik B. Dalı Kodu: ISIC kodu:2411, 2412, 3410<br>Uzmanlık Alanı Kodu:331212, 234141, 234121 | |
| **11. Dağıtım(*):** ☐Sınırlı | ☐Sınırsız |
| **12. Raporun gizlilik durumu:** ☐Gizli | ☐Gizli Değil |